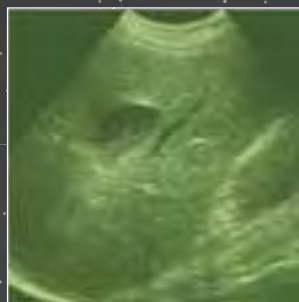


Manual of diagnostic ultrasound

v o l u m e 1



Second edition

cm/s

60
40
20
0
-20

[TIB 1.3]
7.5L40/4.0
SCHILDDR.
100%
48dB ZD4
4.0cm 11B/s

Z
THI
CF5.1MHz
PRF1102Hz
F-Mittel
70dB ZD6

DF5.5MHz
PRF5208Hz
62dB
FT25
FG1.0

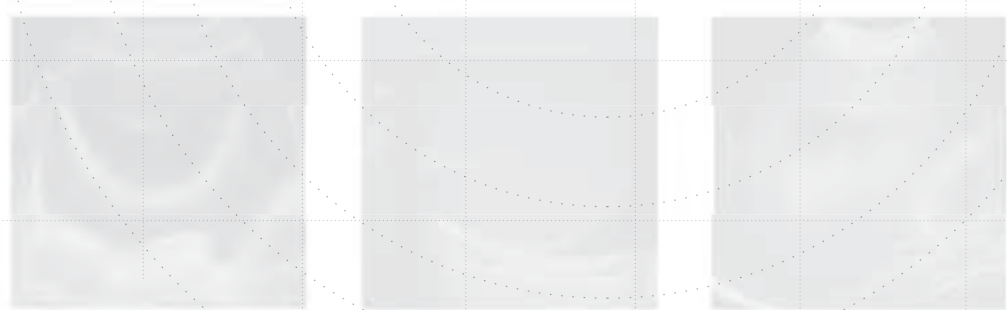


World Health
Organization

0.1

Manual of diagnostic ultrasound

..... v o l u m e 1



Second edition

cm/s



[TIB 1.3]
7.5L40/4.0
SCHILDDR.
100%
48dB ZD4
4.0cm 11B/s

Z
THI
CF5.1MHz
PRF1102Hz
F-Mittel
70dB ZD6

DF5.5MHz
PRF5208Hz
62dB
FT25
FG1.0



**World Health
Organization**

WHO Library Cataloguing-in-Publication Data

WHO manual of diagnostic ultrasound. Vol. 1. -- 2nd ed / edited by Harald Lutz, Elisabetta Buscarini.

1.Diagnostic imaging. 2.Ultrasonography. 3.Pediatrics - instrumentation. I.Lutz, Harald. II.Buscarini, Elisabetta. III. World Health Organization. IV.World Federation for Ultrasound in Medicine and Biology.

ISBN 978 92 4 154745 1

(NLM classification: WN 208)

© **World Health Organization 2011**

All rights reserved. Publications of the World Health Organization can be obtained from WHO Press, World Health Organization, 20 Avenue Appia, 1211 Geneva 27, Switzerland (tel.: +41 22 791 3264; fax: +41 22 791 4857; e-mail: bookorders@who.int). Requests for permission to reproduce or translate WHO publications – whether for sale or for noncommercial distribution – should be addressed to WHO Press, at the above address (fax: +41 22 791 4806; e-mail: permissions@who.int).

The designations employed and the presentation of the material in this publication do not imply the expression of any opinion whatsoever on the part of the World Health Organization concerning the legal status of any country, territory, city or area or of its authorities, or concerning the delimitation of its frontiers or boundaries. Dotted lines on maps represent approximate border lines for which there may not yet be full agreement.

The mention of specific companies or of certain manufacturers' products does not imply that they are endorsed or recommended by the World Health Organization in preference to others of a similar nature that are not mentioned. Errors and omissions excepted, the names of proprietary products are distinguished by initial capital letters.

All reasonable precautions have been taken by the World Health Organization to verify the information contained in this publication. However, the published material is being distributed without warranty of any kind, either expressed or implied. The responsibility for the interpretation and use of the material lies with the reader. In no event shall the World Health Organization be liable for damages arising from its use.

The named editors alone are responsible for the views expressed in this publication.

Production editor: Melanie Lauckner
Design & layout: Sophie Guetaneh Aguetant and Cristina Ortiz

Printed in Malta by Gutenberg Press Ltd.

Contents

Foreword	v	
Acknowledgements	vii	
Chapter 1	1	Basic physics of ultrasound Harald T Lutz, R Soldner
Chapter 2	27	Examination technique Harald T Lutz
Chapter 3	43	Interventional ultrasound Elisabetta Buscarini
Chapter 4	65	Neck Harald T Lutz
Chapter 5	91	Chest Gebhard Mathis
Chapter 6	111	Abdominal cavity and retroperitoneum Harald T Lutz, Michael Kawooya
Chapter 7	139	Liver Byung I Choi, Jae Y Lee
Chapter 8	167	Gallbladder and bile ducts Byung I Choi, Jae Y Lee
Chapter 9	191	Pancreas Byung I Choi, Se H Kim
Chapter 10	207	Spleen Byung I Choi, Jin Y Choi
Chapter 11	221	Gastrointestinal tract Harald T Lutz, Josef Deuerling
Chapter 12	259	Adrenal glands Dennis L L Cochlin
Chapter 13	267	Kidneys and ureters Dennis L L Cochlin, Mark Robinson
Chapter 14	321	Urinary bladder, urethra, prostate and seminal vesicles and penis Dennis L L Cochlin
Chapter 15	347	Scrotum Dennis L L Cochlin
Chapter 16	387	Special aspects of abdominal ultrasound Harald T Lutz, Michael Kawooya
Recommended reading	397	
Glossary	399	
Index	403	

Foreword

No medical treatment can or should be considered or given until a proper diagnosis has been established.

For a considerable number of years after Roentgen first described the use of ionizing radiation – at that time called ‘X-rays’ – for diagnostic imaging in 1895, this remained the only method for visualizing the interior of the body. However, during the second half of the twentieth century new imaging methods, including some based on principles totally different from those of X-rays, were discovered. Ultrasonography was one such method that showed particular potential and greater benefit than X-ray-based imaging.

During the last decade of the twentieth century, use of ultrasonography became increasingly common in medical practice and hospitals around the world, and several scientific publications reported the benefit and even the superiority of ultrasonography over commonly used X-ray techniques, resulting in significant changes in diagnostic imaging procedures.

With increasing use of ultrasonography in medical settings, the need for education and training became clear. Unlike the situation for X-ray-based modalities, no international and few national requirements or recommendations exist for the use of ultrasonography in medical practice. Consequently, fears of ‘malpractice’ due to insufficient education and training soon arose.

WHO took up this challenge and in 1995 published its first training manual in ultrasonography. The expectations of and the need for such a manual were found to be overwhelming. Thousands of copies have been distributed worldwide, and the manual has been translated into several languages. Soon, however, rapid developments and improvements in equipment and indications for the extension of medical ultrasonography into therapy indicated the need for a totally new ultrasonography manual.

The present manual is the first of two volumes. Volume 2 includes paediatric examinations and gynaecology and musculoskeletal examination and treatment. As editors, both volumes have two of the world’s most distinguished experts in ultrasonography: Professor Harald Lutz and Professor Elisabetta Buscarini. Both have worked intensively with clinical ultrasonography for years, in addition to conducting practical training courses all over the world. They are also distinguished representatives of the World Federation for Ultrasound in Medicine and Biology and the Mediterranean and African Society of Ultrasound.

We are convinced that the new publications, which cover modern diagnostic and therapeutic ultrasonography extensively, will benefit and inspire medical professionals in improving ‘health for all’ in both developed and developing countries.

Harald Østensen,
Cluny, France

Acknowledgements

The editors **Harald T Lutz** and **Elisabetta Buscarini** wish to thank all the members of the Board of the World Federation for Ultrasound in Medicine and Biology (WFUMB) for their support and encouragement during preparation of this manual.

Professor Lotfi Hendaoui is gratefully thanked for having carefully read over the completed manuscript.

The editors also express their gratitude to and appreciation of those listed below, who supported preparation of the manuscript by contributing as co-authors and by providing illustrations and competent advice.

- Marcello Caremani:** Department of Infectious Diseases, Public Hospital, Arezzo, Italy
- Jin Young Choi:** Department of Radiology, Yonsei University College of Medicine, Seoul, Republic of Korea
- Josef Deuerling:** Department of Internal Medicine, Klinikum Bayreuth, Bayreuth, Germany
- Klaus Dirks:** Department of Internal Medicine, Klinikum Bayreuth, Bayreuth, Germany
- Hassen A Gharbi:** Department of Radiology, Ibn Zohr, Côté El Khandra, Tunis, Tunisia
- Joon Koo Han:** Department of Radiology 28, Seoul National University Hospital Seoul, Republic of Korea
- Michael Kawooya:** Department of Radiology, Mulago Hospital, Kampala, Uganda
- Ah Young Kim:** Department of Radiology, Asan Medical Center, Ulsan University, Seoul, Republic of Korea
- Se Hyung Kim:** Department of Radiology, Seoul National University Hospital, Seoul, Republic of Korea
- Jae Young Lee:** Department of Radiology, Seoul National University Hospital, Seoul, Republic of Korea
- Jeung Min Lee:** Department of Radiology, Seoul National University Hospital, Seoul, Republic of Korea
- Guido Manfredi:** Department of Gastroenterology, Maggiore Hospital, Crema, Italy
- Mark Robinson:** Department of Radiology, The Royal Gwent Hospital, Newport, Wales
- Richard Soldner:** Engineer, Herzogenaurach, Germany



Chapter 1

Basic physics

Definition	3
Generation of ultrasound	3
Properties of ultrasound	4
Shape of the ultrasound beam	6
	8 Spatial resolution
	9 Echo
	10 Doppler effect
Ultrasound techniques	11
	11 A-mode
	11 B-mode
	12 M-mode or TM-mode
	12 B-scan, two-dimensional
	14 Three- and four-dimensional techniques
	14 B-flow
	14 Doppler techniques
	18 Contrast agents
Artefacts	19
Adverse effects	26

Basic physics

Definition

Ultrasound is the term used to describe sound of frequencies above 20 000 Hertz (Hz), beyond the range of human hearing. Frequencies of 1–30 megahertz (MHz) are typical for diagnostic ultrasound.

Diagnostic ultrasound imaging depends on the computerized analysis of reflected ultrasound waves, which non-invasively build up fine images of internal body structures. The resolution attainable is higher with shorter wavelengths, with the wavelength being inversely proportional to the frequency. However, the use of high frequencies is limited by their greater attenuation (loss of signal strength) in tissue and thus shorter depth of penetration. For this reason, different ranges of frequency are used for examination of different parts of the body:

- 3–5 MHz for abdominal areas
- 5–10 MHz for small and superficial parts and
- 10–30 MHz for the skin or the eyes.

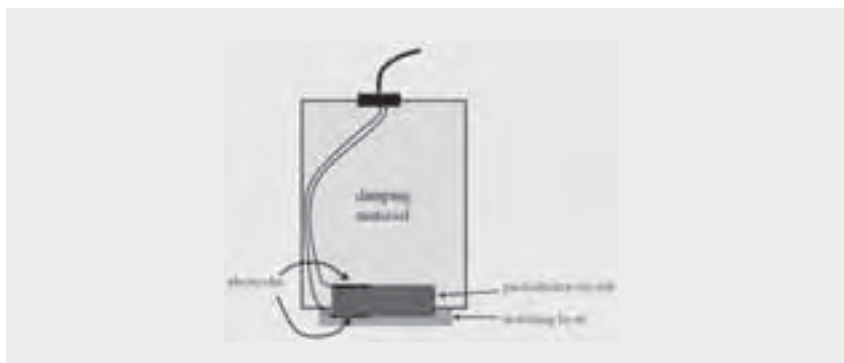
Generation of ultrasound

Piezoelectric crystals or materials are able to convert mechanical pressure (which causes alterations in their thickness) into electrical voltage on their surface (the piezoelectric effect). Conversely, voltage applied to the opposite sides of a piezoelectric material causes an alteration in its thickness (the indirect or reciprocal piezoelectric effect). If the applied electric voltage is alternating, it induces oscillations which are transmitted as ultrasound waves into the surrounding medium. The piezoelectric crystal, therefore, serves as a transducer, which converts electrical energy into mechanical energy and vice versa.

Ultrasound transducers are usually made of thin discs of an artificial ceramic material such as lead zirconate titanate. The thickness (usually 0.1–1 mm) determines the ultrasound frequency. The basic design of a plain transducer is shown in Fig. 1.1.

In most diagnostic applications, ultrasound is emitted in extremely short pulses as a narrow beam comparable to that of a flashlight. When not emitting a pulse (as much as 99% of the time), the same piezoelectric crystal can act as a receiver.

Fig. 1.1. Basic design of a single-element transducer



Properties of ultrasound

Sound is a vibration transmitted through a solid, liquid or gas as mechanical pressure waves that carry kinetic energy. A medium must therefore be present for the propagation of these waves. The type of waves depends on the medium. Ultrasound propagates in a fluid or gas as longitudinal waves, in which the particles of the medium vibrate to and fro along the direction of propagation, alternately compressing and rarefying the material. In solids such as bone, ultrasound can be transmitted as both longitudinal and transverse waves; in the latter case, the particles move perpendicularly to the direction of propagation. The **velocity of sound** depends on the density and compressibility of the medium. In pure water, it is 1492 m/s (20 °C), for example. The relationship between frequency (f), velocity (c) and wavelength (λ) is given by the relationship:

$$\lambda = \frac{c}{f} \quad (1.1)$$

As it does in water, ultrasound propagates in soft tissue as longitudinal waves, with an average velocity of around 1540 m/s (fatty tissue, 1470 m/s; muscle, 1570 m/s). The construction of images with ultrasound is based on the measurement of distances, which relies on this almost constant propagation velocity. The velocity in bone (ca. 3600 m/s) and cartilage is, however, much higher and can create misleading effects in images, referred to as artefacts (see below).

The wavelength of ultrasound influences the **resolution** of the images that can be obtained; the higher the frequency, the shorter the wavelength and the better the resolution. However, attenuation is also greater at higher frequencies.

The kinetic energy of sound waves is transformed into heat (thermal energy) in the medium when sound waves are absorbed. The use of ultrasound for thermotherapy was the first use of ultrasound in medicine.

Energy is lost as the wave overcomes the natural resistance of the particles in the medium to displacement, i.e. the viscosity of the medium. Thus, absorption increases with the viscosity of the medium and contributes to the attenuation of the ultrasound beam. Absorption increases with the frequency of the ultrasound.

Bone absorbs ultrasound much more than soft tissue, so that, in general, ultrasound is suitable for examining only the surfaces of bones. Ultrasound energy cannot reach

the areas behind bones. Therefore, ultrasound images show a black zone behind bones, called an **acoustic shadow**, if the frequencies used are not very low (see Fig. 5.2).

Reflection, scattering, diffraction and refraction (all well-known optical phenomena) are also forms of interaction between ultrasound and the medium. Together with absorption, they cause attenuation of an ultrasound beam on its way through the medium. The total attenuation in a medium is expressed in terms of the distance within the medium at which the intensity of ultrasound is reduced to 50% of its initial level, called the 'half-value thickness'.

In soft tissue, attenuation by absorption is approximately 0.5 decibels (dB) per centimetre of tissue and per megahertz. Attenuation limits the depth at which examination with ultrasound of a certain frequency is possible; this distance is called the 'penetration depth'. In this connection, it should be noted that the reflected ultrasound echoes also have to pass back out through the same tissue to be detected. Energy loss suffered by distant reflected echoes must be compensated for in the processing of the signal by the ultrasound unit using echo gain techniques ((depth gain compensation (DGC) or time gain compensation (TGC)) to construct an image with homogeneous density over the varying depth of penetration (see section on Adjustment of the equipment in Chapter 2 and Fig. 2.4).

Reflection and refraction occur at acoustic boundaries (interfaces), in much the same way as they do in optics. Refraction is the change of direction that a beam undergoes when it passes from one medium to another. Acoustic interfaces exist between media with different acoustic properties. The acoustic properties of a medium are quantified in terms of its **acoustic impedance**, which is a measure of the degree to which the medium impedes the motion that constitutes the sound wave. The acoustic impedance (z) depends on the density (d) of the medium and the sound velocity (c) in the medium, as shown in the expression:

$$z = dc \quad (1.2)$$

The difference between the acoustic impedance of different biological tissues and organs is very small. Therefore, only a very small fraction of the ultrasound pulse is reflected, and most of the energy is transmitted (Fig. 1.2). This is a precondition for the construction of ultrasound images by analysing echoes from successive reflectors at different depths.

The greater the difference in acoustic impedance between two media, the higher the fraction of the ultrasound energy that is reflected at their interface and the higher the attenuation of the transmitted part. Reflection at a smooth boundary that has a diameter greater than that of the ultrasound beam is called 'specular reflection' (see Fig. 1.3).

Air and gas reflect almost the entire energy of an ultrasound pulse arriving through a tissue. Therefore, an **acoustic shadow** is seen behind gas bubbles. For this reason, ultrasound is not suitable for examining tissues containing air, such as the healthy lungs. For the same reason, a coupling agent is necessary to eliminate air between the transducer and the skin.

The boundaries of tissues, including organ surfaces and vessel walls, are not smooth, but are seen as 'rough' by the ultrasound beam, i.e. there are irregularities at a scale similar to the wavelength of the ultrasound. These interfaces cause non-specular reflections, known as back-scattering, over a large angle. Some of these reflections will reach the transducer and contribute to the construction of the image (Fig. 1.3).

Fig. 1.2. Specular reflection. (a) Transducer emitting an ultrasound pulse. (b) Normally, most of the energy is transmitted at biological interfaces. (c) Gas causes total reflection

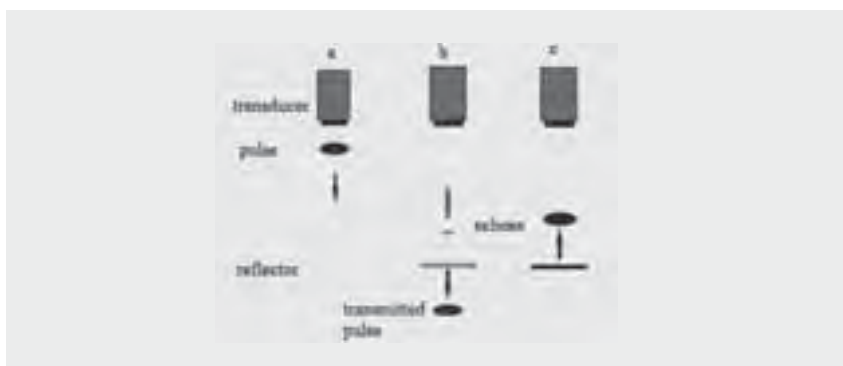
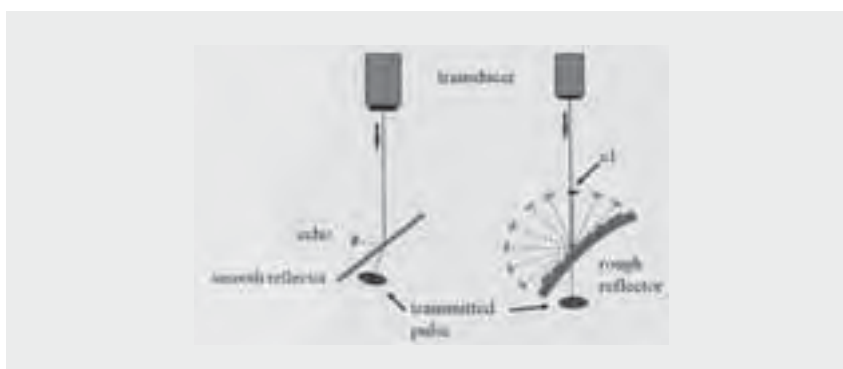


Fig. 1.3. Specular reflection. Smooth interface (left), rough interface (right). Back-scattering is characteristic of biological tissues. The back-scattered echo e1 will reach the transducer



A similar effect is seen with very small reflectors, those whose diameters are similar to that of the wavelength of the ultrasound beam. These reflectors are called 'scatterers'. They reflect (scatter) ultrasound over a wide range of angles, too (Fig. 1.4).

Shape of the ultrasound beam

The three-dimensional **ultrasound field** from a focused transducer can be described as a beam shape. Fig. 1.5 is a two-dimensional depiction of the three-dimensional beam shape. An important distinction is made between the near field (called the Fresnel zone) between the transducer and the focus and the divergent far field (called the Fraunhofer zone) beyond the focus. The border of the beam is not smooth, as the energy decreases away from its axis.

Fig. 1.4. Scatterer. Part of the back-scattered echoes (e7) will reach the transducer

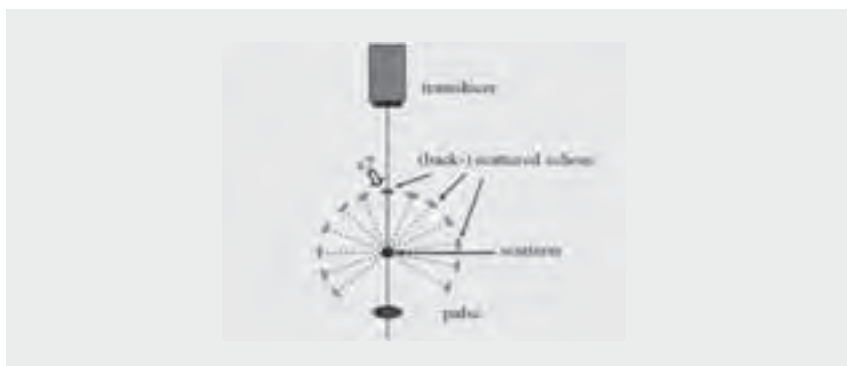
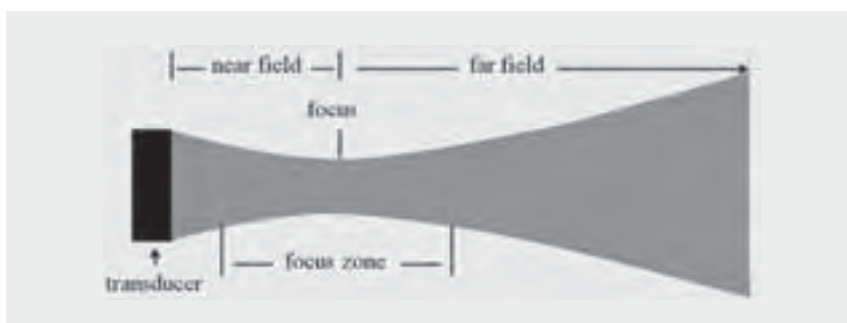


Fig. 1.5. Ultrasound field



The focus zone is the narrowest section of the beam, defined as the section with a diameter no more than twice the transverse diameter of the beam at the actual focus. If attenuation is ignored, the focus is also the area of highest intensity. The length of the near field, the position of the focus and the divergence of the far field depend on the frequency and the diameter (or aperture) of the active surface of the transducer. In the case of a plane circular transducer of radius R , the near field length (L_0) is given by the expression:

$$L_0 \sim \frac{0.8R^2}{\lambda} \quad (1.3)$$

The divergence angle (α) of the ultrasound beam in the far field is given by the expression:

$$\frac{\sin \alpha}{2} \sim \frac{0.6\lambda}{R} \quad (1.4)$$

The diameter of the beam in the near field corresponds roughly to the radius of the transducer. A small aperture and a large wavelength (low frequency) lead to a

Fig. 1.6. Focusing of transducers. Ultrasound field of a plane and a concave transducer (left) and of multiarray transducers, electronically focused for short and far distances and depths; (see also Fig. 1.7)

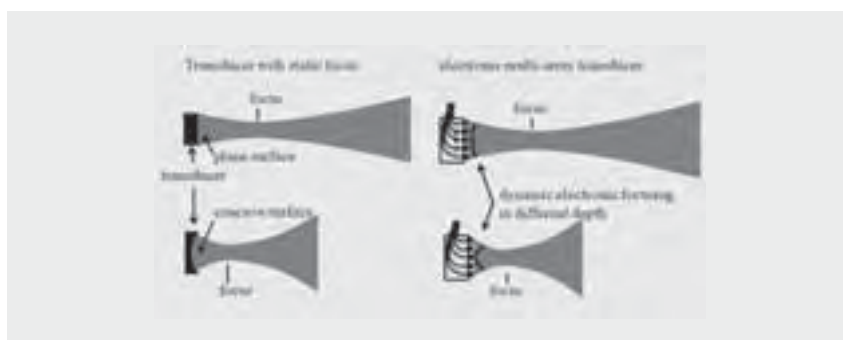
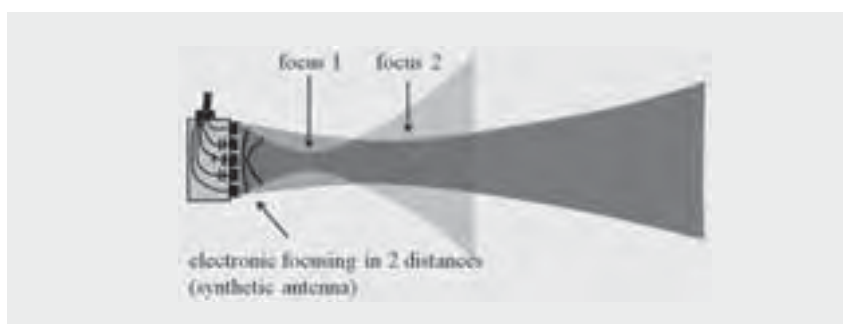


Fig. 1.7. Dynamic electronic focusing during receive to improve lateral resolution over a larger depth range



short near field and greater divergence of the far field, while a larger aperture or higher frequency gives a longer near field but less divergence. The focal distance, L_0 , as well as the diameter of the beam at the focal point can be modified by additional focusing, such as by use of a concave transducer (Fig. 1.6) or an acoustic lens (static focus). The use of electronic means for delaying parts of the signal for the different crystals in an array system enables variable focusing of the composite ultrasound beam, adapted to different depths during receive (dynamic focusing; Fig. 1.6 and Fig. 1.7).

The form and especially the diameter of the beam strongly influence the **lateral resolution** and thus the quality of the ultrasound image. The focus zone is the zone of best resolution and should always be positioned to coincide with the region of interest. This is another reason for using different transducers to examine different regions of the body; for example, transducers with higher frequencies and mechanical focusing should be used for short distances (small-part scanner). Most modern transducers have electronic focusing to allow adaption of the aperture to specific requirements (dynamic focusing, Fig. 1.7).

Spatial resolution

Spatial resolution is defined as the minimum distance between two objects that are still distinguishable. The lateral and the axial resolution must be differentiated in ultrasound images.

Lateral resolution (Fig. 1.8) depends on the diameter of the ultrasound beam. It varies in the axial direction, being best in the focus zone. As many array transducers can be focused in only one plane, because the crystals are arranged in a single line, lateral resolution is particularly poor perpendicular to that plane.

The axial resolution (Fig. 1.9) depends on the pulse length and improves as the length of the pulse shortens. Wide-band transducers (transducers with a high transmission bandwidth, e.g. 3–7 MHz) are suitable for emitting short pulses down to nearly one wavelength.

Fig. 1.8. Lateral resolution. The objects at position 'a' can be depicted separately because their separation is greater than the diameter of the ultrasound beam in the focus zone. The distance between the objects at 'b' is too small to allow them to be distinguished. The objects at 'c' are the same distance apart as those at 'a' but cannot be separated because the diameter of the beam is greater outside the focus zone

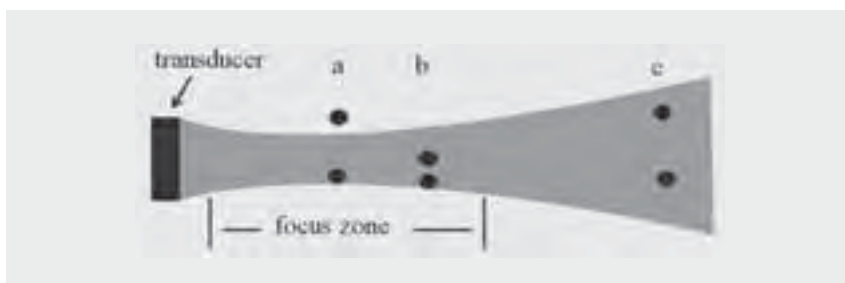
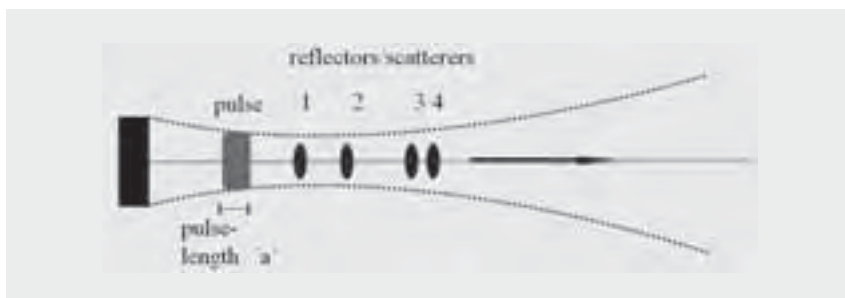


Fig. 1.9. Axial resolution. The objects at positions '1' and '2' can be depicted separately because their distance is greater than the pulse length a , whereas the distance between the objects at '3' and '4' is too small for them to be depicted separately



Echo

Echo is the usual term for the reflected or back-scattered parts of the emitted ultrasound pulses that reach the transducer. For each echo, the intensity and time delay are measured

at the transducer and electronically processed to allow calculation of the distance travelled. The displayed results form the basis of diagnostic ultrasound images.

The origin of echoes reflected from broad boundaries, such as the surface of organs or the walls of large vessels, is easily identified. However, scatterers that are very small in relation to the ultrasound beam exist at high density in the soft tissues and organs. Because of their large number, single scatterers cannot be registered separately by the ultrasound beam, and the superimposed signals cannot be related to specific anatomical structures. These image components are called 'speckle'.

Although the idea that each echo generated in the tissue is displayed on the screen is an oversimplification, it is reasonable to describe all echoes from an area, an organ or a tumour as an **echo pattern** or **echo structure** (see Fig. 2.12 and Fig. 2.13).

Doppler effect

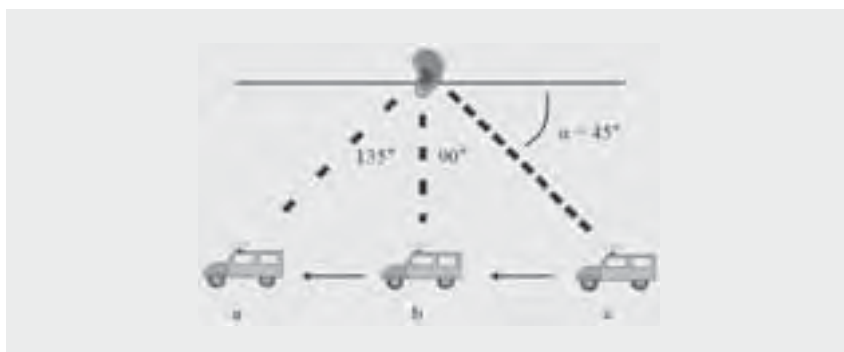
The **Doppler effect** was originally postulated by the Austrian scientist Christian Doppler in relation to the colours of double stars. The effect is responsible for changes in the frequency of waves emitted by moving objects as detected by a stationary observer: the perceived frequency is higher if the object is moving towards the observer and lower if it is moving away. The difference in frequency (Δf) is called the **Doppler frequency shift**, **Doppler shift** or **Doppler frequency**. The Doppler frequency increases with the speed of the moving object.

The Doppler shift depends on the emitted frequency (f), the velocity of the object (V) and the angle (α) between the observer and the direction of the movement of the emitter (Fig. 1.10), as described by the formula (where c is the velocity of sound in the medium being transversed):

$$\Delta f = \frac{f}{c} V \cos \alpha \quad (1.5)$$

When the angle α is 90° (observation perpendicular to the direction of movement), no Doppler shift occurs ($\cos 90^\circ = 0$)

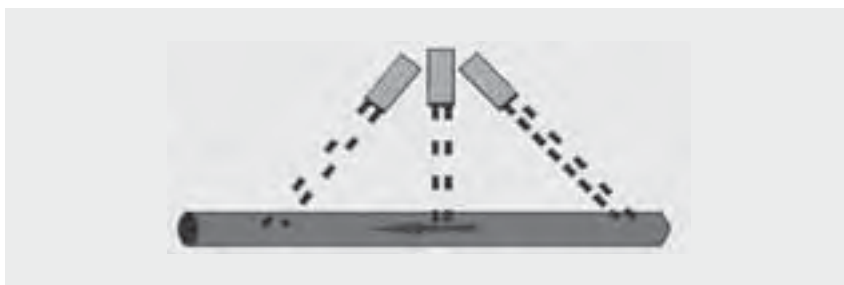
Fig. 1.10. Doppler effect. The observer hears the correct frequency from the car in position 'b' ($\alpha = 90^\circ$), whereas the signal from position 'a' ($\alpha = 45^\circ$) sounds lower and that from position 'c' ($\alpha = 135^\circ$) higher than the emitted sound



In medicine, Doppler techniques are used mainly to analyse blood flow (Fig. 1.11). The observed Doppler frequency can be used to calculate blood velocity because the velocity of the ultrasound is known and the angle of the vessels to the beam direction can be measured, allowing angle correction. It must be noted that a Doppler shift occurs twice in this situation: first, when the ultrasound beam hits the moving blood cells and, second, when the echoes are reflected back by the moving blood cells. The blood velocity, V , is calculated from the Doppler shift by the formula:

$$V = c \cdot \frac{\Delta f}{2f} \cdot \cos \alpha \quad (1.6)$$

Fig. 1.11. Doppler analysis of blood flow (arrow). The Doppler shift occurs twice. The shift observed depends on the orientation of the blood vessel relative to the transducer



Physiological blood flow causes a Doppler shift of 50–16 000 Hz (frequencies in the audible range), if ultrasound frequencies of 2–10 MHz are used. The equipment can be set up to emit sounds at the Doppler frequency to help the operator monitor the outcome of the examination.

Ultrasound techniques

The echo principle forms the basis of all common ultrasound techniques. The distance between the transducer and the reflector or scatterer in the tissue is measured by the time between the emission of a pulse and reception of its echo. Additionally, the intensity of the echo can be measured. With Doppler techniques, comparison of the Doppler shift of the echo with the emitted frequency gives information about any movement of the reflector. The various ultrasound techniques used are described below.

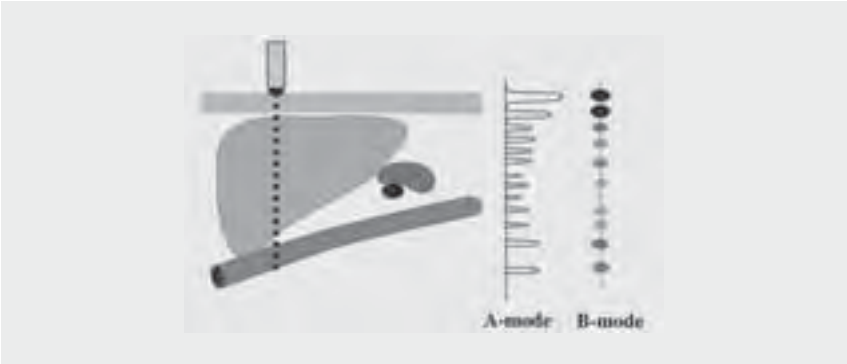
A-mode

A-mode (A-scan, amplitude modulation) is a one-dimensional examination technique in which a transducer with a single crystal is used (Fig. 1.12). The echoes are displayed on the screen along a time (distance) axis as peaks proportional to the intensity (amplitude) of each signal. The method is rarely used today, as it conveys limited information, e.g. measurement of distances.

B-mode

B-mode (brightness modulation) is a similar technique, but the echoes are displayed as points of different grey-scale brightness corresponding to the intensity (amplitude) of each signal (Fig. 1.12).

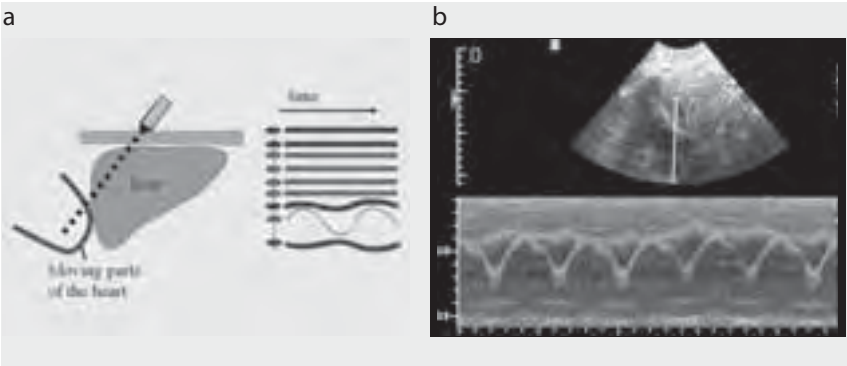
Fig. 1.12. A-mode and one-dimensional B-mode. The peak heights in A-mode and the intensity of the spots in B-mode are proportional to the strength of the echo at the relevant distance



M-mode or TM-mode

M-mode or TM-mode (time motion) is used to analyse moving structures, such as heart valves. The echoes generated by a stationary transducer (one-dimensional B-mode) are recorded continuously over time (Fig. 1.13).

Fig. 1.13. TM-mode. (a) The echoes generated by a stationary transducer when plotted over time form lines from stationary structures or curves from moving parts. (b) Original TM-mode image (lower image) corresponding to the marked region in the B-scan in the upper image (liver and parts of the heart)

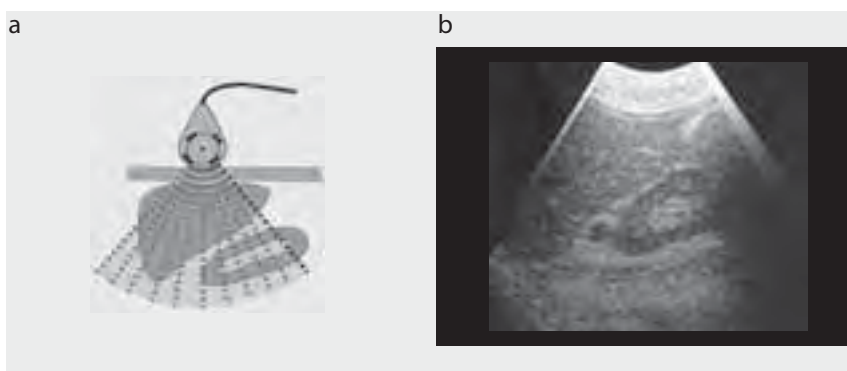


B-scan, two-dimensional

The arrangement of many (e.g. 256) one-dimensional lines in one plane makes it possible to build up a two-dimensional (2D) ultrasound image (2D B-scan). The single lines are generated one after the other by moving (rotating or swinging) transducers or by electronic multielement transducers.

Rotating transducers with two to four crystals mounted on a wheel and swinging transducers ('wobblers') produce a sector image with diverging lines (mechanical sector scanner; Fig. 1.14).

Fig. 1.14. Two-dimensional B-scan. (a) A rotating transducer generates echoes line by line. (b) In this early image (from 1980), the single lines composing the ultrasound image are still visible

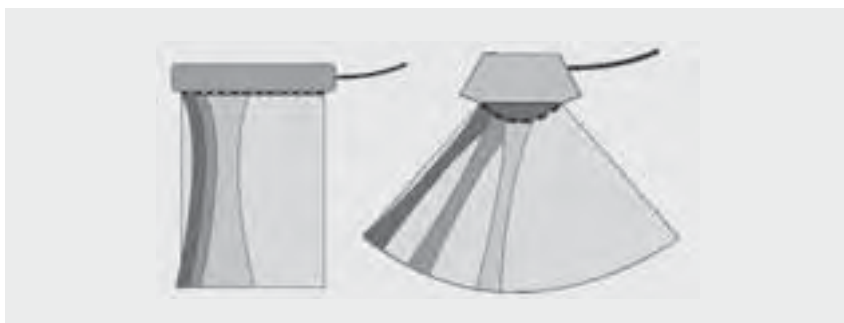


Electronic transducers are made from a large number of separate elements arranged on a plane (**linear array**) or a curved surface (**curved array**). A group of elements is triggered simultaneously to form a single composite ultrasound beam that will generate one line of the image. The whole two-dimensional image is constructed step-by-step, by stimulating one group after the other over the whole array (Fig. 1.15). The lines can run parallel to form a rectangular (linear array) or a divergent image (curved array). The **phased array technique** requires use of another type of electronic multielement transducer, mainly for echocardiography. In this case, exactly delayed electronic excitation of the elements is used to generate successive ultrasound beams in different directions so that a sector image results (electronic sector scanner).

Construction of the image in fractions of a second allows direct observation of movements in real time. A sequence of at least 15 images per second is needed for real-time observation, which limits the number of lines for each image (up to 256) and, consequently, the width of the images, because of the relatively slow velocity of sound. The **panoramic-scan technique** was developed to overcome this limitation. With the use of high-speed image processors, several real-time images are constructed to make one large (panoramic) image of an entire body region without loss of information, but no longer in real time.

A more recent technique is **tissue harmonic imaging**, in which the second harmonic frequencies generated in tissue by ultrasound along the propagation path are used to construct an image of higher quality because of the increased lateral resolution arising from the narrower harmonic beam. The echoes of gas-filled microbubbles

Fig. 1.15. Linear and curved array transducer, showing ultrasound beams generated by groups of elements



(contrast agents) are rich in harmonics as well. Thus microbubbles can be detected by Doppler schemes even in very small vessels with very low flow at the microvascular level (**contrast harmonic imaging**).

Many technical advances have been made in the electronic focusing of array transducers (**beam forming**) to improve spatial resolution, by elongating the zone of best lateral resolution and suppressing side lobes (points of higher sound energy falling outside the main beam). Furthermore, use of complex pulses from wide-band transducers can improve axial resolution and penetration depth. The elements of the array transducers are stimulated individually by precisely timed electronic signals to form a synthetic antenna for transmitting composite ultrasound pulses and receiving echoes adapted to a specific depth. Parallel processing allows complex image construction without delay.

Three- and four-dimensional techniques

The main prerequisite for construction of **three-dimensional (3D)** ultrasound images is very fast data acquisition. The transducer is moved by hand or mechanically perpendicular to the scanning plane over the region of interest.

The collected data are processed at high speed, so that real-time presentation on the screen is possible. This is called the **four-dimensional (4D) technique** ($4D = 3D + \text{real time}$). The 3D image can be displayed in various ways, such as transparent views of the entire volume of interest or images of surfaces, as used in obstetrics and not only for medical purposes. It is also possible to select two-dimensional images in any plane, especially those that cannot be obtained by a 2D B-scan (Fig. 1.16).

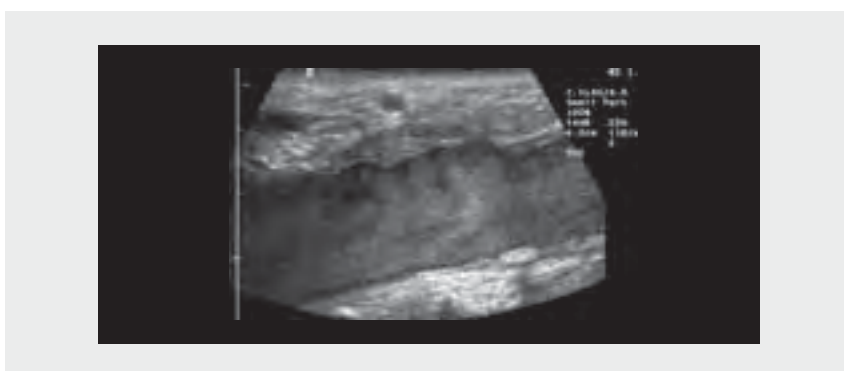
B-flow

B-flow is a special B-scan technique that can be used to show movement without relying upon the Doppler effect. The echoes from moving scatterers (particularly blood cells in blood vessels) are separated from stationary scatterers by electronic comparison of echoes from successive pulses (autocorrelation). These very weak echoes are amplified and depicted as moving dots on the screen. This technique is effective in showing the inner surface of blood vessels, but, unlike Doppler methods (see below), it provides no information about flow velocity (Fig. 1.17).

Fig. 1.16. 3D ultrasound image of the liver. The 3D data collected (left, image 3) can provide 2D sections in different planes (right, images 1, 2 and 4)



Fig. 1.17. B-flow image of an aorta with arteriosclerosis. This technique gives a clear delineation of the inner surface of the vessel (+...+ measures the outer diameter of the aorta)



Doppler techniques

In these techniques, the **Doppler effect** (see above) is used to provide further information in various ways, as discussed below. They are especially important for examining blood flow.

Continuous wave Doppler

The transducer consists of two crystals, one permanently emitting ultrasound and the other receiving all the echoes. No information is provided about the distance of the reflector(s), but high flow velocities can be measured (Fig. 1.18).

Pulsed wave Doppler

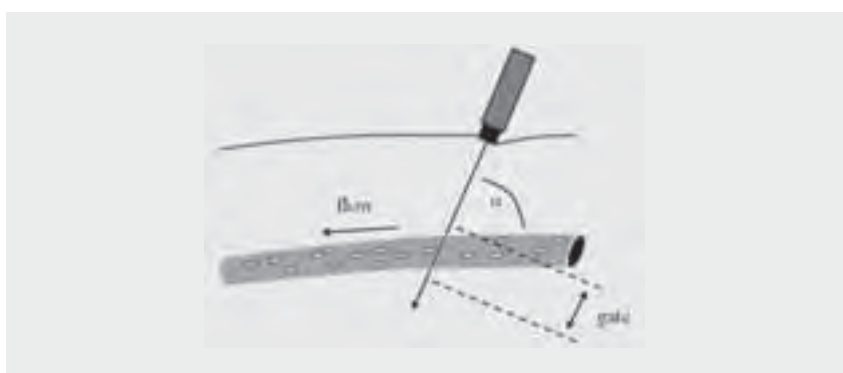
In this technique, ultrasound is emitted in very short pulses. All echoes arriving at the transducer between the pulses in a certain time interval (termed the gate) are registered and analysed (Fig. 1.19). A general problem with all pulsed Doppler techniques is the analysis of high velocities: the range for the measurement of Doppler frequencies is

limited by the pulse repetition frequency (PRF). When the Doppler frequency is higher than the pulse repetition frequency, high velocities are displayed as low velocities in the opposite direction (spectral Doppler) or in the wrong colour (colour Doppler). This phenomenon is known as 'aliasing' and is directly comparable to the effect seen in movies where car wheels rotating above a certain speed appear to be turning backward. A correct display is possible only for Doppler frequencies within the range \pm one half the pulse repetition frequency, known as the **Nyquist limit**. As a consequence, Doppler examination of higher velocities requires lower ultrasound frequencies and a high pulse repetition frequency, whereas low velocities can be analysed with higher frequencies, which allow better resolution.

Fig. 1.18. Schematic representation of the principle of continuous wave Doppler



Fig. 1.19. Schematic representation of pulsed wave Doppler. The gate is adjusted to the distance of the vessel and the echoes within the gate are analysed (the Doppler angle α is 55° in this example)

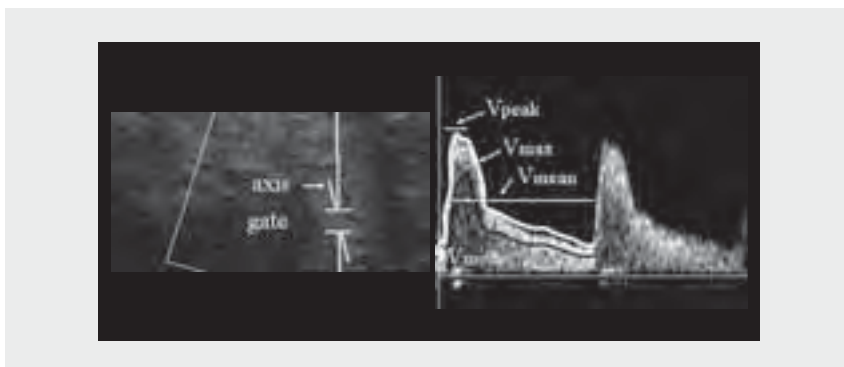


Spectral Doppler

The flow of blood cells in vessels is uneven, being faster in the centre. Doppler analysis, therefore, shows a spectrum of different velocities towards or away from the transducer, observed as a range of frequencies. All this information can be displayed together on the screen. The velocity is displayed on the vertical axis. Flow towards the transducer is positive (above the baseline), while flow away is negative (below the baseline). The number of signals for each velocity determines the brightness of the corresponding point on the screen. The abscissa corresponds to the time base. The **spectral Doppler**

approach combined with the B-scan technique is called the **duplex technique**. The B-scan shows the location of the vessel being examined and the angle between it and the ultrasound beam, referred to as the Doppler angle. This angle should always be less than 60° , and if possible around 30° , to obtain acceptable results. The integrated display demonstrates the detailed characteristics of the flow. The combination of B-scan with colour Doppler and spectral Doppler is called the **triplex technique** (Fig. 1.20).

Fig. 1.20. Spectral Doppler, triplex technique. The upper B-scan shows the vessel, the Doppler angle (axis arrow) and the gate. The lower part of the image shows the spectrum of the velocities over time (two cycles). Note the different velocities: peak velocity in systole (V_{peak}), maximal velocity over time (V_{max} , white plot), most frequent velocity (V_{mode} , black plot) and average velocity (V_{mean}).



Additionally, the cross-section of the vessel can be determined from the image. The volume blood flow (Vol) can then be calculated by multiplying the cross-section (A) by the average (over time and across the vessel) flow velocity (TAV_{mean}):

$$Vol = A \cdot TAV_{\text{mean}} \quad (1.7)$$

However, measurement of the cross-section and the Doppler angle, which affects the calculated flow velocity, is difficult and often imprecise.

The velocity curves in a Doppler display yield indirect information about the blood flow and about the resistance of the vessel to flow. Highly resistant arteries show very low flow or even no flow in late diastole, whereas less resistant arteries show higher rates of end-diastolic flow. Indices that are independent of the Doppler angle can be calculated to characterize the flow in the vessels, showing the relation between the systolic peak velocity (V_{max}) and the minimal end-diastolic flow (V_{min}). The commonest index used is the **resistance index (RI)**:

$$RI = \frac{(V_{\text{max}} - V_{\text{min}})}{V_{\text{max}}} \quad (1.8)$$

The **pulsatility index (PI)** is another common index used to characterize oscillations in blood flow, including the time-averaged maximal velocity (TAV_{\max}):

$$PI = \frac{(V_{\max} - V_{\min})}{TAV_{\max}} \quad (1.9)$$

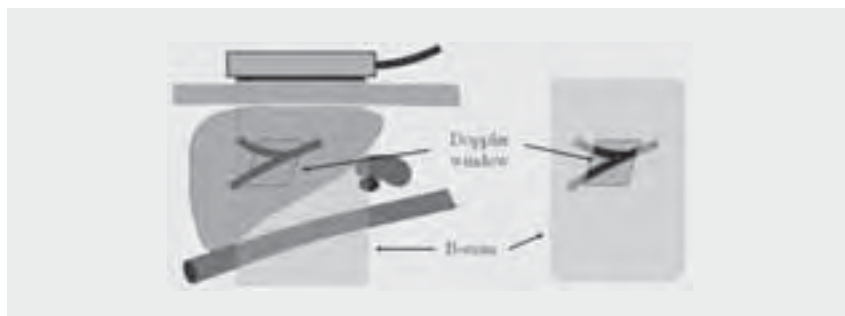
Narrowing of a vessel (stenosis) causes acceleration of the flow within the stenotic section (in a closed system), and post-stenotic turbulence is seen as ‘spectral broadening’ on a spectral Doppler display. The grade of the stenosis (St) (as a percentage) can be estimated from the calculated average flow velocity before (V_1) and within (V_2) the stenotic section of the vessel using the formula:

$$St = 100(1 - \frac{V_1}{V_2}) \quad (1.10)$$

Colour Doppler and **power Doppler** displays are used as duplex systems integrated into the B-scan image.

Colour Doppler (CD) imaging displays the average blood velocity in a vessel, based on the mean Doppler frequency shift of the scatterers (the blood cells). The echoes arising from stationary reflectors and scatterers are displayed as grey-scale pixels to form the B-scan image. The echoes from moving scatterers are analysed by the Doppler technique separately in a selected window and are displayed in the same image as colour-coded pixels (Fig. 1.21). The direction of the flow is shown by different colours, usually red and blue. The disadvantages of colour Doppler are the angle dependence and aliasing artefacts.

Fig. 1.21. Colour Doppler. The echoes from moving targets (blood cells) within the window are colour-coded and depicted here in black (see also Fig. 4.11)



Power Doppler (PD, also known as **colour Doppler energy** or **ultrasound angiography**) is based on the total integrated power of the Doppler signal. In general, it is up to five times more sensitive in detecting blood flow than colour Doppler, being in particular more sensitive to slow blood flow in small vessels; however, it gives no information about the direction of flow.

Contrast agents

The echoes from blood cells in the vessels are much weaker than those arising in tissue. Therefore, contrast agents administered intravenously into the systemic circulation were initially used to obtain stronger signals from blood flow. These agents are microbubbles, which are more or less stabilized or encapsulated gas bubbles, and are somewhat smaller than red blood cells. Use of these contrast agents considerably improves the visibility of small vessels and slow flow with colour and power Doppler. However, the most important advantage of contrast agents is that they allow a more detailed image of the static and dynamic vascularity of organs or tumours. Analysis of the appearance of the contrast agents in the early phase after application (fill-in) and later (wash-out) shows characteristic patterns of various tumours (dynamic enhancement pattern), and enables their differentiation. Another benefit is that the contrast between lesions and the surrounding normal tissue may increase because of their different vascularity. Thus, small lesions, which are not seen in conventional ultrasound images because of their low contrast, become visible.

Special software programmes and equipment are needed when contrast agents are used. Contrast harmonic imaging is a technique similar to tissue harmonic imaging (see above) for improving the signals from microbubbles.

Artefacts

Artefacts are features of an ultrasound image that do not correspond to real structures, i.e. they do not represent a real acoustic interface with regard to shape, intensity or location (Table 1.1, Table 1.2, Fig. 1.22, Fig. 1.23, Fig. 1.24, Fig. 1.25, Fig. 1.26, Fig. 1.27, Fig. 1.28, Fig. 1.29, Fig. 1.30, Fig. 1.31, Fig. 1.32). Features that result from incorrect adjustment of the instrument settings are, by this definition, not true artefacts.

Artefacts may adversely affect image quality, but they are not difficult to recognize in the majority of cases. In certain situations, they hamper correct diagnosis (e.g. cysts) or lead to false diagnosis of a pathological condition where none exists. In other cases, they may actually facilitate diagnosis (e.g. stones).

Table 1.1. Common B-scan artefacts

Term/origin	Appearance	Diagnostic significance
Acoustic shadow (see Fig. 1.22, Fig. 1.23): total reflection on a strong reflector (gas, foreign body) or extensive absorption (bones)	Echo-free zone behind the interface, a complete shadow . Less than total weakening of the ultrasound causes an incomplete shadow . Echoes from behind the interface are still seen but appear very weak. Shadows behind gas often show a second superimposed artefact ('dirty shadow').	Limits the examination of body regions behind gas or bones but is useful for diagnosing stones, calcifications or foreign bodies.
Tangential artefact (lateral shadow) : total lateral deflection of the sound beam onto the sides of smooth structures (cysts, vessels)	Small, echo-free, dark zone behind both flanks of such a structure, like a shadow	Regarded as a sign of a cyst or a benign tumour with a capsule
Echo enhancement (acoustic enhancement) (Fig. 1.24): structures that attenuate ultrasound less than the surrounding tissue lead to over-amplification of the echoes behind.	Echoes behind such structures appear too bright.	Regarded as a sonographic symptom of a cystic lesion but sometimes also seen behind benign and malignant tumours
Reverberation (Fig. 1.25): echoes are reflected partially by interfaces on their way back (internal reflections) or at the surface of the transducer itself. The echo is then reflected for a second time at the interface of its origin but twice the time is needed before it is recorded by the transducer. This may occur several times, the echoes becoming weaker after each reflection.	The structures that cause internal reflections are displayed two or more times at double or multiple distances from the transducer, always in the same order as the original structures, but weaker.	These echoes become especially conspicuous in echo-free areas close to the transducer (bladder, gallbladder, cysts). As they occur mainly in the abdominal wall, they can be identified, because they do not move with the abdominal structures during breathing.
Mirror artefact (Fig. 1.26): a strong smooth reflector reflects the beam to the side, where it causes further reflections or back-scatter. These echoes follow the same path back to the transducer and are wrongly displayed in straight extension of the original beam direction (a special type of internal reflection or reverberation).	These artefacts are seen only in echo-free areas. Structures of the liver seen above the diaphragm (the surface of the air-filled lung acting as the mirror) are a typical example.	An image or lesion of the liver or the kidney may, for example, be seen above the diaphragm and be misinterpreted as a lesion of the lung.
Comet tail artefact (or ring-down artefact) (Fig. 1.27): if two interfaces lie close together, they can cause many internal reflections at very short intervals and send a large number of echoes back to the transducer.	In the ultrasound image, a small bright 'tail' is seen behind these interfaces, sometimes for only a very short time.	This artefact is typical of a group of small air bubbles ('dirty shadow') and of the wall of the gallbladder in cholesterosis. It also occurs behind puncture needles if their angle to the ultrasound beam is around 90°.
Partial volume effect (Fig. 1.28): if an ultrasound beam hits a cyst smaller than the beam cross-section, the echoes from the wall appear to come from inside the cyst (artificial sedimentation).	Small cystic lesions show echoes inside.	Small cysts may be misinterpreted as solid lesions.
Overpenetration : the bladder and other large fluid-filled structures do not attenuate the ultrasound pulses. They can generate reflections beyond the selected depth that return late or only after the next pulse. These echoes are displayed in the image as if generated by the second pulse.	Echoes appear within a normally echo-free area, such as the bladder.	Such wrong echoes, called 'ghost echoes', must be distinguished from real echoes by changing the scan direction.
Velocity artefact (Fig. 1.29): if an ultrasound beam passes through a structure with a considerably higher sound velocity (e.g. cartilage), echoes from structures beyond are displayed closer to the transducer.	Structures behind tissues with higher sound velocity are distorted in the ultrasound image.	The border of the lung appears to undulate behind the ribs due to such distortion.

Table 1.2. Common disturbances and artefacts in Doppler techniques

Term/origin	Appearance	Diagnostic significance
Tissue vibration (bruit): restriction of blood flow by a stenosis or by an arteriovenous fistula causes vibrations of the surrounding tissue, which are transmitted by the pulsating blood pressure.	Disseminated colour pixels in the tissue around a stenosis.	Indication of a severe stenosis
Flash: corresponds to the vibration artefact. The pulsation of the heart is transmitted to the adjacent structures, e.g. the cranial parts of the liver.	A short but intense colour coding of all pixels within the Doppler window during systole	Disturbs examination of the vessels in the region close to the heart
Blooming (Fig. 1.30): amplification of the signals causes 'broadening' of the vessels.	The area of colour-coded pixels is broader than the diameter of the vessel.	Blurred border of the vessel and inaccurate demarcation of the inner surface of the wall
Twinkling (Fig. 1.31): caused by certain stones, calcifications and foreign bodies with a rough surface.	Colour-coded stones or calcifications with a mosaic-like pattern	Sometimes helpful for detecting small kidney stones
Change of angle of incidence: the ultrasound beam impinges on a vessel running across the scanning plane at different angles.	Despite a constant flow velocity in one direction, the signals from the vessel are displayed in different colours depending on the angle between the vessel and the ultrasound beam. If it is 'hidden' at an angle of 90° , no coloured pixel is seen.	The inhomogeneous depiction of the vessel is not an artefact but a correct depiction, depending on the actual angle of each part of the image.

Fig. 1.22. (a) Several gallstones (arrow) cause a complete acoustic shadow (S), whereas a small 4-mm gallstone (b) causes only an incomplete shadow (S). The small shadow in (b) at the edge of the gallbladder (arrow) corresponds to a tangential artefact (see Fig. 1.24)

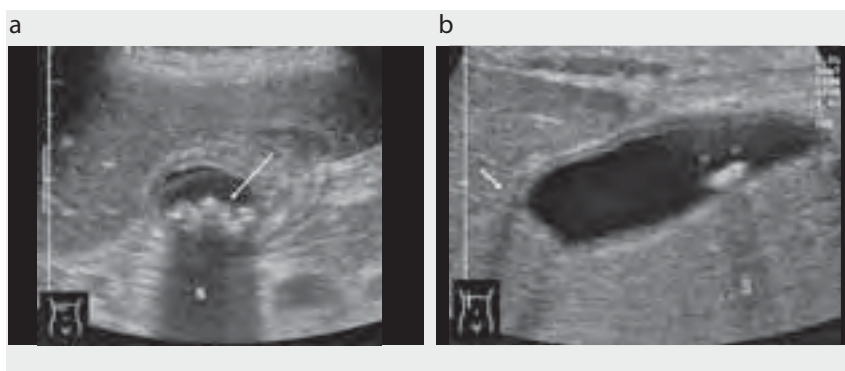


Fig. 1.23. Air bubbles cause 'dirty' shadows. (a) Gas in an abscess (arrow) causes a strong echo, a shadow and reverberation artefacts, which superimpose the shadow (A, abscess; I, terminal ileum). (b) Air in the jejunum causes a 'curtain' of shadows and reverberation artefacts, which cover the whole region behind the intestine

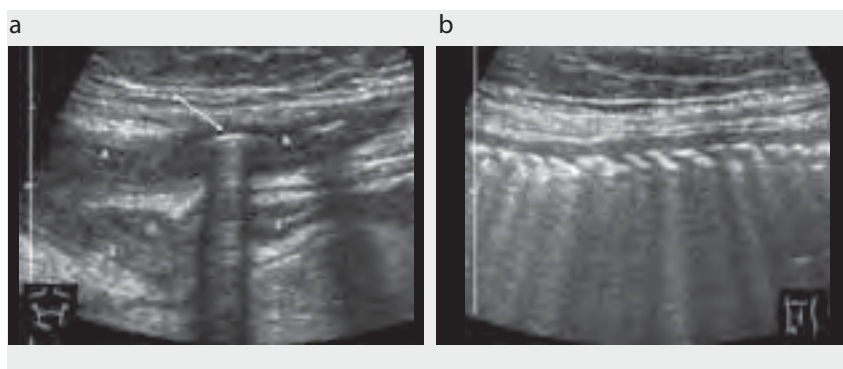


Fig. 1.24. A small cyst in the liver causes two artefacts. A brighter zone behind the cyst is caused by echo enhancement, whereas slight shadows on both sides of this zone are tangential artefacts due to the smooth border of the cyst



Fig. 1.25. Reverberation artefacts. (a) A 'cloud' of small artefacts (arrow) is seen in the gallbladder. (b) The structures between the wall and the border of the air (1) are repeated several times behind this border (2)

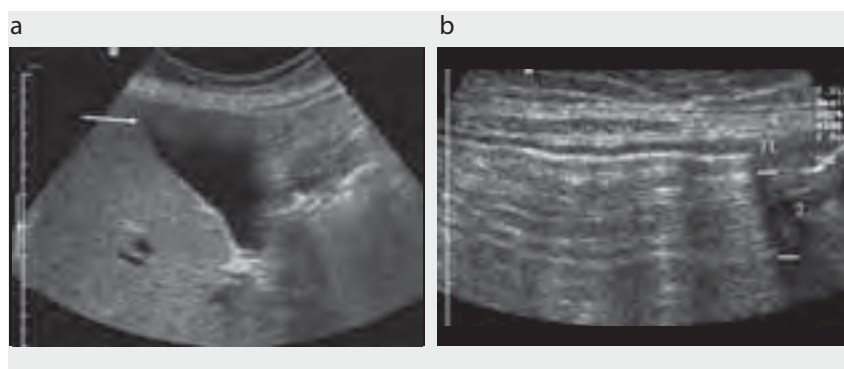


Fig. 1.26. Mirror artefact. The air-containing lung behind the diaphragm reflects all the ultrasound pulses. (a) Structures of the liver are seen behind this border (arrow) as artefacts. (b) The cross-section of a vessel indicates the direction of the original pulse reflected by this mirror (arrow). The echoes from the path between the mirror and the vessel and back are depicted falsely along a straight line (dotted line) behind the diaphragm

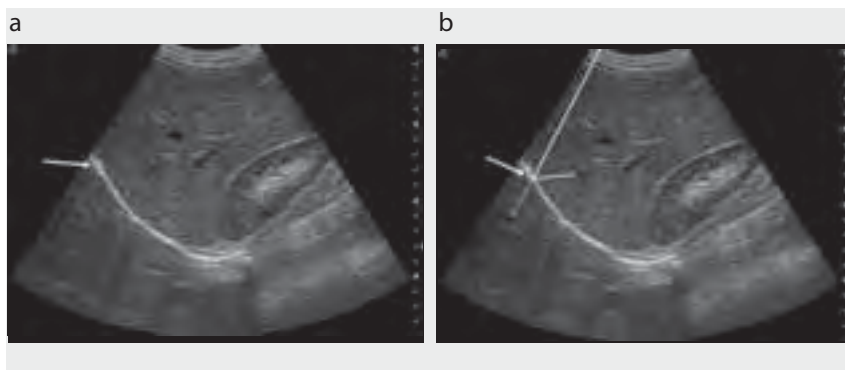


Fig. 1.27. Comet tail (or ring-down) artefact. The small artefacts (broad open arrow) are typical of cholesterosis of the gallbladder (see Fig. 8.17). A shadow (S) is caused by a gallstone (thin arrow)

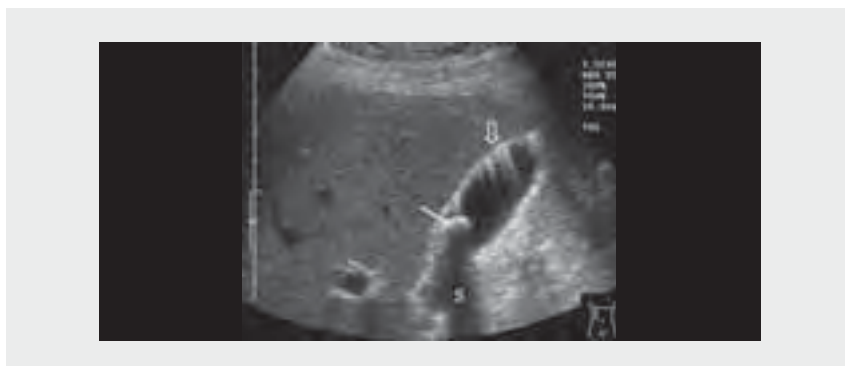


Fig. 1.28. Partial volume effect. (a) The cyst (c) is smaller than the diameter of the ultrasound beam. The beam generates weak echoes from the wall, which are depicted within the cyst. (b) These artefacts are seen in two small cysts (arrows) of the right kidney (RN). The other larger cysts (z) are echo free. The lesion (T) at the lower pole is a true echo-poor small carcinoma. This image illustrates very well the diagnosis problems that are sometimes caused by artefacts

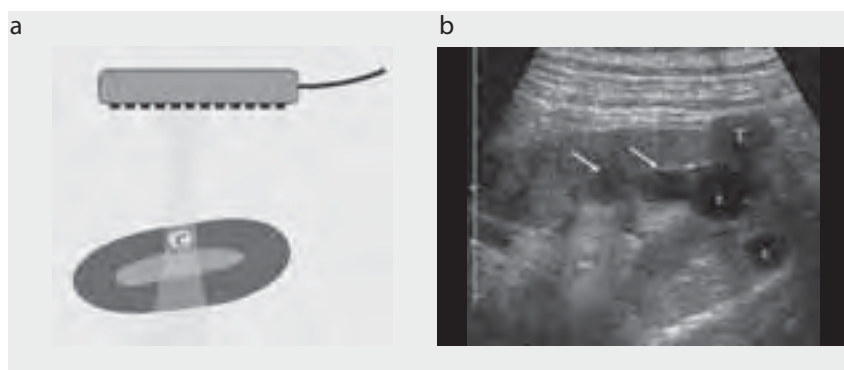


Fig. 1.29. Velocity artefact. The higher sound velocity in the cartilage (car) of the ribs causes distortion of the echoes at the border of the lung (arrows), so that the contour appears to be undulating (see also Fig. 5.2; int, intercostal muscles)

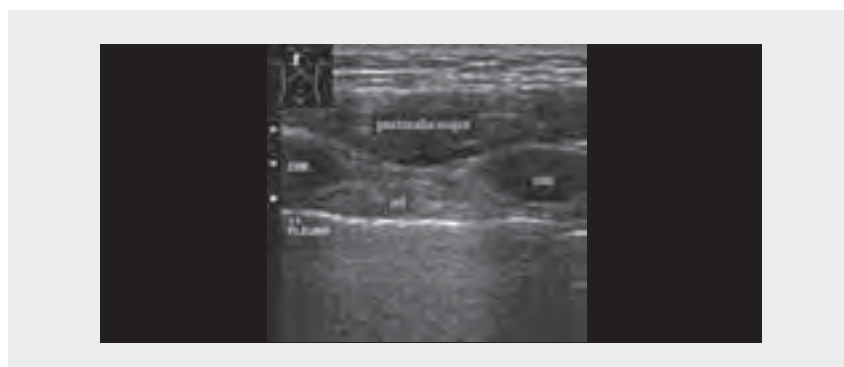


Fig. 1.30. Blooming: (a) the colour-coded signals (white and black) show a wider diameter of the splenic vessel than that correctly measured by B-scan (b)

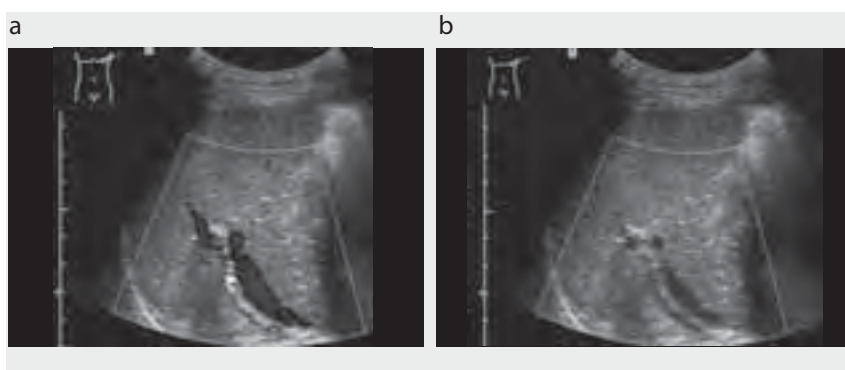


Fig. 1.31. 'Twinkling'. (a) B-scan shows a strong echo of a renal stone and an incomplete shadow (arrow). (b) With colour Doppler, the stone (arrow) is colour-coded with a mosaic-like multicoloured pattern (here black and white spots)

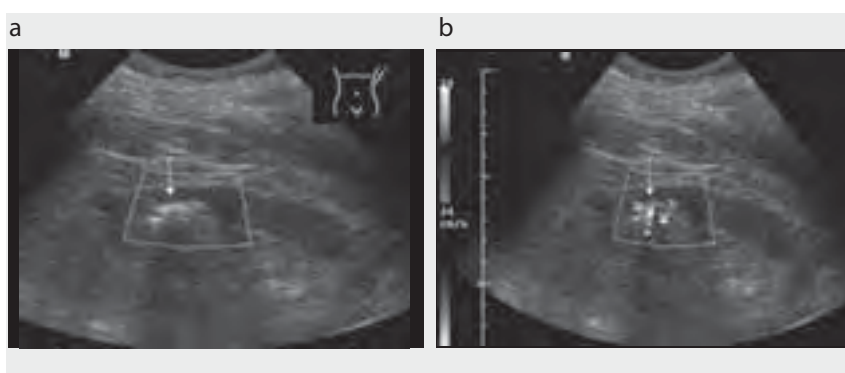


Fig. 1.32. Change of angle of incidence. The curved vessel (iliac artery) is oriented at different angles with respect to the ultrasound beam (thick arrows). The constant flow in one direction (thin arrows) is Doppler-coded red in some sections (seen here as white) and blue in others (black arrows)



Adverse effects

The kinetic energy of ultrasound waves can cause adverse effects in tissue. Non-thermal effects include cavitation, direct mechanical damage to cells by acceleration, movement of particles in fluid (acoustic streaming) and aggregation of particles or cells. Cavitation is the formation of voids, or bubbles, in a biological structure during the rarefaction phase of a sound wave. These bubbles may grow with changes in pressure or collapse during the positive pressure phase. The risk of cavitation is low at the ultrasound intensities used in medical diagnosis. Furthermore, diagnostic ultrasound is applied in very short pulses. Nevertheless, as very small gas bubbles may serve as cavitation centres, the recent introduction of microbubble contrast agents has stimulated and renewed discussion about this phenomenon.

Direct mechanical damage to cell membranes, the occurrence of high temperatures or formation of free radicals may also occur. However, the Committee on Ultrasound Safety of the World Federation for Ultrasound in Medicine and Biology has stated that no adverse biological effects have been seen in the large number of studies that have been carried out to date. A **mechanical index** has been introduced to indicate the relative risk for adverse biological effects resulting from mechanical effects during an ultrasound examination. This index is calculated in real time by the ultrasound equipment and displayed so that the operator is aware of any risk.

The generation of heat in tissues is an important limiting factor in the diagnostic use of ultrasound. The temperature rise in tissue depends on the absorbed ultrasound energy and the volume within which the absorption occurs. The energy absorbed is therefore higher with stationary ultrasound emitters (transducer fixed, e.g. Doppler, TM-mode) than with scanning methods (transducer moved during examination, e.g. B-scan). Furthermore, the thermal effect is reduced by convection, especially in the bloodstream. The embryo is particularly sensitive to long exposure to ultrasound, especially during prolonged Doppler examinations.

The **thermal index** (TI) is displayed in real time as an indication of the maximum temperature rise that may occur in a tissue during a prolonged ultrasound examination. Depending on the method used, the appropriate index to use is specified as:

- TIS for superficial tissue (e.g. the thyroid or the eyes); this indicator can also be used for endoscopic ultrasound;
- TIC for superficial bones (e.g. examination of the brain through the skull);
- TIB for bone tissue in the ultrasound beam (e.g. examination of a fetus).

Ultrasound that produces a rise in temperature of less than 1 °C above the normal physiological level of 37 °C is deemed without risk by the Committee on Ultrasound Safety of the World Federation for Ultrasound in Medicine and Biology.

For more details see chapter on Safety in Volume 2 of this manual.

Examination technique: general rules and recommendations

Range of application	29
General indications (B-scan and duplex techniques)	29
Preparation	30
Positioning	30
Coupling agents	30
Equipment	31
Adjustment of the equipment	31
Guidelines for the examination	34
Documentation	36
Interpretation of the ultrasound image	36
40	Duplex technique

Examination technique: general rules and recommendations

Range of application

All body regions that are not situated behind expanses of bone or air-containing tissue, such as the lungs, are accessible to transcutaneous ultrasound. Bone surfaces (fractures, osteolytic lesions) and the surfaces of the lungs or air-void parts can also be demonstrated. Examinations through thin, flat bones are possible at lower frequencies. It is also possible to bypass obstacles with endoprobes (endoscopic sonography). Thus, transcutaneous ultrasound is used mainly for evaluating:

- neck: thyroid gland, lymph nodes, abscesses, vessels (angiology);
- chest: wall, pleura, peripherally situated disorders of the lung, mediastinal tumours and the heart (echocardiography);
- abdomen, retroperitoneum and small pelvis: parenchymatous organs, fluid-containing structures, gastrointestinal tract, great vessels and lymph nodes, tumours and abnormal fluid collections; and
- extremities (joints, muscles and connective tissue, vessels).

General indications (B-scan and duplex techniques)

The general indications are:

- presence, position, size and shape of organs;
- stasis, concretions and dysfunction of hollow organs and structures;
- tumour diagnosis and differentiation of focal lesions;
- inflammatory diseases;
- metabolic diseases causing macroscopic alterations of organs;
- abnormal fluid collection in body cavities or organs, including ultrasound-guided diagnostic and therapeutic interventions;
- evaluating transplants;
- diagnosis of congenital defects and malformations.

Additionally, ultrasound is particularly suitable for checks in the management of chronic diseases and for screening, because it is risk-free, comfortable for patients and cheaper than other imaging modalities.

Preparation

In general, no preparation is needed for an ultrasound examination; however, for certain examinations of the abdomen, a period of fasting is useful or necessary. To avoid problems due to meteorism, dietary restrictions (no gas-producing foods), physical exercise (walking before the examination) and even premedication (antifoaming agents) are recommended. Special preparation is only necessary for certain examinations and these are discussed in the relevant chapters of this manual.

Positioning

The ultrasound examination is usually carried out with the patient in the supine position. As further described in the specific chapters, it is often useful to turn the patient in an oblique position or to scan from the back in a prone position, e.g. when scanning the kidneys. Ultrasound also allows examination of the patient in a sitting or standing position, which may help in certain situations to diagnose stones or fluid collection (e.g. pleural effusion).

Coupling agents

A coupling agent is necessary to ensure good contact between the transducer and the skin and to avoid artefacts caused by the presence of air between them. The best coupling agents are water-soluble gels, which are commercially available. Water is suitable for very short examinations. Disinfectant fluids can also be used for short coupling of the transducer during guided punctures. Oil has the disadvantage of dissolving rubber or plastic parts of the transducer.

The composition of a common coupling gel is as follows:

- 10.0 g carbomer
- 0.25 g ethylenediaminetetraacetic acid (EDTA)
- 75.0 g propylene glycol
- 12.5 g triethanolamine and up to 500 ml demineralized water.

Dissolve the EDTA in 400 ml of water. When the EDTA has dissolved, add the propylene glycol. Then add the carbomer to the solution and stir, if possible with a high-speed stirrer, until the mixture forms a gel without bubbles. Add up to 500 ml of demineralized water to the gel.

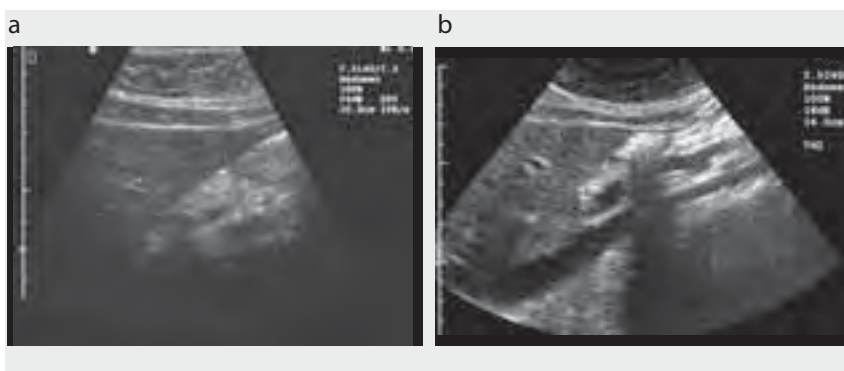
Precaution: Be careful not to transmit infectious material from one patient to the next via the transducer or the coupling gel. The transducer and any other parts that come into direct contact with the patient must be cleaned after each examination. The minimum requirements are to wipe the transducer after each examination and to clean it with a suitable disinfectant every day and after the examination of any patient who may be infectious.

A suitable method for infectious patients, e.g. those infected with human immunodeficiency virus (HIV) and with open wounds or other skin lesions, is to slip a disposable glove over the transducer and to smear some jelly onto the active surface of the transducer.

Equipment

Generally, modern ultrasound equipment consists of 'all-round scanners'. Two transducers, usually a curved array for the range 3–5 MHz and a linear array for the range greater than 5 MHz to 10 MHz, as a 'small-part scanner' can be used as 'general-purpose scanners' for examination of all body regions with the B-scan technique (Fig. 2.1).

Fig. 2.1. Choice of transducer and frequency. Generally, superficial structures are examined at 7.5 MHz; however, this frequency is not in general suitable for abdominal work and is limited to examination of superficial structures. (a) At 7.5 MHz, only the ventral surface of the liver can be displayed. (b) The liver and the adjacent structures can be examined completely at 3.5 MHz



Examinations of the skin and eyes and the use of endoprobes require special transducers and more expensive equipment to enable the use of higher frequencies. For echocardiography, different transducers, i.e. electronic sector scanners (phased array technique) are required.

An integrated Doppler technique is necessary for echocardiography and angiology, and is also useful for most other applications. Special software is needed for the use of contrast agents.

Adjustment of the equipment

Correct adjustment of an ultrasound scanner is not difficult, as the instruments offer a wide range of possible settings. Most instruments have a standard setting for each transducer and each body region. This standard can be adapted to the needs of each operator.

When starting with these standards, only slight adaptation to the individual patient is necessary.

- The choice of frequency (and transducer) depends on the penetration depth needed. For examination of the abdomen, it may be useful to start with a lower frequency (curved array, 3.5 MHz) and to use a higher frequency if the region of interest is close to the transducer, e.g. the bowel (Fig. 2.1, Fig. 11.26).
- Adaptation to the penetration depth needed: the whole screen should be used for the region of interest (Fig. 2.2).
- The mechanical index should be as low as possible (< 0.7 in adults).

- The time gain compensation (TGC) setting must compensate for attenuation, e.g. depending on the abdominal wall, to obtain a homogeneous image. It is useful to find a good TGC setting when scanning a homogeneous section of the tissue, e.g. the right liver lobe in the abdomen, before moving the transducer to the region of interest (Fig. 2.3, Fig. 2.4, Fig. 2.5).
- The focus, or zone of best resolution, should always be adjusted to the point of interest.

Fig. 2.2. Use of the screen. (a) Incorrect adaptation of the screen: the region of interest fills only a small part of the screen. (b) Correct adaptation of the screen

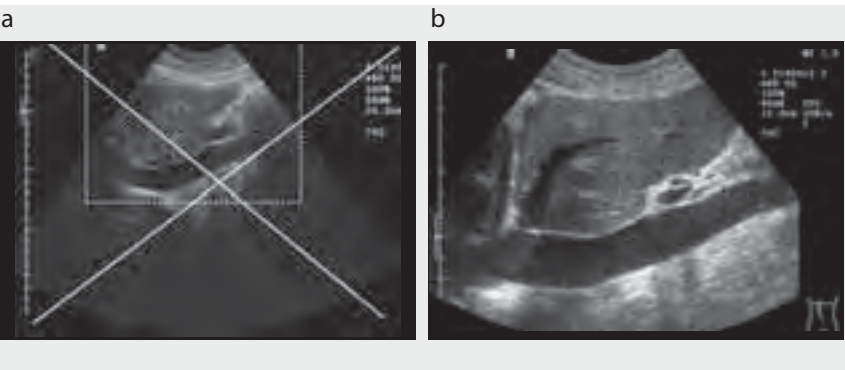


Fig. 2.3. (a) Operating console of an ultrasound machine. Control knobs must be adjusted for each patient. R (range), penetration depth; F (focus), region of best resolution; TGC, time (depth) gain compensation (see Fig. 2.4); Z (zoom), enlarges regions of interest; G, Doppler gain; V, Doppler velocity (pulse repetition frequency). (b) B-image (not the same equipment as in (a)), shows correct (homogeneous pattern of normal liver tissue), TGC curve (arrow) and focus zone, which should be slightly deeper and level with the focal nodular hyperplasia lesion. The thermal index (TIS) and the mechanical index (MI) are indicated. Note that these indices are considerably higher in the colour Doppler image (B-scan 0.6 and 0.5, respectively, versus Doppler 2.3 and 0.8). (c) The Doppler velocity and the Doppler window are correctly adjusted to the size of the lesion and the expected velocity range in the vessels

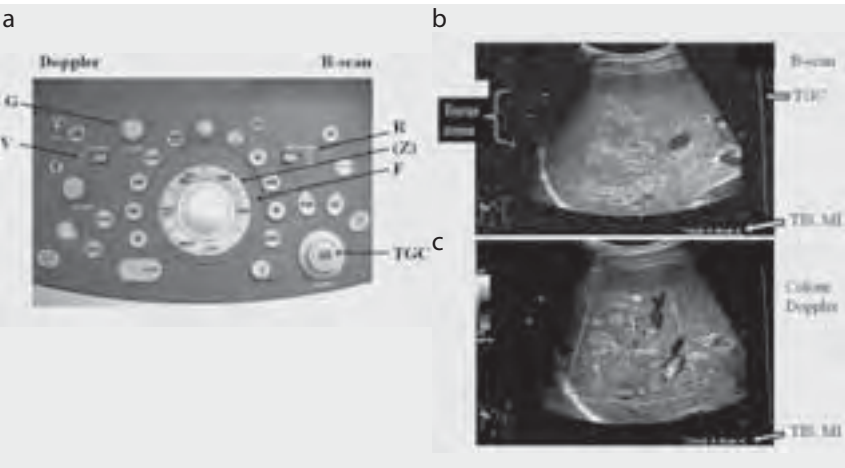


Fig. 2.4. Time gain compensation (TGC). The TGC is always adjusted according to each patient's circumstances. (a) An overall gain in compensation (B-mode: gain) and gradual regulation are possible. (b) The loss of intensity, or decline in the echoes at a greater distance, is compensated for by the TGC, as shown in the diagram and (c) the ultrasound image with the displayed TGC line (arrow) for 3.5 MHz. This compensation is not sufficient for 7 MHz (see Fig. 2.1)

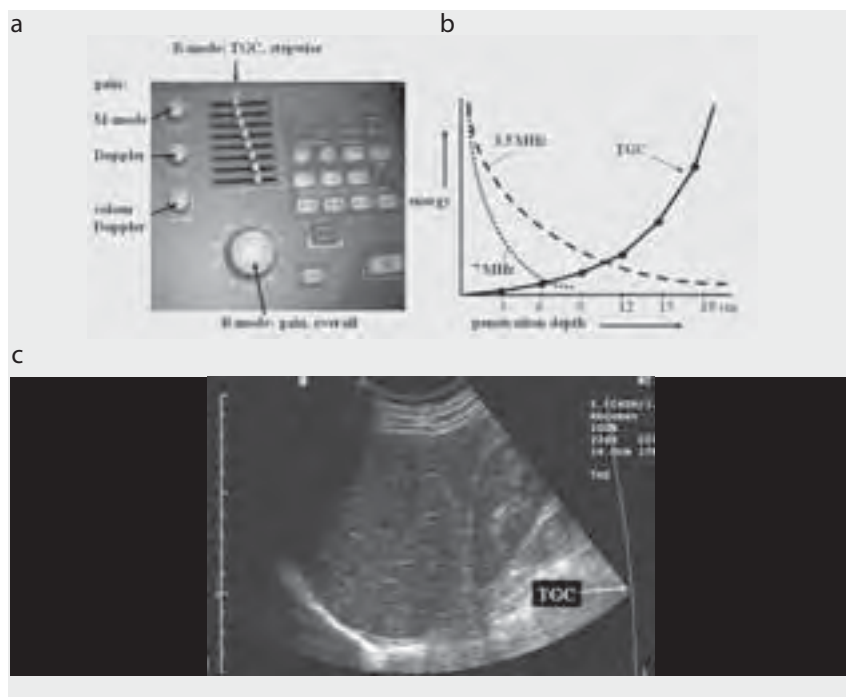
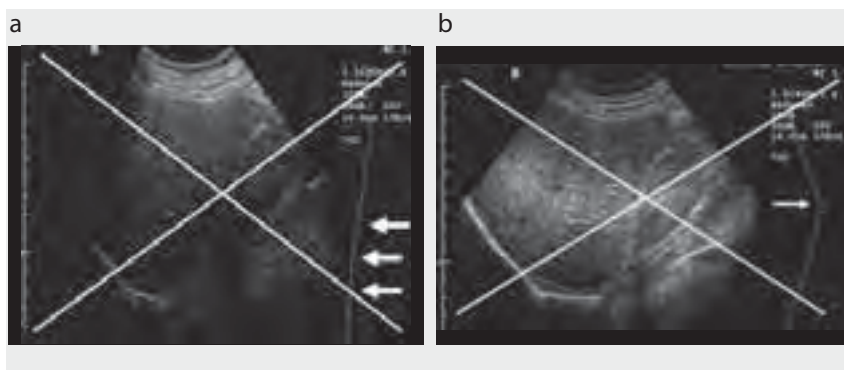


Fig. 2.5. TGC adjustment. Two examples of incorrect adjustment: (a) The lower part of the ultrasound image is too dark because the TGC adjustment is too weak, whereas in (b) the adjustment for the middle part is too high, causing an inhomogeneous image of the liver with a zone that is too bright in the middle part



- The zoom should be used mainly for the final investigation of detail and for preparing the documentation.
- If there are problems, use of the image optimizer knob and returning to the standard settings may help.

Guidelines for the examination

- Know the patient's problem and medical history. An advantage of ultrasound is that the patient's doctor can carry out the examination, and this provides a good opportunity to talk to the patient about his or her problem.
- Make sure that the settings of the equipment and the orientation of the transducer are correct in relation to the image. This will avoid misinterpretations due to inhomogeneous images with areas that are too dark or too bright and with artefacts.
- Conduct a systematic and complete examination of the whole body region, even if there is an obvious palpable mass or a localized point of pain.
- Start with an anatomically constant area and move to the more variable area (e.g. from the liver to the region of the pancreas or the intestine).
- Move the transducer in a slow constant pattern, while maintaining the defined scanning plane. Hold the transducer motionless when the patient moves, e.g. during respiration. It is possible to move a transducer in many directions by tilting it in the scanning plane and moving it perpendicularly, but with a combination of all these movements the less experienced operator will lose the orientation of the image (Fig. 2.6, Fig. 2.7).
- Use anatomically constant, easily visualized structures for orientation (e.g. liver, aorta or fluid-filled bladder) and normal structures for comparison (e.g. right and left kidney or kidney and liver).
- Examine each organ, structure or tumour in at least two planes. **In this way, one can avoid missing small lesions or misinterpreting artefacts as real alterations.**
- Use palpation to displace fluid or gas from the bowel, to test the consistency of tumours and organs and to localize points of pain.
- Continue the entire examination even if pathological conditions are found. Only a complete examination will avoid that only a less important alteration (e.g. gallstones) is found but the main diagnosis (e.g. pancreatic cancer) is missed.
- In clinically difficult situations or when the findings are doubtful, repeat the examination a short time later. Such repeat examinations can be carried out even at the bedside. This is particularly useful with trauma patients and patients in intensive care.

Fig. 2.6. Movements of a transducer. The transducer can be moved in its scanning plane in a longitudinal direction (a), turned about itself (b), or tilted in the scanning plane (c) or in a perpendicular direction (d)

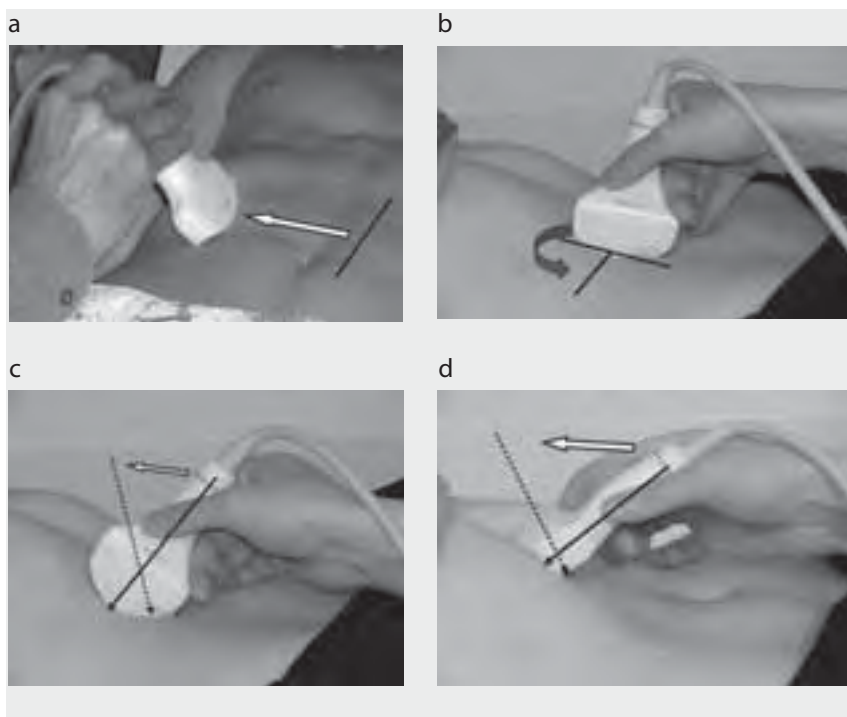
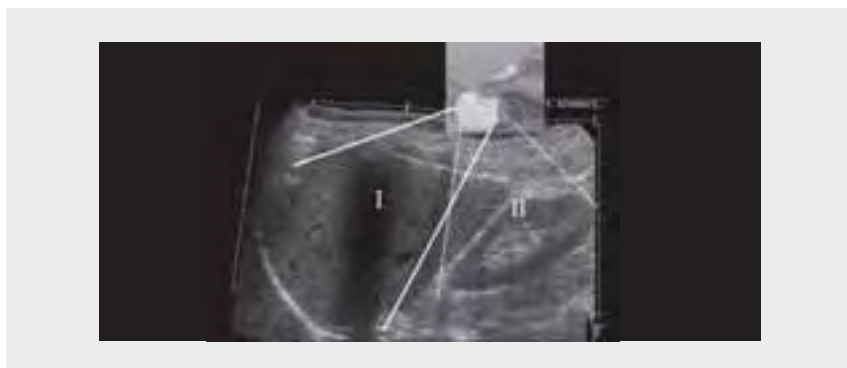


Fig. 2.7. Imaging of the right liver lobe and the right kidney obtained by tilting the transducer in different directions (I and II)



Documentation

As a rule, both a written report and pictorial documentation should be prepared for each ultrasound examination.

The written report should include:

- a description of the problem that led to the examination;
- a list of the organs (region) examined (generally, it is not necessary to describe normal findings but to note measurements only);
- a description of pathological findings (the descriptions should be concise and clear, but without over-interpretation.); and
- the diagnosis or decision.

Pictorial documentation of pathological findings in two planes is necessary, but documentation of a normal finding (one representative scan of the organ or body region examined) is also useful, e.g. for later check-up examinations.

Interpretation of the ultrasound image

Organs, structures within organs, vessels, tumours and fluid collections are evaluated by B-scan in terms of their:

- presence (aplasia?);
- position (displaced?);
- outer contour or border (which gives information about the surface of an organ or tumour as well as about its relation to the adjacent structures);
- mobility (fixed?);
- consistency (palpation under ultrasonic observation);
- echo pattern; and
- attenuation.

Evaluation of the **presence**, **position** and **size** of an organ is based on the known normal anatomy. A simple determination of organ diameter is sufficient for most routine evaluations, provided the shape is normal. The volume (V) of round- or oval-shaped organs is calculated on the basis of their three perpendicular diameters a , b and c , following the formula for an ellipsoid:

$$V = 0.5 \cdot a \cdot b \cdot c \quad (2.1)$$

Formulas for special problems, e.g. pleural effusion, are discussed in specific chapters of this book. The volume of organs and structures with complicated shapes can be calculated by the 3D technique.

Evaluation of the **contour** of an organ, and particularly of a neoplastic lesion, should give information about both the smooth or irregular surface and any sharp or blurred (ill-defined) demarcation lines (Fig. 2.8, Fig. 2.9, Fig. 2.10). The latter should include the relation to the surrounding tissue, e.g. any overlap with a natural border, such as a capsule, or infiltration into adjacent structures. The possibilities of contour evaluation are limited by the imaging geometry of ultrasound. The fine surface irregularities of a cirrhotic liver, for example, can be shown, especially since the surface

Fig. 2.8. Evaluation of the margin or contour of a lesion (e.g. in the liver). The margin of both lesions is sharp. The cyst (a) is echo free, the haemangioma (b) shows a homogeneous echo-rich pattern

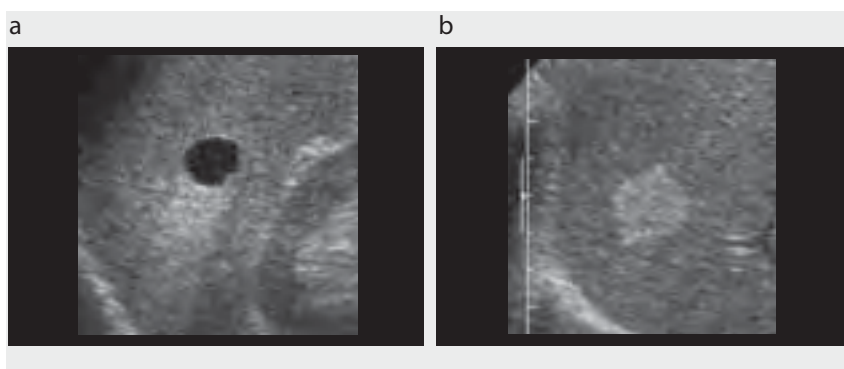
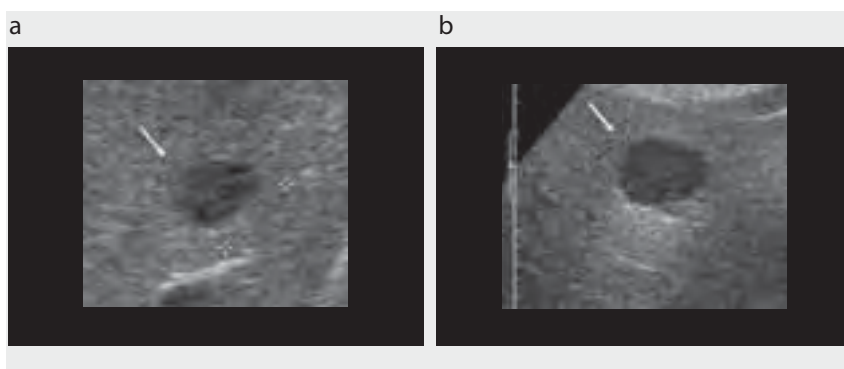


Fig. 2.9. Evaluation of the contour (margin) of two echo-poor liver lesions. (a) The echo-poor metastasis has a blurred outline, particularly at the cranial side (arrow), whereas the malignant lymphoma (b) shows a partial (dorsal side), rather sharp but altogether irregular outline. Slight echo enhancement is seen behind the lymphoma



is approximately perpendicular to the ultrasound beam (Fig. 2.11). The contour of an organ such as the pancreas, however, may appear to be irregular, particularly on the sides, as a result of the coarse boundary echoes.

Evaluation of the **echo pattern** (also known as echo structure, echo texture, echogenicity) of an organ, tissue or tumour is based on an analysis of the intensity and distribution of the internal echoes that are not due to discernible anatomical structures, such as vessels, septa or ducts. Single echoes are either weak, average or strong (Fig. 2.12).

The **echo pattern** is analysed on the basis of the number and strength of the echoes and their distribution (Fig. 2.13):

- echo free – echo poor (hypoechoogenic) – average – echo rich (hyperechoogenic); and
- homogeneous or inhomogeneous.

Fig. 2.10. Contour sign. (a) The lesion in the liver has a smooth outline and a tangential artefact (see Fig. 1.24), but is nevertheless a hepatocellular carcinoma (HCC), probably with a capsule. The pattern is average, similar to that of the surrounding liver tissue. (b) The metastasis in the abdominal wall shows an irregular shape and an echo-poor pattern

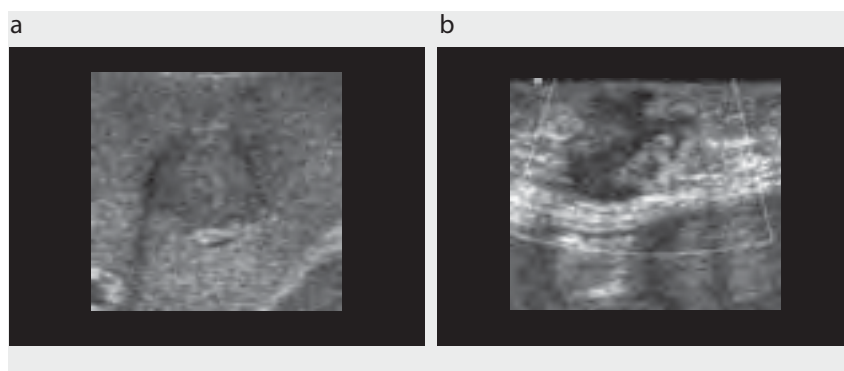
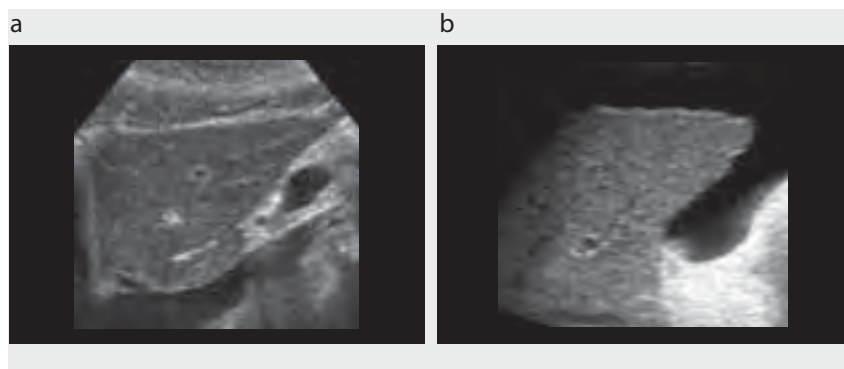


Fig. 2.11. Surface of the liver. (a) The normal healthy liver has a smooth surface. The echo structure of the normal liver is homogeneous and of normal brightness. (b) The cirrhotic liver has an irregular surface. (The echo pattern of the cirrhotic liver is slightly inhomogeneous (coarsened))



Echo free: no (real) echoes within a lesion, e.g. a cyst (Fig. 2.8, Fig. 2.13). This diagnosis requires the correct gain and the identification of artefacts (see section on Artifacts in Chapter 1). Furthermore, only fluid in the strict physical sense is really echo free. Other types of fluid (e.g. blood, abscesses or exudates) contain small particles (e.g. blood cells, fibrin) and cause weak echoes (Fig. 2.12).

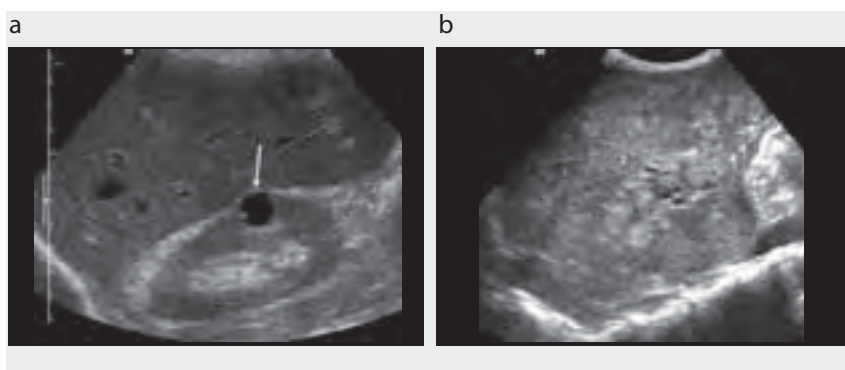
Echo poor: an echo pattern consisting of only a few weak echoes (see Fig. 2.9).

An echo pattern appears to be **echo rich** if the tissue causes many weak echoes or a few strong echoes. In both situations, this region appears 'bright' on the screen. For the first type of echo-rich pattern, the term 'echo dense' is occasionally used. Generally, none of these types of echo-rich pattern is differentiated (Fig. 2.8, Fig. 2.9, Fig. 2.10, Fig. 2.11, Fig. 2.12, Fig. 2.13, Fig. 2.14).

Fig. 2.12. Quality of echoes. The echoes in the upper part of the left lesion are weak, while those of the liver are average. In the right lesion, strong echoes caused by gas are seen. Both lesions (abscesses) show an inhomogeneous pattern; the one on the left is echo poor and the other partially echo rich. Behind the right-hand lesion, a tangential artefact is seen

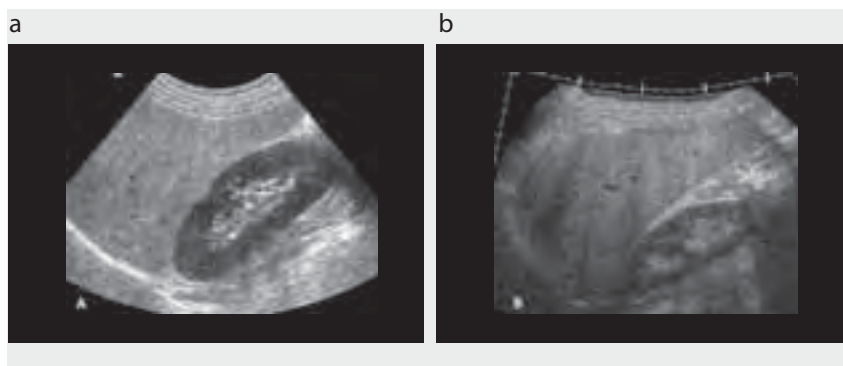


Fig. 2.13. Echo structure (echo pattern). (a) The ultrasonic structure of the liver and the parenchyma of the kidney are echo poor and homogeneous; the pattern in the centre of the kidney is echo rich. A small cyst (arrow) is echo free. (b) The liver shows an inhomogeneous echo-rich structure caused by echo-rich metastases



Increased **attenuation** of ultrasound in an organ may indicate pathological alterations, such as fibrosis; however, experience is needed to recognize this sonographic symptom, as no objective parameters exist (Fig. 2.14).

Fig. 2.14. Attenuation. (a) The fatty liver shows a typical homogeneous echo-rich pattern. (b) The echo structure of the left liver is echo rich near the ventral surface, but the dorsal parts appear more echo poor. Provided the adjustment of the TGC is correct, this indicates higher than average attenuation of the ultrasound, as seen in fibrosis



Duplex technique

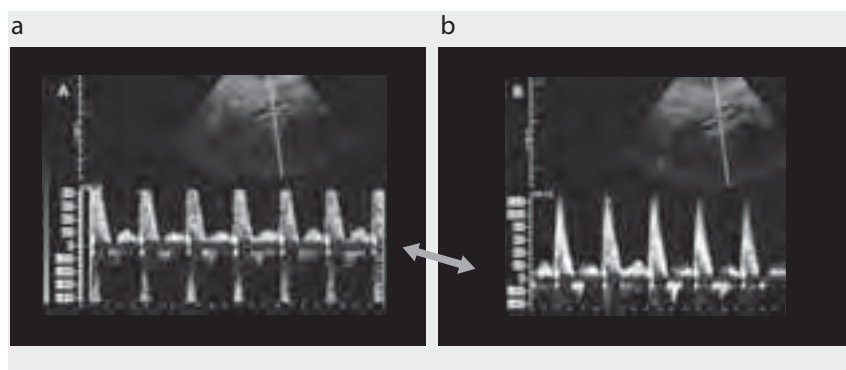
In interpreting Doppler information in an ultrasound image, account should be taken of the principal problems and limitations of the Doppler technique: angle dependency and aliasing.

A suitable angle ($< 60^\circ$) must be found for the ultrasound beam to reach the vessel of interest, especially if measurements (spectral Doppler) are to be made. The angle is less problematic for colour Doppler imaging, but colour pixels may be missed if the angle is close to 90° (see Fig. 1.32). Power Doppler images are not affected by this problem but give no information about the flow direction.

The window for the Doppler examination should be as small as possible, as its width and length determine the time needed for the construction of one image and, therefore, the image frequency (Fig. 1.19, Fig. 1.20, Fig. 1.21). The distal border of the window, or the penetration depth for the Doppler ultrasound, limits the pulse repetition frequency because a second pulse can be emitted only if the echoes of the adjusted depth have reached the transducer. The pulse repetition frequency limits the flow velocity, which can be depicted without aliasing (see section on Doppler techniques in Chapter 1). Initially, it is useful to adjust the settings to a relatively low velocity (17–24 cm/s) to depict the slow flow velocities in the veins. For the same reason, the filter should be low to avoid suppressing slow flow signals with those caused by the movement of the wall. For the examination of veins and arteries, the wall filter should be adjusted to 50–100 Hz and 200 Hz, respectively. If aliasing (see section on Doppler techniques in Chapter 1) occurs in the arteries, the pulse repetition frequency can gradually be adapted to higher velocities. The baseline can also be shifted to avoid aliasing in the arteries (Fig. 2.15) because the velocity in the veins in the opposite direction is slow.

The gain of the Doppler signals should be high so that single colour pixels are seen in the tissue, especially if thrombosis is suspected. If no colour-coded signals are seen in a vessel, the angle and adjustment, particularly of the pulse repetition frequency, should be checked. If they are correct, spectral Doppler should also be used to obtain a definite diagnosis.

Fig. 2.15. Aliasing. (a) The spectral Doppler depiction (duplex technique) of the flow in the aorta shows aliasing. The peak velocity signals, 80–120 cm/s, are shown below the baseline (arrow). (b) Correct depiction as a result of shifting the baseline (arrow)



In an artery, the colour Doppler technique will yield high systolic flow and give a good signal. In diastole, however, the flow may become very slow or even reverse (high-resistance flow), resulting in a weak signal and an unsatisfactory image of the vessel. With persistence, it is possible to extend the peak flow to get a better colour Doppler image (Fig. 2.16).

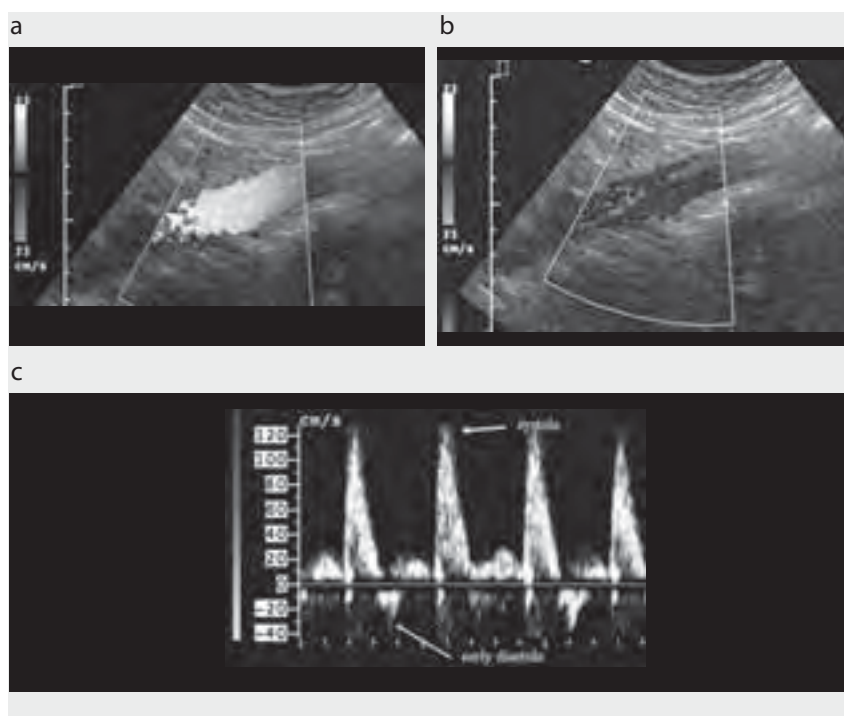
B-scan provides information about the anatomy of vessels, including diagnoses of dilatation, aneurysms and alterations of the wall and stenosis. Thrombosis in a vessel can also be demonstrated.

The colour Doppler technique permits detection of small vessels and gives information about flow and direction. Power Doppler is more sensitive for examining small vessels and slow flow but does not provide information about the direction of flow. In particular, it is used to estimate the vascularity of a structure or a mass.

Estimation of flow velocity from the brightness of colour pixels is rather approximate. Even turbulent flow, caused by stenosis, is not reliable.

Use of spectral Doppler (triplex technique) is needed for a more accurate analysis of the flow, e.g. direction, velocity and dynamic course. A condition required for an exact analysis is a Doppler angle of $< 60^\circ$ (best, $\sim 30^\circ$), which may be difficult to achieve in the abdomen. Each measurement should be made at least three times, and the average finding should be used. Attention should be paid to specific conditions, such as a change in flow, which depend on the activity of the region or tissues it supplies.

Fig. 2.16. Colour Doppler and spectral Doppler of the abdominal aorta. (a) The colour Doppler image shows red (here bright) signals, because it is made in systole, whereas the image in (b) shows blue signals (here dark), indicating reverse flow in early diastole. Both phases are indicated in the spectral Doppler (c)





Chapter 3

Interventional ultrasound

Definitions	45
Ultrasound-guided procedures: general clinical rules	46
	46 Diagnostic procedures
	54 Diagnostic or therapeutic procedures
	55 Therapeutic procedures
Complications of interventional ultrasonography	62
	62 Diagnostic procedures
	62 Therapeutic procedures

Interventional ultrasound

Definitions

Interventional ultrasound is defined as any diagnostic or therapeutic procedure performed under ultrasound guidance for any tissue or organ that is visualized by ultrasound.

Diagnostic procedures: ultrasound-guided aspiration of fluid or cystic fluid for biochemical or cytological and culture examinations as well as for cytological or tissue sampling with fine (outer calibre < 1 mm) or coarse needles for microscopic examination. The needle calibre is generally expressed in terms of gauges (Table 3.1).

Table 3.1. Needle calibre: conversion from millimetres to gauge

Millimetres (mm)	Gauge
Fine needle: calibre ≤ 1 mm	
0.5	23
0.6	22
0.7	21
0.8	20
0.9	19
Coarse needle: calibre ≥ 1 mm	
1.0	18
1.1	17
1.3	16
1.4	15
1.6	14
1.8	13
2.0	12

Therapeutic procedures: drainage of fluid collections (e.g. abscesses, parasitic cysts) by needle or catheter; injection into a tumour or echinococcal cyst of necrotizing substances (e.g. ethanol) and positioning of radiofrequency needle electrodes to obtain a thermal lesion.

Over the past 10 years, due to improvements in imaging techniques, indications for diagnostic procedures have progressively decreased and they have been replaced by imaging and/or laboratory data when they are considered sufficient for diagnosis.

Indications for therapeutic procedures have been increasing, so that there is now, for example, consensus that percutaneous abscess drainage is the treatment of choice for abdominal abscesses.

Ultrasound-guided procedures: general clinical rules

Ultrasound-guided diagnostic procedures should be performed only if a diagnosis cannot be made with other less or non-invasive methods (i.e. diagnostic imaging).

Pathological diagnostic confirmation should imply a definite benefit for the patient.

Therapeutic procedures should be as effective, or more effective, than more conventional invasive methods (e.g. surgery).

Before any ultrasound-guided procedure is carried out, a coagulation parameter check is mandatory: prothrombin activity should be 50% or greater, the international normalized ratio less than 1.5 and the platelet count 50 000 per ml or more.

Before any ultrasound-guided procedure is performed, the patient's informed consent should be obtained.

Contraindications: Uncooperative patients; severe blood-clotting impairment (patients must be asked about their intake of anticoagulant or antiaggregant drugs.)

Diagnostic procedures

Ultrasound-guided diagnostic procedures include cytological or tissue sampling and fluid collection by needle aspiration.

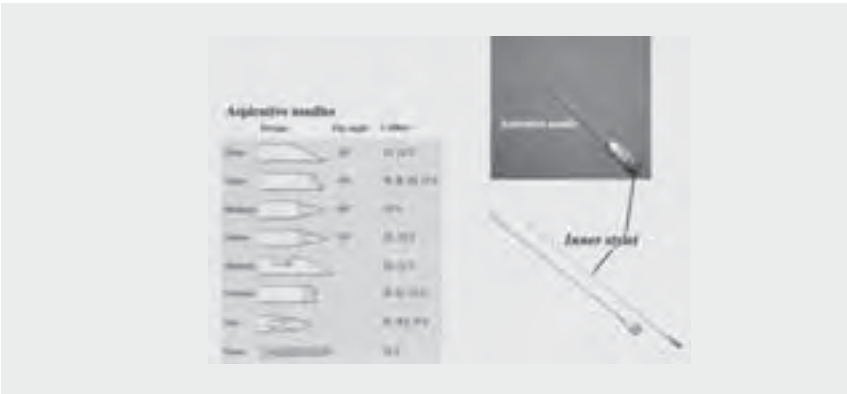
Technical notes

Needles

Fine needles are subdivided into aspirative needles for cytological sampling and cutting needles for tissue sampling (Fig. 3.1, Fig. 3.2).

Aspirative needles have an inner removable stylet. The prototype of aspirative needles was the spinal needle (Fig. 3.1). Cellular material is collected by aspiration, which is obtained by connecting the needle to a 10-ml syringe (which can also be connected to an aspiration handle).

Fig. 3.1. Types of aspirative needle and inner stylet



The main types of cutting needles are the Menghini (end-cutting needle) (Fig. 3.2) and the Tru-Cut (side-cutting needle). The Menghini needle has an inner retractable stylet attached to the syringe piston to avoid aspiration of the tissue core when suction is applied. The Tru-Cut needle has an outer cutting cannula and an inner one with a 20-mm notch, in which the biopsy specimen is trapped. The notch is located immediately before the tip (Table 3.2).

Fluid aspiration can be performed with either fine or coarse aspirative needles, depending on the fluid characteristics (e.g. viscosity, presence of debris).

Fig. 3.2. End-cutting needle showing needle tip



Table 3.2. Types of needles with relevant calibre and cost in US\$ (averaged worldwide, for 2009)

Type	Calibre (gauge)	Cost (US\$)
Aspirative		
Chiba	18–22	12
Spinal	18–25	6
Cutting		
Menghini	15–23	35
Tru-Cut	14–20	20

Approach

The approach depends on the target organ and the site of the focal lesion and can be either subcostal or intercostal. The depth of the target is calculated.

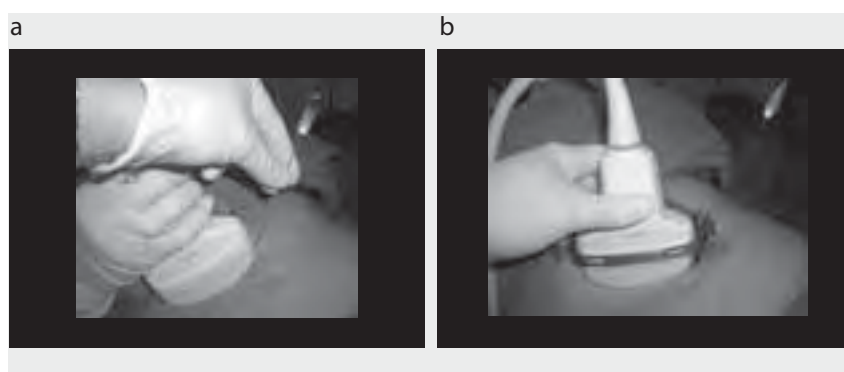
Biopsy with aspirative needle

The skin of the patient is disinfected with iodine, which also serves as a sterile contact medium. The fine needle is guided towards the target either with the **free-hand technique** or with the help of a **guidance apparatus** attached to the probe or directly introduced through the biopsy channel of the transducer (Fig. 3.3).

Fine needles can be inserted directly into the skin and subcutaneous tissue and then directed to the target. The tip of the needle should be seen on the ultrasound screen during the biopsy. Lesion areas, which are usually necrotic (echo poor, central), should

be avoided during sampling to improve the quality and quantity of the material collected (see Fig. 3.4). When the needle tip is in the correct position, the inner stylet is removed and the needle is attached to the syringe. Suction is applied, and the needle is moved backward and forward five to ten times. The syringe's piston is released before the needle is withdrawn to avoid contamination with material from different tissue layers.

Fig. 3.3. (a) In the free-hand technique, the needle is inserted close to the probe and the needle track is monitored by slight adjustments to the probe's inclination. (b) The needle is inserted into the channel of the guidance apparatus connected to the probe



The biopsy needle is disconnected, and the syringe is filled with air and reconnected to the biopsy needle. The material inside the needle is sprayed onto slides and smeared. It is preferable to check the adequacy of the material collected by immediate staining; if this is not possible, the biopsy should be repeated two or three times to ensure that an adequate sample has been obtained.

Biopsy with cutting needle

Cutting needles, even those of calibre < 1 mm, have a blunter tip than aspirative needles. Therefore, a local anaesthetic (e.g. 2–3 ml lidocaine) is infiltrated subcutaneously into the muscle layer after the skin has been disinfected. This is particularly necessary when larger calibre needles (< 18 gauge) are used. The skin is then pricked with a small lancet to facilitate the entrance of the needle. The biopsy is performed according to the type of needle. The Menghini needle is introduced into the superior margin of the target, suction is applied to the syringe and the needle is advanced rapidly for 2–3 cm and retracted. The Tru-Cut needle is also positioned at the proximal border of the target. The internal cannula is advanced, the tissue is trapped in the notch and finally cut by the outer sheath.

Post-biopsy control

The patient's vital parameters should be observed for 2 h after the intervention, especially if the biopsy was performed with a coarse needle or if the patient's coagulative status is abnormal although within the suggested limits. Thereafter, in the absence of any troubling signs or symptoms, the patient can be discharged with the recommendation to seek advice for any medical complaint within the following 7 days.

A negative biopsy result does not rule out a malignancy or, conversely, the need to confirm the benign nature of the biopsied lesion formally.

Indications

Liver

Malignant tumours

Ultrasound-guided biopsy is very accurate for diagnosing malignant liver tumours (Fig. 3.4, Fig. 3.5, Fig. 3.6, Fig. 3.7). Metastases can be typed by examining a cytological sample obtained with an aspirative needle (fine-needle biopsy (FNB)); sensitivity is very high at 92.7% and specificity is 100%. Cytological typing of hepatocellular carcinoma (HCC) can present some difficulties because, in well-differentiated forms, tumour hepatocytes are very similar to normal hepatocytes, whereas in poorly differentiated forms the hepatic histotype can be misinterpreted and an erroneous diagnosis of metastasis made. In such cases, it is advisable to perform a double biopsy: one for cytological examination (fine-needle biopsy with an aspirative needle) and one for histology (fine-needle biopsy with a cutting needle). In this way, sensitivity is increased to 97.5% and the specificity is 100%. According to current diagnostic policy, a biopsy should not be performed on nodular lesions with an α -fetoprotein value higher than 400 ng/ml or if two imaging techniques confirm a diagnosis of HCC.

Fig. 3.4. Fine-needle biopsy of a large hepatic lesion: hepatocellular carcinoma. Note that on the needle track a portion of normal parenchyma is interposed between the lesion and liver capsule; the needle is directed to the more echo-rich area of the tumour to improve the sampling adequacy



Fig. 3.5. Fine-needle biopsy of a small hepatic lesion: liver metastasis

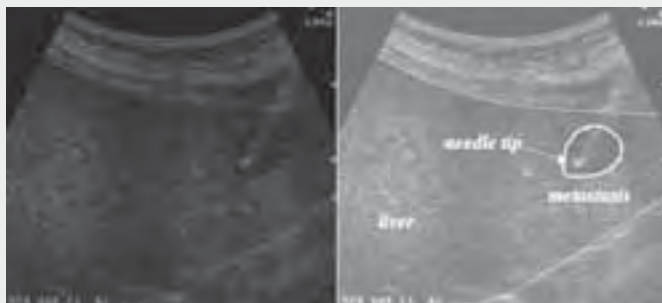
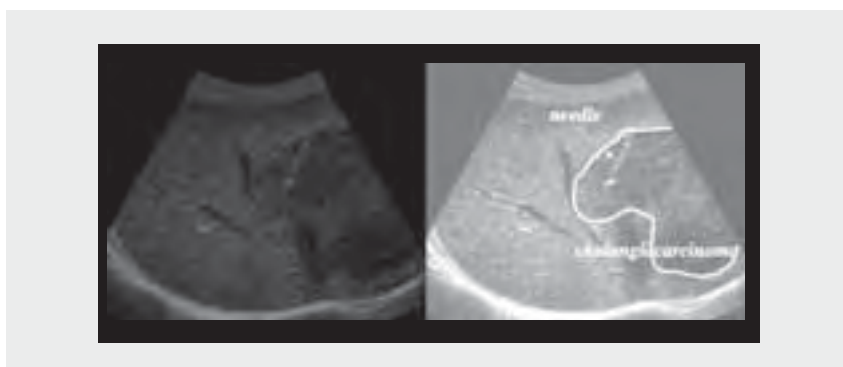


Fig. 3.6. Fine-needle biopsy of a small, ill-defined hepatic lesion: cholangiocarcinoma



Fig. 3.7. Fine-needle biopsy of a large hepatic lesion with irregular borders: cholangiocarcinoma



Benign tumours

Haemangioma is the commonest benign liver tumour, and generally ultrasound is diagnostic. In some instances, however, its presentation can be very atypical and puncture is advised. Unfortunately, the diagnostic accuracy of fine-needle biopsy is not satisfactory because the material obtained is filled with blood, and few endothelial cells are present. Furthermore, major complications (haemorrhage) or even death has been reported after biopsy of liver haemangioma.

Two other benign liver tumours – much rarer than angioma – are adenoma and focal nodular hyperplasia, which is really a pseudotumour. Imaging with a combination of at least two coincident techniques generally suffices to characterize focal nodular hyperplasia, while diagnosis of an adenoma is more difficult. A combination biopsy (cytology and histology) should be performed with caution because both focal nodular hyperplasia and adenoma have rich vascularization. Histological sampling is better performed with coarse cutting needles (1.2–1.4 mm).

Simple cysts and hydatid cyst

Generally, ultrasonic diagnosis of simple cysts is to be recommended. In an oncological context, however, a pathological diagnosis may be necessary. Cystic fluid can easily be aspirated and a cytological examination performed.

Hydatid cysts are usually diagnosed by a combination of serology and imaging. In some cases, an examination of the aspirated fluid may be useful. Experience has shown that puncturing a hydatid cyst is only rarely complicated by anaphylactic shock.

Pyogenic abscess and amoebic abscess

Material obtained by ultrasound-guided aspiration of pyogenic abscess is creamy-yellow and foul-smelling. Multiple sets of culture increase the diagnostic yield of blood cultures. Ultrasound-guided aspiration of an amoebic abscess should be performed when the diagnosis is uncertain. The aspirated fluid is viscous, yellow or dark-brown ('anchovy sauce'). In both these forms, the aspiration should be performed with 19- to 20-gauge needles because of the viscosity of the material.

Chronic liver disease (cirrhosis, chronic hepatitis)

When clinical, laboratory and imaging data require histological confirmation, a biopsy can be performed with a subcostal or intercostal approach. A cutting needle (14–18 gauge) can be used.

Gallbladder

The gallbladder can be punctured under ultrasound guidance, using a transhepatic approach, to diagnose gallbladder masses.

Pancreas

Pancreatic masses

The pathological diagnosis of a pancreatic mass ensures correct management of patients (Fig. 3.8, Fig. 3.9). If the tumour is resectable, surgery can be carried out to avoid the time and difficulties involved in intraoperative biopsy. In patients with non-resectable tumours, appropriate palliative treatment can be planned. Moreover, fine-needle biopsy allows diagnosis of malignancies other than adenocarcinoma, such as neuroendocrine tumours, lymphoma or metastases, which require different management. In one series of 510 patients with pancreatic masses, either benign or malignant, the diagnostic effectiveness of fine-needle biopsy was found to be very high (Table 3.3), except for neuroendocrine tumours.

Fig. 3.8. Fine-needle biopsy of a large pancreatic lesion: pancreatic carcinoma

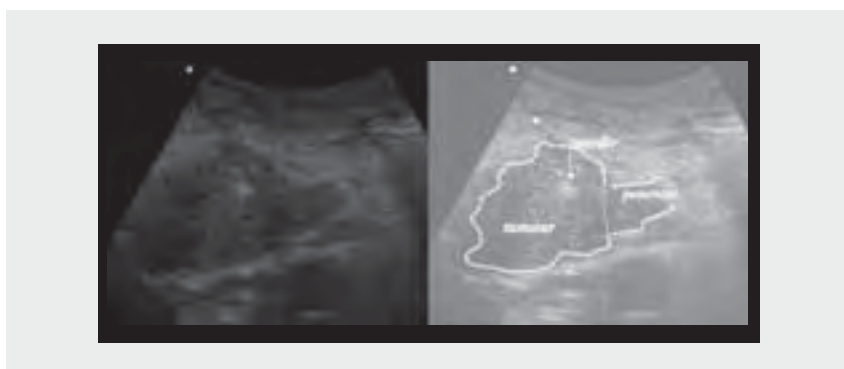


Fig. 3.9. Fine-needle biopsy of a large cystic pancreatic lesion: pancreatic cystadenoma. Bioptic access was transhepatic



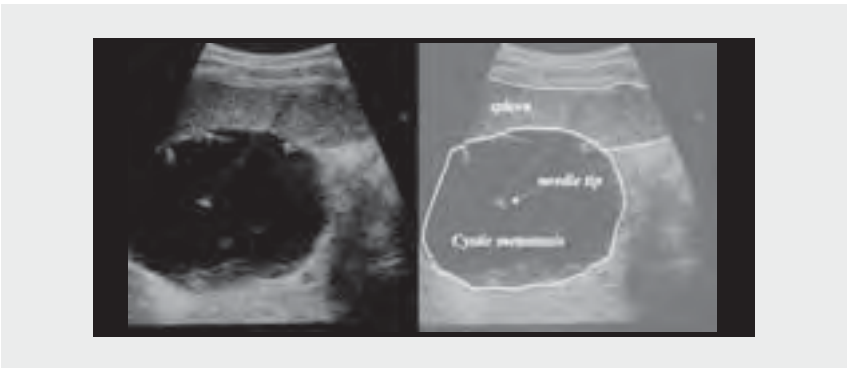
Table 3.3. Results of different fine-needle biopsy procedures for the diagnosis of pancreatic lesions; the differences in the results are not statistically significant

	Cytology (287 patients)	Histology (95 patients)	Cytology + histology (128 patients)
Sensitivity (%)	87	94	97
Specificity (%)	100	100	100

Spleen

Spleen biopsies are performed infrequently because of the risk of post-procedural bleeding. Moreover, the indications for spleen biopsy, which include staging or restaging of lymphoma, are decreasing. Spleen biopsy can, however, be a highly effective diagnostic tool in selected cases of focal lesions, organomegaly or fever of unknown origin. In addition, it has an acceptable complication rate (Fig. 3.10).

Fig. 3.10. Fine-needle biopsy of a large cystic lesion of the spleen: metastasis



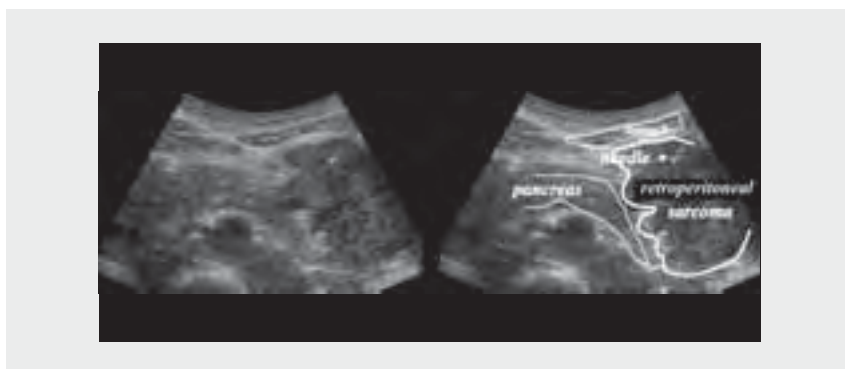
Kidney

Imaging techniques cannot always differentiate between a benign and a malignant kidney mass. In such instances, fine-needle biopsy is easy to perform, with satisfactory diagnostic accuracy. Cutting needles (18 gauge) guided by ultrasound can readily be used to obtain kidney tissue to characterize diffuse nephropathy.

Gastrointestinal masses

The origin of gastrointestinal masses varies, occurring either in the gastrointestinal tract or independently of it. Intestinal gas, which degrades the ultrasound image, can be displaced by compressing the intestine with the probe. Sampling is preferably performed with a fine aspirative needle (cytology examination). A liquid mass can easily be aspirated with a fine needle. Many potential pathological conditions are possible: haematoma, very large kidney cysts or ovarian cysts, mesenteric cysts, lymphangioma, atypical location of a pancreatic pseudocyst, necrotic tumours and hydatid cysts. The aspirated material should be used for culture, cytological examinations and laboratory tests, such as amylase and tumour markers. Other retroperitoneal or abdominal (lymphadenopathy) masses can also be aspirated under ultrasound guidance (Fig. 3.11, Fig. 3.12).

Fig. 3.11. Fine-needle biopsy of a huge retroperitoneal mass: sarcoma



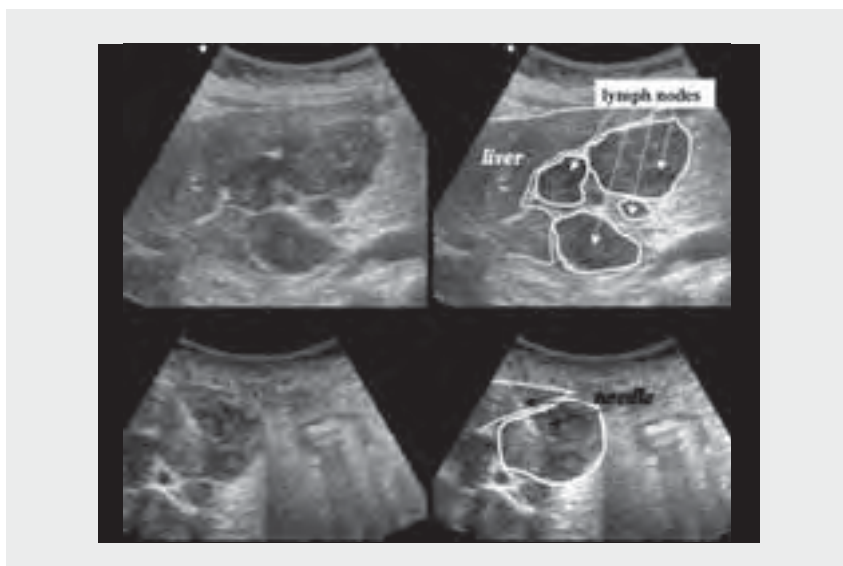
Lung

Ultrasonography is a useful alternative to other imaging techniques (e.g. fluoroscopy and computed tomography (CT)) to guide biopsy of subpleural lung lesions. The technique is simple and rapid and can be carried out at the bedside.

Bone

Although sonography cannot be used to study bone lesions, ultrasound images are clear enough to perform an ultrasound-guided biopsy on some patients with lytic lesions characterized by disruption of the cortical structure. Within these limits, the diagnostic accuracy is very good.

Fig. 3.12. Fine-needle biopsy of abdominal lymphadenopathy; the biopsy access was transhepatic



Diagnostic or therapeutic procedures

Pericardiocentesis, **pleurocentesis** and **paracentesis** are procedures with either a diagnostic or therapeutic purpose.

Pericardiocentesis

Ultrasound guidance reduces the risks for lung or heart injury, and the procedure is much safer and easier than the previously used blind puncture technique. Cytological and culture examinations can establish the diagnosis in many instances. Generally, the procedure has a simultaneous therapeutic value, when the amount of pericardial fluid could interfere with cardiac contractions. Sometimes, a permanent catheter may be necessary, which can be positioned by the Seldinger technique (see section on Catheter insertion techniques in this chapter).

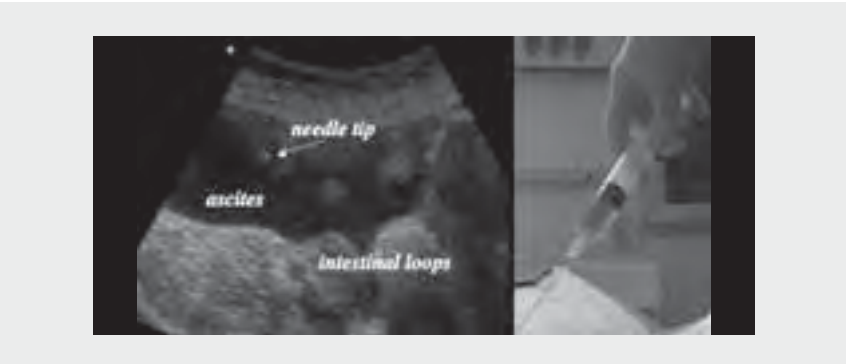
Pleurocentesis

The procedure is still performed with a blind technique, in which the fluid collected is substantial. Ultrasound guidance facilitates correct needle insertion and positioning, particularly when small amounts of fluid or septated collections are involved.

Paracentesis

Ultrasound guidance ensures the correct positioning of the needle when the sample to be collected is small or loculated (Fig. 3.13).

Fig. 3.13. Paracentesis: correct positioning of the needle



Therapeutic procedures

Abdominal abscess drainage is the first line of treatment for infected or symptomatic fluid collection. Almost all abscesses are amenable to percutaneous drainage. When a coexisting problem, such as a bowel leak, requires surgery, drainage provides useful temporization for the surgeon. Catheter insertion procedures include the trocar and Seldinger techniques. Ultrasound, CT and fluoroscopy are the imaging guidance systems most commonly used. Preferably, the procedure is performed by positioning a large catheter under ultrasound guidance. The catheter is left in situ until draining has stopped.

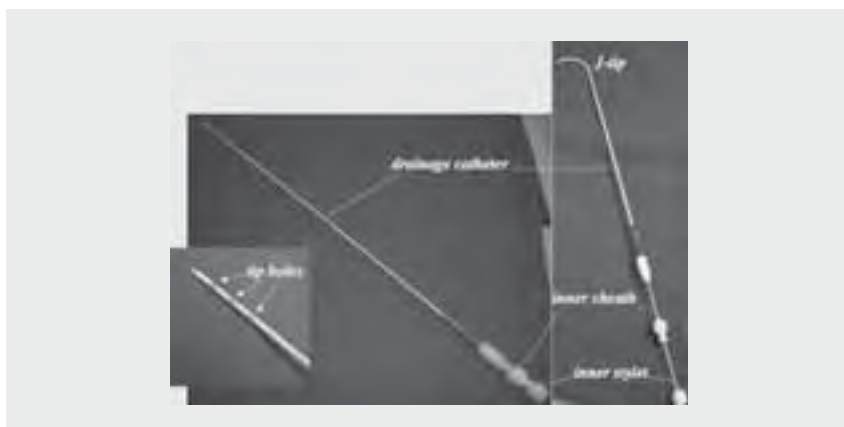
Technical notes

Catheters of different lengths and calibres are available (Table 3.4). Most are characterized by a terminal part configured as a ‘pigtail’ (or J-shaped), which can prevent inadvertent catheter withdrawal (Fig. 3.14).

Table 3.4. Conversion from French units to inches and millimetres

French catheter scale (outside diameter)	Inches	mm
4	0.053	1.35
6	0.079	2
8	0.105	2.7
10	0.131	3.3
12	0.158	4
14	0.184	4.7
16	0.210	5.3
18	0.236	6
20	0.263	6.7
22	0.288	7.3
24	0.315	8

Fig. 3.14. Catheter structure. Withdrawal of the inner stylet and sheath allows the tip to assume a J-shaped curvature



Catheter insertion techniques

Basically, there are two methods for inserting a catheter into an abscess: the trocar technique and the Seldinger technique.

Trocar technique

A catheter mounted on a trocar is directly inserted into the collection site. The depth of the target should be accurately measured and the track of the trocar carefully followed on the ultrasound screen. When the calibre of the catheter is large (> 8 French), accurate placement can be made by using a guiding needle previously inserted into the abscess. Thereafter, a small skin incision is made alongside the needle, and the trocar is advanced parallel to the guiding needle. When the catheter is in position, the inner stylet of the trocar is retracted, some millilitres of pus aspirated, and the trocar then removed.

Seldinger technique

An 18 to 20-gauge needle is inserted into the collection site and a guide wire passed through the needle. After needle insertion and aspiration of a few millilitres of fluid, a guide wire is inserted and the needle is withdrawn. The catheter is directed over the guide and into place at the collection site. The first step of the procedure is realized under ultrasound guidance. It may be necessary to use dilators of increasing calibre to obtain an adequate track for introduction of the catheter.

An advantage of the trocar technique is its relative simplicity, whereas the Seldinger technique allows more accurate location of the catheter.

Management of the catheter

A primary mechanism for internal catheter retention is the catheter configuration. The so-called pigtail-shaped catheter or J-shaped tip (Fig. 3.14), which is widely used, prevents inadvertent catheter withdrawal. The catheter should be fixed externally by suturing it to the patient's skin. Most catheters have external fixation devices.

Once abscess decompression has been achieved, the catheter should be flushed every 8–12 h with 10–15 ml of saline to clear it and to eliminate plugs, which may cause obstruction. The procedure should be performed cautiously to avoid catheter dislodgement. Catheter output, the characteristics of the drained material and any changes in these characteristics should be carefully recorded. Output reduction while the abscess is incompletely drained may indicate the presence of a clog in the tube, in which case the catheter should be changed. Suspicion of a fistula with adjacent organs or other structures should be confirmed by injecting contrast fluid into the abscess through the catheter. The presence of sepsis should delay this radiological check.

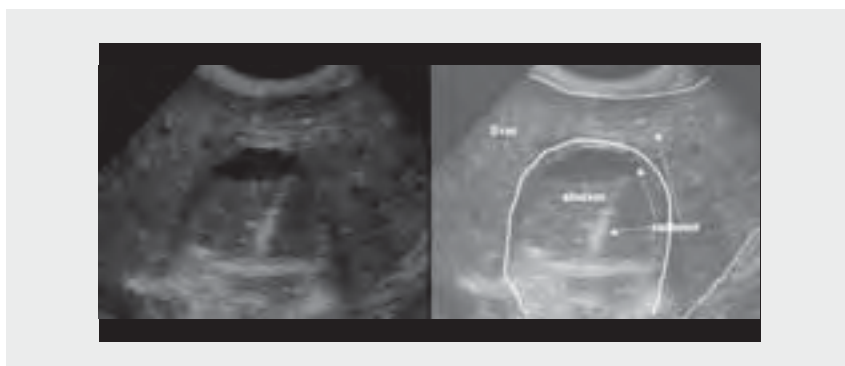
Indications

Liver

Pyogenic abscess

The pus is characteristically creamy and unpleasant smelling. Needle aspiration (even with a fine needle) is recommended as the first diagnostic procedure, as it allows assessment of the thickness of the purulent material and, thus, facilitates the choice of catheter. A first culture should be performed. If the abscess is large, use of a catheter is generally mandatory (Fig. 3.15, Fig. 3.16). It is left in situ for a few days after drainage has stopped (with the catheter open).

Fig. 3.15. Catheter drainage of a large pyogenic abscess of the liver



Amoebic abscess

The pus is yellow or dark-brown ('anchovy sauce') and, typically, odourless. The treatment is similar to that described for pyogenic abscess. The results of percutaneous drainage are very satisfactory for both kinds of abscess.

Echinococcal cyst

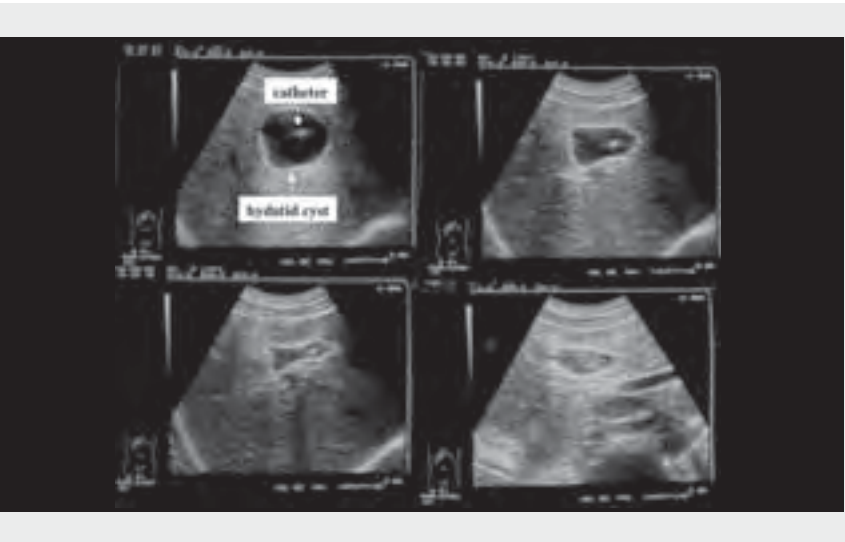
Hydatid cyst can be treated by ultrasound-guided puncture with the PAIR technique (puncture, aspiration of contents, injection of scolicide solution and reaspiration of the injected liquid), which represents an alternative to surgery and medical treatment. Preliminary aspiration of cystic fluid (10–20 ml) for parasitological and biological examination is performed. The fluid is typically as limpid as pure water. The therapeutic procedure (Fig. 3.17) is generally performed with a 14–18 gauge needle, preferably with a transhepatic approach. Catheter insertion is only sometimes useful but is mandatory for large cysts and thick material. After fluid aspiration, 95% ethanol or 30% hypertonic

saline solution is introduced in a quantity equivalent to about one third of the aspirated fluid to ensure an effective concentration of the scolicide in the cyst. After 10 min, the ethanol or saline solution is reaspirated. A variation involves repeating the ethanol injection (about 100 ml) every 3 days without reaspiration. Treatment with a specific drug is advisable. The procedure is effective and safe: prolonged follow-up has not shown leakage of hydatid fluid or passage of ethanol or saline solution into the bile system. The operator must, however, bear in mind the risk of chemical cholangitis; therefore, a rapid test for bilirubin should be performed on the fluid from the cyst, before scolicide injection.

Fig. 3.16. Pus from a pyogenic abscess is yellow (a), whereas that from amoebic abscess is typically brown (b)



Fig. 3.17. PAIR technique study of a hepatic hydatid cyst. The catheter is clearly visible inside the cyst. Reaspiration of scolicide progressively empties the cyst



Pancreas

Pancreatic pseudocyst

These are collections of pancreatic juice encapsulated by a connective wall of varying thickness, without an epithelial lining. They originate from the pancreas and, in many instances, communicate with pancreatic ducts. They are usually found within or adjacent to the pancreas in the lesser peritoneal sac. Occasionally, pseudocysts dissect the mesentery and can be found anywhere in the abdomen. Two pathogenic mechanisms are responsible for pseudocyst development. In the first, there is an episode of acute pancreatitis with gland inflammation, exudates and eventual disruption of the ductular system. The second mechanism is related to the course of chronic pancreatitis. Most pseudocysts resolve with conservative management. When the presumed duration of collection of pancreatic juice is less than 6 weeks, treatment should be avoided to allow maturation of the pseudocyst wall. Percutaneous drainage of pseudocysts requires the use of large-bore catheters, as the collection fluid is rich in fibrin plugs and gross necrotic debris. The time needed to cure pseudocysts by percutaneous drainage is generally very long and sometimes takes months. **Pancreatic abscesses** (Fig. 3.18) and other **abdominal collections** (Fig. 3.19) can also be drained under ultrasound guidance.

Fig. 3.18. (a–d) Catheter drainage of a large pancreatic collection. The catheter is visible within the collection (black and white arrows), which is progressively emptied

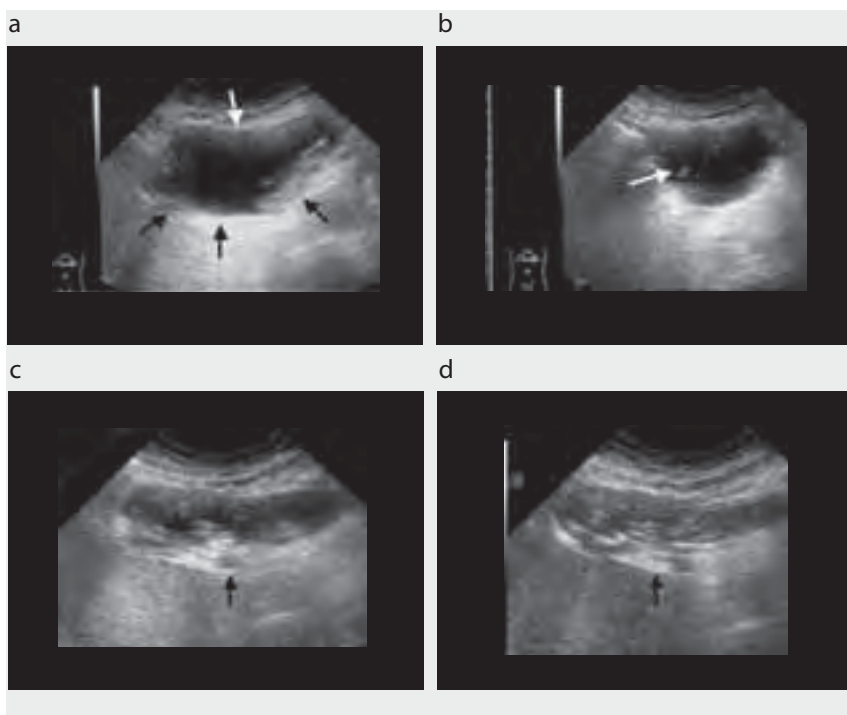
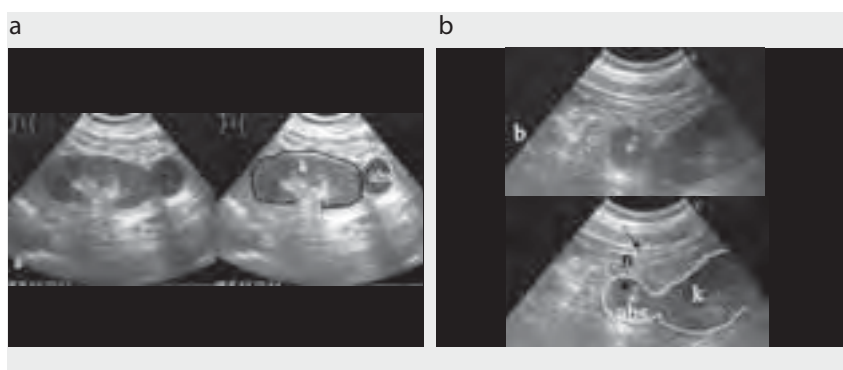


Fig. 3.19. (a, b) Needle drainage of a renal abscess (abs) due to *Escherichia coli*. The needle (n) track is marked with arrows; k, kidney



Percutaneous treatment of malignant liver tumours

Metastases of HCC and colorectal cancer are the most frequent liver malignancies, for which the only prospect for cure is surgical resection. Liver transplantation is the therapy of choice only in selected cases of HCC. The number of patients suitable for liver resection is sharply limited by many factors: multicentre tumours, non-resectable location, advanced liver cirrhosis and comorbidity. Methods for local tumour ablation have thus been proposed, and some ultrasound-guided procedures have gained ground.

HCC can be treated by ultrasound-guided procedures, such as percutaneous ethanol injection, or by creating a thermal lesion with a radiofrequency electrode (radiofrequency ablation). It is generally accepted that single tumours of less than 5 cm in diameter or multiple tumours (diameter < 3 cm) can be treated. The results obtained appear similar to those for surgical resection. Percutaneous ethanol injection (Fig. 3.20) is a more straightforward procedure, but it requires many sessions. It is performed, without anaesthesia, by inserting, under ultrasound guidance, a fine needle (22 gauge) into different tumour sites. Access is intercostal or subcostal, and 2–5 ml of 95% ethanol is injected at each session. The injection is generally painful, although is rarely judged unbearable. The total amount of injected ethanol can be calculated from Shiina's formula, in which a correction factor is introduced into the sphere volume calculation: $\frac{4}{3} \pi (r + 0.5)^3$, where r is the tumour radius and 0.5 the correction factor.

In radiofrequency ablation (Fig. 3.21), the patient is connected to the radiofrequency generator by an active electrode and a dispersive electrode. A mild sedative is administered, before the skin is pricked with a small lancet under local anaesthesia. Access is intercostal or subcostal. The radiofrequency generator is activated, and a temperature of about 100 °C is reached around the electrode tip and maintained for 10–20 min. Recent approaches to wider thermal necrosis have centred on modifying the needle electrodes: expandable electrodes enlarge the surface of the active electrode by means of extensible hooks (expandable system); and internal cooling of the needle electrode prevents adjacent tissue desiccation and hence allows higher power input (cooled system).

The results obtained by either percutaneous ethanol injection or radiofrequency ablation are examined by techniques such as CT and magnetic resonance imaging (MRI). In a substantial proportion of cases, the tumour is found to be completely necrotized at the end of treatment. Studies of the long-term therapeutic efficacy of

Fig. 3.20. Percutaneous ethanol injection of a small HCC located in segment 8 of the liver: ethanol is injected after the needle tip is demonstrated in the tumour

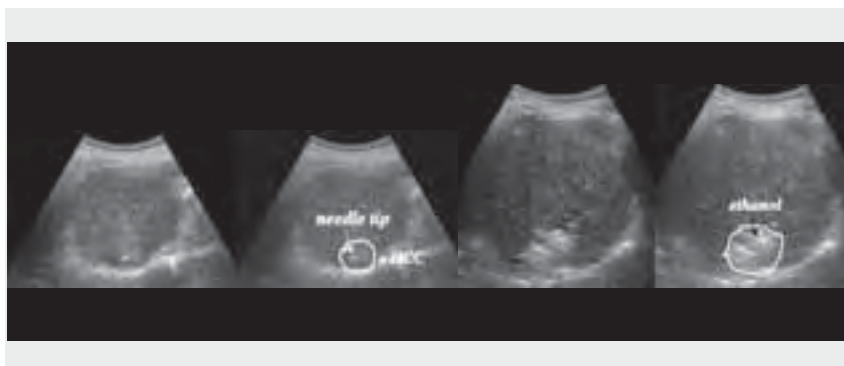
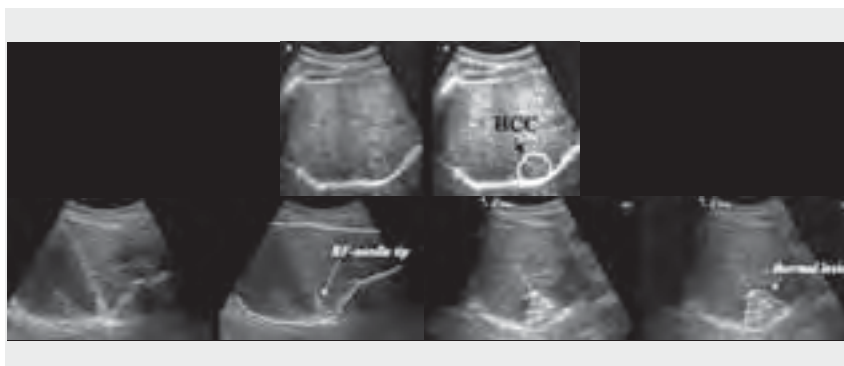


Fig. 3.21. Radiofrequency thermal ablation of a small HCC located in segment 8 of the liver. After the needle-electrode hooks are deployed within the tumour, exposure to radiofrequency (RF) is activated until completion of thermal ablation



percutaneous ethanol injection and radiofrequency ablation for small HCCs show similar survival rates (about 40–50% at 5 years), which are comparable to those after surgical resection. Recurrences after these procedures are high (65–90% at 5 years), with a disease-free survival rate of about 25% at 3 years. A lower incidence of local recurrence is seen with radiofrequency ablation. Another advantage of this procedure is that tumour ablation can be achieved in only one or two sessions, while a large number of sessions are required for percutaneous ethanol injection over many weeks.

Percutaneous ethanol injection is ineffective for treating liver metastases, and this indication for the procedure has been abandoned. The percutaneous therapeutic option is offered by radiofrequency ablation, which has been used to treat metastases from colorectal cancer and is associated with almost the same number and kind of limitations as those for HCC.

Complications of interventional ultrasonography

Complications of diagnostic and therapeutic procedures have been examined in many multicentre studies. Studies carried out in a single institution are rare because few centres carry out enough procedures to be able to make such analyses. However, multicentre studies tend to underreport data, and data on therapeutic procedures are, in some settings, difficult to analyse. As some of these procedures (particularly drainage of abdominal abscesses and pancreatic collections) are carried out on severely ill patients, it is difficult or impossible to distinguish between procedure-related complications and the disease outcome. For local treatment of liver tumours (by percutaneous ethanol injection or radiofrequency ablation), the patient's condition is relatively good and patients are closely followed after treatment. Complications due to these two procedures are, thus, clearly reported.

Diagnostic procedures

The risks associated with these diagnostic procedures are low: the mortality rate in the multicentre surveys lies in the range 0.001–0.031%. In a recent survey of 16 648 ultrasound-guided liver procedures in one centre, no deaths were observed. The rate of major complications has been estimated as 0.05%, one third of which is due to haemorrhage. One problem that is still the subject of discussion is tumour seeding along the needle track; however, the risk seems to be low (three cases in 100 000 biopsies).

The major caveats to performing ultrasound-guided diagnostic procedures are as follows:

- The risk increases with the use of large needles.
- Puncture of vascular lesions (haemangioma, angiosarcoma) presents a high risk for bleeding.
- It is hazardous to biopsy a normal pancreas because of a false impression of the presence of a 'mass'.
- Pancreatitis may occur after biopsy; the risk for puncturing a pheochromocytoma is high and should be avoided (diagnosis on the basis of imaging and clinical syndrome).
- Puncture of carcinoid metastases to the liver can cause a carcinoid crisis (somatostatin analogues should be available during puncture).
- Puncture of a hydatid cyst may cause anaphylaxis (check serology whenever such a lesion is suspected; resuscitation drugs and instruments should be available during puncture).
- An aneurysm may be misinterpreted as a lesion (check the lesion with colour Doppler ultrasound before biopsy).

Therapeutic procedures

Percutaneous ethanol injection

In a multicentre survey of 1066 patients with small HCC (greatest diameter, < 5 cm) treated for a mean of 6.7 sessions with a fine needle, one death occurred (0.09%) and 34 major complications (3.2%) were found, 9 of which were haemorrhagic.

Radiofrequency ablation

In two large multicentre studies involving two different techniques (the cooled system and the expandable system), the mortality rate ranged from 0.09% to 0.3%. The major complication rate was 2.2–3.2%. Tumour seeding was observed in 0.04–0.3% of cases.

Treatment of hydatid cyst

No major complications were found in 163 patients with echinococcal cysts treated by PAIR. However, in a large series treated by alcohol injection, without reaspiration, one death was observed due to anaphylactic shock.



Chapter 4

Neck

Indications	67
Examination technique	67
67	Equipment, transducer
67	Preparation
67	Position of the patient
67	Scanning technique
Normal findings	68
68	Thyroid gland
70	Parathyroid glands
70	Oesophagus
70	Vessels
70	Lymph nodes
70	Muscles
Pathological findings	71
71	Thyroid
81	Parathyroid glands
81	Branchial cervical cysts
83	Primary tumours in the neck
83	Inflammation of the soft tissue
83	Lymph node diseases
Differential diagnosis	86
86	Goitre
87	Small thyroid
87	Echo-poor nodule
88	Other lesions and masses in the neck
Ultrasound-guided fine-needle biopsy	88

Neck

Indications

The indications for ultrasonography of the neck are:

- diseases of the thyroid gland
- suspected parathyroidal adenoma
- malignant lymphoma, staging and follow-up
- palpable masses (lymph nodes, tumours, cervical cysts)
- abscesses.

Examination technique

Equipment, transducer

A linear or curved array is used, at least 5 MHz or, better, 7.5–10 MHz.

If an abdominal transducer of only 3 MHz is available, a water bag placed between the transducer and the skin permits a rough examination of the neck.

The Doppler technique is useful, especially for examining the thyroid (differentiation of toxic adenomas, diagnosis of autoimmune disorders and some thyroid carcinomas) and for differentiation of enlarged lymph nodes.

Preparation

No specific preparation is necessary.

Position of the patient

The preferred position for examining a patient is supine, with the neck hyper-extended (neck roll). Examination in a sitting position is also possible.

Scanning technique

The initial scans (B-scan) should be transverse, with the strong echoes of the air in the trachea (marking the midline) and the large vessels on both sides used as 'landmarks'. These scans should be followed by longitudinal scans (see Fig. 4.1, Fig. 4.2).

Afterwards, if indicated, examination, with colour Doppler of the whole thyroid gland (Grave-Basedow disease) or nodules and enlarged lymph nodes and tumours, may be necessary, always after the B-scan technique is used.

Fig. 4.1. (a) Topography of the thyroid (Th). (b) Typical transverse scan. Smm, sternocleidomastoid muscle; Stm, sternothyroidal muscle; Om, omohyoid muscle; Ca, common carotid artery; Jv, jugular vein; Tr, trachea; P, parathyroid gland; Rn, recurrent nerve; Vn, vagus nerve; O, oesophagus

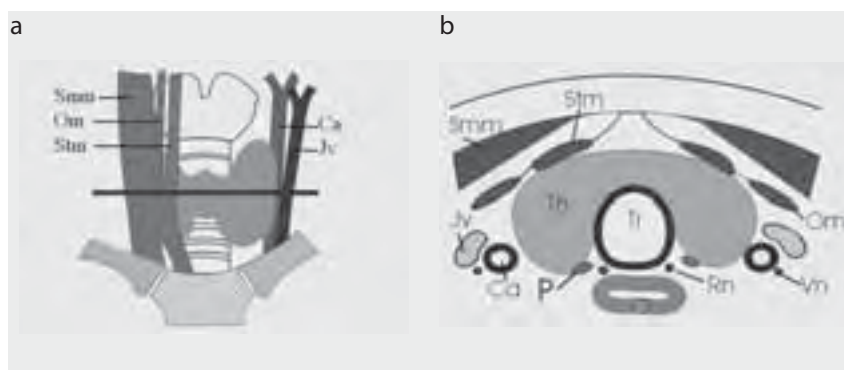
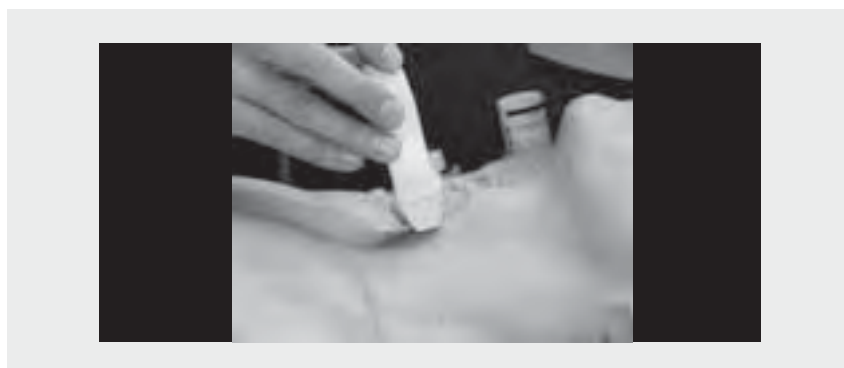


Fig. 4.2. Transducer placement corresponding to Fig. 4.1, Fig. 4.2, Fig. 4.3



Normal findings

Thyroid gland

The thyroid is shaped like the letter 'H', with an oval lobe on each side of the trachea connected by the isthmus (Fig. 4.3, Fig. 4.4). The pyramidal process, originating from the isthmus and developing in the midline upwards, is a rare inborn variant. Abnormalities, such as the sublingual thyroid or a unilateral gland, are also very rare.

The two lower arteries (inferior thyroid artery) enter the capsule of the thyroid on the dorsal side of the lower poles. The two upper arteries (superior thyroid artery) originating from the external carotid artery enter the upper poles.

The thyroid gland consists of small lobules, each containing around 25 follicles. The content of the follicles depends on their function. It also determines the echo pattern (Fig. 4.3).

The echopattern of the thyroid gland is homogeneous and echo rich (normofollicular stage), giving a strong contrast to the echo-poor pattern of the surrounding muscles,

Fig. 4.3. (a) Transverse scan of the normal thyroid (Th), panoramic view. The echo-rich pattern of the thyroid contrasts well with the muscles (**Fig. 4.1**). The air in the trachea (Tr) causes an acoustic shadow and reverberation artefacts. Note the large vessels on both sides. Jv, jugular vein; Ca, common carotid artery; Om, omohyoid muscle; Smm, sternocleidomastoid muscle; Stm, sternothyroidal muscle. (b) Schematic representation of the relation between thyroid function and sonographic pattern. Macrofollicular echo-rich nodules are typical of endemic goitre, normofollicular pattern is the normal finding. A microfollicular echo-poor pattern is typical in Grave-Basedow disease, and an echo-poor pattern caused by cellular infiltration is seen in Hashimoto thyroiditis and in carcinomas

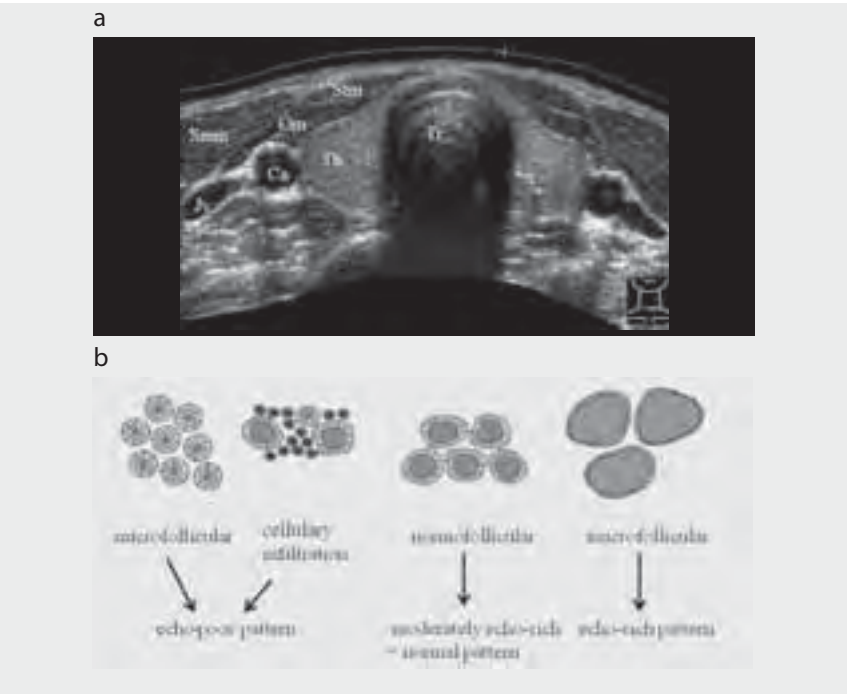
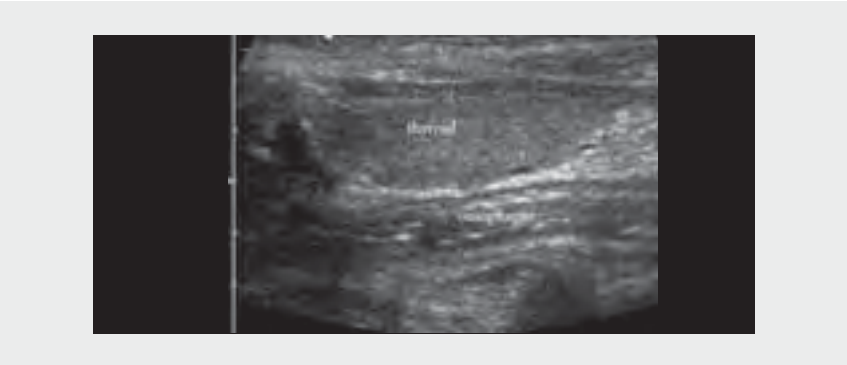


Fig. 4.4. Normal left lobe (31 × 9 mm) and oesophagus, longitudinal scan



which can serve as a reference. The outline is regular and smooth. The bright echoes behind the isthmus are caused by air within the trachea. The section of the lobes is round or triangular in transverse scans and oval in longitudinal scans (Fig. 4.3, Fig. 4.4).

The size of each lobe is 5–6 cm (length (*a*)) × 2–4 cm (width (*b*)) × 1–2.5 cm (thickness (*c*)). The volume of the whole gland is up to 20 ml in females and 25 ml in males and is determined by adding the volumes (*V*) of both lobes, each calculated from the formula:

$$V = 0.5 \cdot a \cdot b \cdot c \quad (4.1)$$

The intensive blood circulation can be demonstrated with colour and power Doppler techniques. The peak flow velocity in the thyroid arteries is less than 25 cm/s.

Parathyroid glands

Usually, normal parathyroid glands cannot be found by ultrasound. However, it may be possible to visualize them if a good quality machine with a high frequency (> 7 MHz) is used and if the location of the glands is normal – close to the superior or inferior thyroid artery.

Oesophagus

The cervical oesophagus can be seen in longitudinal scans behind the thyroid as a tubular or target-like structure if this area is scanned with the transducer moved to the left-hand side to avoid the shadow of air within the trachea (Fig. 4.3, Fig. 4.4).

Vessels

The large vessels (the carotid artery and the jugular vein) are behind the sternocleidomastoid muscles and lateral to the thyroid gland. The jugular vein shows as an oval shape and may collapse in certain phases of respiration or from the pressure of the transducer. The carotid artery is round and shows stronger wall echoes than the vein (Fig. 4.3).

Lymph nodes

The number of the lymph nodes is especially high in the neck. High-frequency ultrasound frequently demonstrates normal lymph nodes, which are usually oval, with a maximum diameter of 8 mm. The pattern is echo poor with an echo-rich hilus. In older people, the pattern becomes increasingly echo rich due to fatty degeneration, mostly starting from the hilus (see Fig. 4.5). The lymph nodes of older people are more difficult to detect because of their low contrast with the surrounding soft tissue. The normal vessels, which branch out symmetrically from the hilus ('hilar vascularity'), can be evaluated with high-resolution power Doppler.

Muscles

The muscles are echo poor with a striated structure. They are important as anatomical landmarks and serve as a reference point for evaluating the echo pattern of the thyroid.

Fig. 4.5. Normal lymph node (arrow) between vessels (Jv (jugular vein), Ca (common carotid artery)) and muscle (Smm (sternocleidomastoid muscle)). The oval shape and the echo-rich hilus are characteristic



Pathological findings

Thyroid

Congenital abnormalities

Failure of the thyroid to descend during embryogenesis leads to an ectopic thyroid or to an abnormal lobe in the midline (pyramidal lobe). The size of the isthmus is variable. The absence of one lobe is very rare. Abnormalities of the vessels are more common, e.g. a fifth artery (thyroid ima artery).

Endemic goitre (iodine-deficiency goitre)

Endemic goitre is very common in areas of iodine deficiency. Enlargement of the thyroid is a lifelong disorder in which the thyroid is enlarged with a homogeneous, echo-rich pattern in the early stage of the disorder (Fig. 4.6, see also Fig. 4.5).

The pattern becomes inhomogeneous (nodular goitre, Fig. 4.7), mainly in middle-aged patients, because of inhomogeneous growth of the cells and the development of macrofollicular echo-rich nodules. Degenerative alterations, such as cystic degeneration of the nodules and calcification, may also occur. Liquid parts of the nodules are echo free and may imitate cysts. Calcifications cause strong echoes, sometimes with acoustic shadows.

Autoimmune disorders of the thyroid

A common sonographic finding in autoimmune disorders of the thyroid is an echo-poor pattern.

Grave-Basedow disease

In this disease, autoantibodies against the thyroid-stimulating hormone receptor stimulate the thyroid in the same way as the hormone. The disease occurs more often in young (female) adults, but can be seen at any age. The younger the patient, the more characteristic are the symptoms of hyperthyroidism.

Fig. 4.6. Simple goitre (iodine deficiency) with a volume of 54 ml

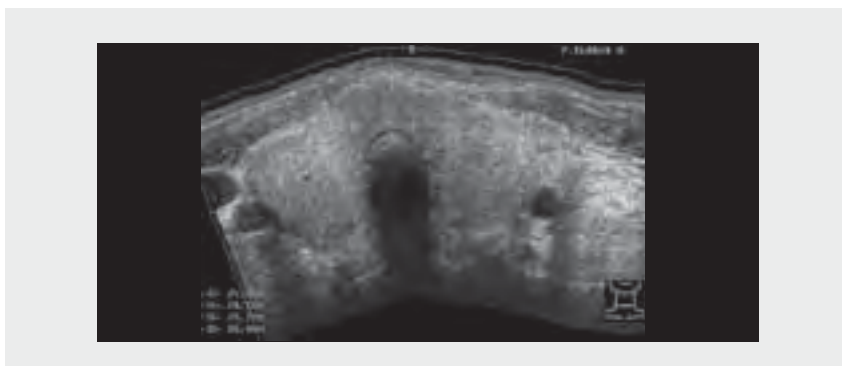
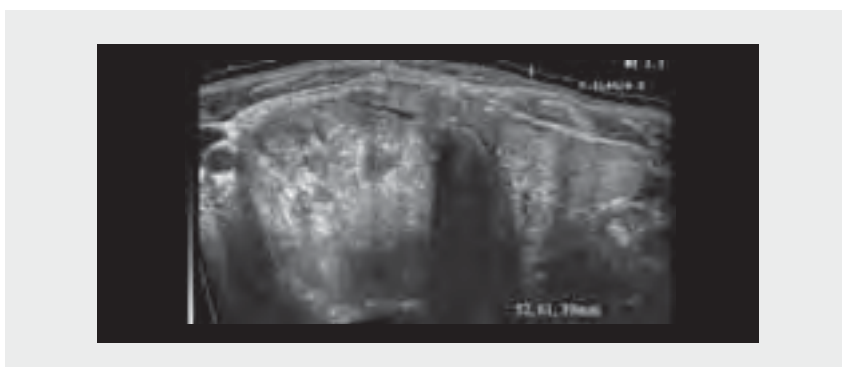


Fig. 4.7. Nodular goitre (iodine deficiency) with a volume of 96 ml. Typical inhomogeneous and echo-rich pattern



Ultrasound can be used to visualize a moderately enlarged thyroid with a characteristic echo-poor, homogeneous or slightly inhomogeneous pattern corresponding histologically to hyperplastic but empty follicles (Fig. 4.8).

Colour and power Doppler examinations demonstrate striking hypervascularity (Fig. 4.9). The flow in the feeding arteries is rapid, at more than 100 cm/s; a decrease to less than 40 cm/s on treatment is interpreted as a sign of a good prognosis.

Focal lesions (nodules) within the echo-poor thyroid in Grave-Basedow disease are independent of the basic disease and should be considered separately.

Autoimmune thyroiditis (Hashimoto thyroiditis)

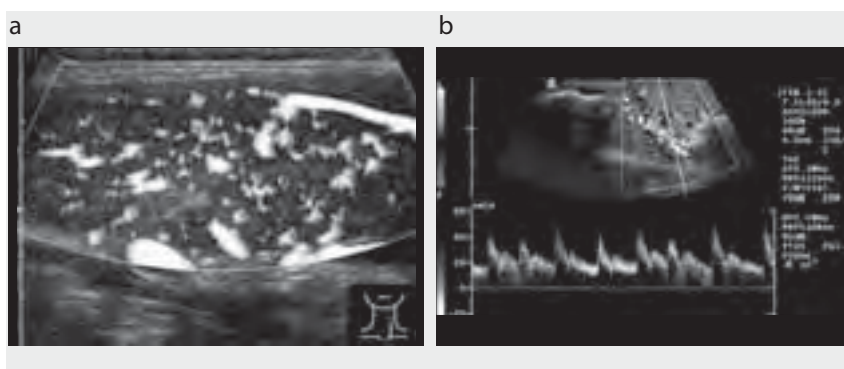
In this disease, lymphoplasmacellular infiltration slowly destroys the gland. This infiltration causes an echo-poor pattern of the thyroid, which develops over a long time. In the initial stage, the gland may be slightly enlarged; in the later (atrophic) stage, however, the thyroid becomes small with a volume of less than 10 ml (Fig. 4.10).

Colour Doppler ultrasound demonstrates hypervascularity, which is not as marked as in Grave-Basedow disease. The flow in the feeding arteries is less rapid.

Fig. 4.8. Grave-Basedow disease. The moderately enlarged thyroid shows a characteristically echo-poor pattern without contrast with the muscles (m, M). The outline of the right lobe is marked. The image is composed of transverse scans of the right and left lobes. Ca, common carotid artery



Fig. 4.9. Grave-Basedow disease. (a) Colour Doppler (white) demonstrates hypervascularity. (b) Spectral Doppler shows the acceleration of the flow in the feeding artery (ca. 50 cm/s)



In the early stage, hyperfunction may occur, and differentiation from Grave-Basedow disease becomes difficult. The typical clinical feature of the later stage is hypothyroidism.

Toxic adenoma, toxic goitre

The proliferation of autonomic cells, stimulated by iodine deficiency, leads to autonomic, toxic nodules or a diffuse functional autonomy causing hormone production independent of stimulation by thyroid-stimulating hormone. When the volume of the autonomic tissue is greater than 5–10 ml (depending on the iodine supply), hyperthyroidism results. The incidence of this type of hyperthyroidism is, therefore, higher than that of Grave-Basedow disease in areas of iodine deficiency. The disorder develops in a long-standing simple goitre and is seen mainly in the elderly (Fig. 4.11).

Fig. 4.10. Hashimoto thyroiditis. Note: (a) the echo-poor pattern (B-scan) of the small gland; (b) hypervascularity (power Doppler). Smm, sternocleidomastoid muscle; Ca, common carotid artery; Jv, jugular vein

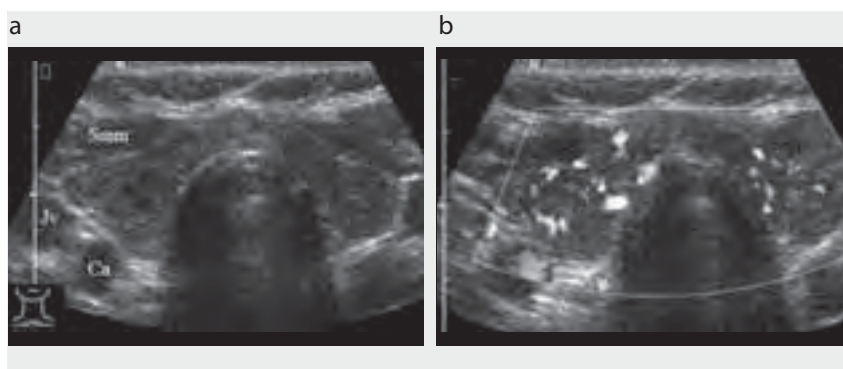
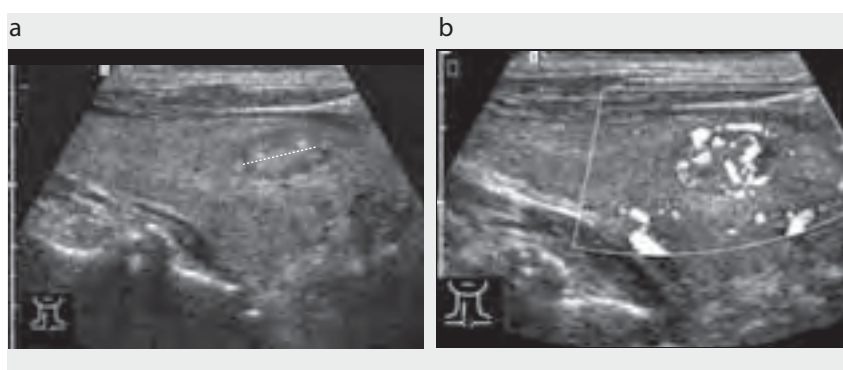


Fig. 4.11. Toxic adenoma. (a) Oval nodule (9 mm) with echo-poor halo. (b) Doppler technique shows a hypervascular pattern and the vascular halo



A typical autonomous adenoma is echo poor. The Doppler technique demonstrates hypervascularity (compared with the surrounding tissue) within the nodule and a halo consisting of vessels. Warm or toxic nodules may show a more echo-rich pattern in up to 30% of people, and hypervascularity may be missing in regressive nodules. Currently, there are no reliable sonographic signs to indicate the warm or toxic nature of a nodule. There is therefore no specific echo pattern for diffuse autonomy. A diagnosis of toxic nodule can be assumed only if others (e.g. Grave-Basedow disease, toxic adenoma) are excluded (Table 4.1).

Caution! Highly differentiated carcinomas of the thyroid are also hypervascular but without a halo.

Hypothyroidism

In adults, hypothyroidism is a consequence of the loss of thyroid tissue caused by thyroiditis, radiation therapy to the neck, radioiodine ablation or surgical resection of the thyroid. In most cases, ultrasound demonstrates a small thyroid (< 10 ml). A

Table 4.1. Clinical and sonographic differential diagnosis of hyperthyroidism

Ultrasound B-scan	Doppler	Additional aspects	Disorder
Symmetric goitre, echo-poor pattern	Hypervascularity, high velocity	Anti-TSH ophthalmopathy	Grave-Basedow disease
Moderate enlargement, echo-poor pattern	Hypervascularity	Anti-thyroid peroxidase	Hashimoto thyroiditis (initial stage)
Nodule, echo-poor, halo	Hypervascular halo	TSH	Toxic adenoma
Normal thyroid	Normal finding	TSH	Diffuse autonomy or thyreotoxicosis caused by drugs

TSH, thyroid-stimulating hormone.

characteristic echo-poor pattern is found in the late, atrophic stage of Hashimoto thyroiditis. The echo pattern in other cases is relatively normal or less homogeneous.

Thyroiditis

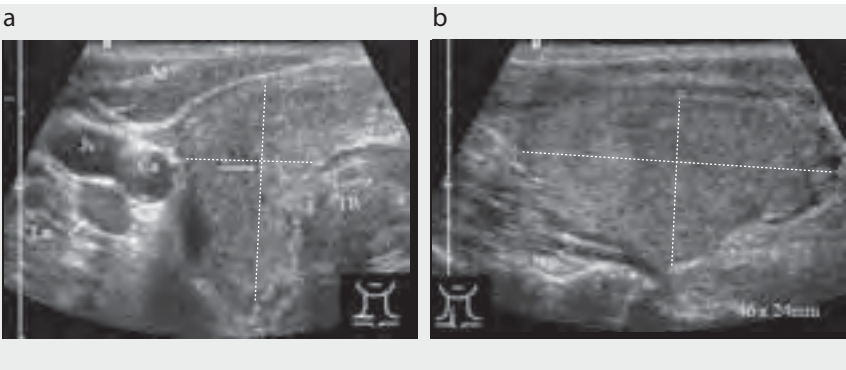
Pyogenic thyroiditis is very rare. Symptoms such as tenderness, swelling and redness are more often caused by pyogenic inflammation of the soft tissue around the thyroid. Ultrasound demonstrates dislocation of the thyroid and inflammation of the soft tissue (see below).

Subacute thyroiditis (giant cell thyroiditis, de Quervain thyroiditis) is thought to be viral in origin, because this disease often follows respiratory tract infections. Pain radiating to the mandible and the ear is a typical symptom.

An ultrasound B-scan shows an echo-poor area with a blurred margin. The gland may be slightly enlarged (Fig. 4.12). The lesions are more or less hypovascular than the surrounding thyroid tissue.

Chronic fibrosing thyroiditis (Riedel thyroiditis) is extremely rare. An irregular echo pattern caused by blurred echo-poor, nodular lesions is reported in a few cases.

Fig. 4.12. De Quervain thyroiditis. (a) Transverse (30 × 20 mm) and (b) longitudinal (46 × 24 mm) scan of the left lobe. Note the inflamed lymph node (Ln, 9 mm × 6 mm). The border of the slightly echo-poor inflamed area is better seen in the longitudinal scan. Ca, common carotid artery, Jv, jugular vein, M, muscles, TR, trachea

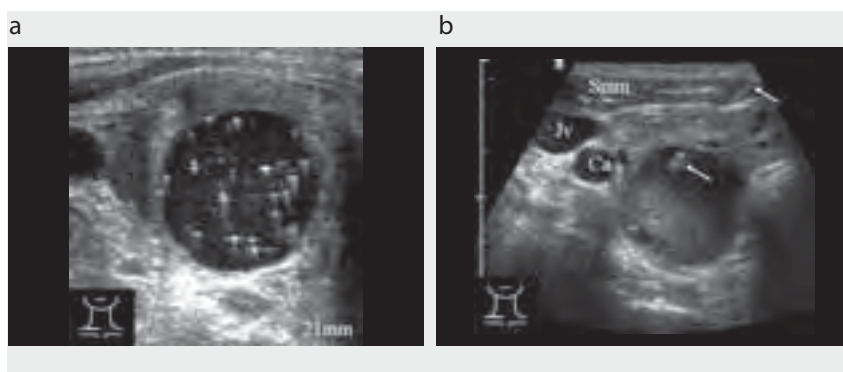


Focal lesions

Cysts and cystic lesions

True cysts of the thyroid are very rare, and most cystic echo-free lesions are cystic-degenerated nodules. The echo pattern of the solid parts determines its clinical classification. A typical event is the sudden onset of pain coupled with a palpable swelling caused by bleeding into the cyst (e.g. when practising sports). In these cases, ultrasound demonstrates a cloud of echoes floating in the fluid. The puncture shows brownish fluid ('chocolate cyst') (Fig. 4.13).

Fig. 4.13. Cystic lesions of the thyroid with haemorrhage ('chocolate cysts'). (a) Floating echoes (21 mm). (b) Sedimented blood cells. Note the echoes of the puncture needle (arrows). Ca, common carotid artery; Jv, jugular vein; Smm, sternocleidomastoid muscle



Solid nodules

Nodules in the thyroid are found in up to 50% of asymptomatic persons. Malignant tumours of the thyroid are rare. Nevertheless, differentiation of benign and malignant nodules is a challenge in the ultrasonic diagnosis of the thyroid.

Benign lesions

True adenomas are encapsulated, grow slowly and are mainly microfollicular. Adenomas vary in their function. Warm or toxic adenomas are highly differentiated and can accumulate iodine independently of thyroid-stimulating hormone regulation (see above).

Depending on the follicular structure, adenomas are mostly echo poor (microfollicular, Fig. 4.14) or more echo rich and rather homogeneous. Their contour is smooth. An echo-poor halo (B-scan) with vessels around the nodule is characteristic of a benign adenoma and is, therefore, best demonstrated with colour Doppler. Warm adenomas often show hypervascularity (Fig. 4.15).

Hyperplastic nodules develop over several years in cases of endemic goitre, caused by the differential growth ability of the thyroid cells. These lesions are not true neoplasms. Owing to their normofollicular or macrofollicular structure, they are often echo rich with an echo-poor halo. Degenerative alterations, such as cystic parts or calcifications, are common, causing a complex sonographic pattern with echo-free areas and strong echoes (Fig. 4.16, Fig. 4.17).

Fig. 4.14. Adenoma (21 mm) with a complex echo pattern caused by calcification, regressive cystic components and an echo-poor halo

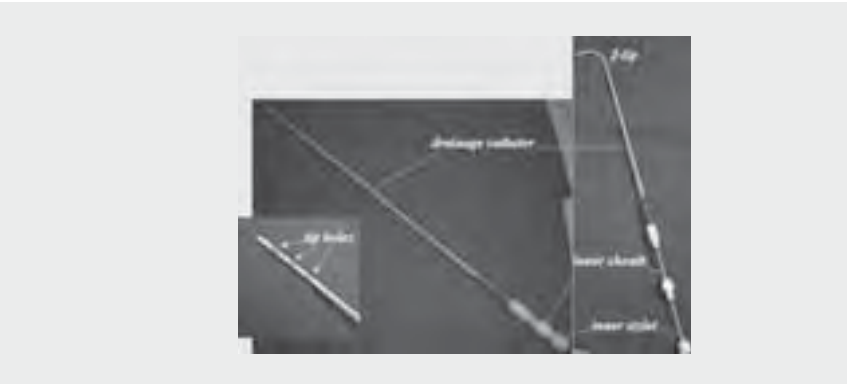


Fig. 4.15. (a) B-scan of an adenoma of the thyroid. shows an echo-poor pattern and a halo. (b) Power Doppler shows signals in the nodule and the vascular halo

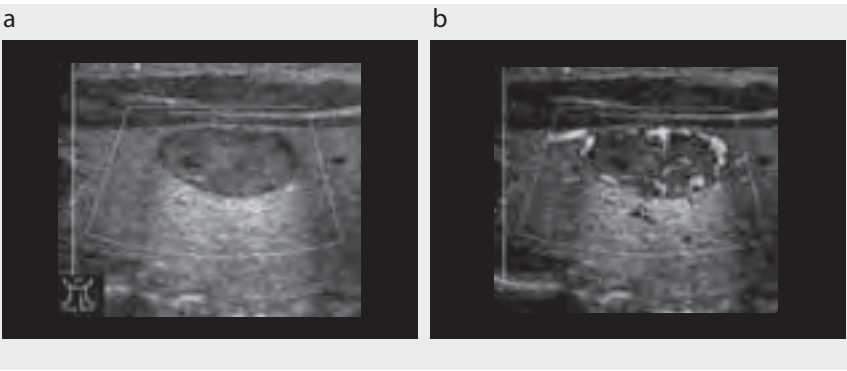
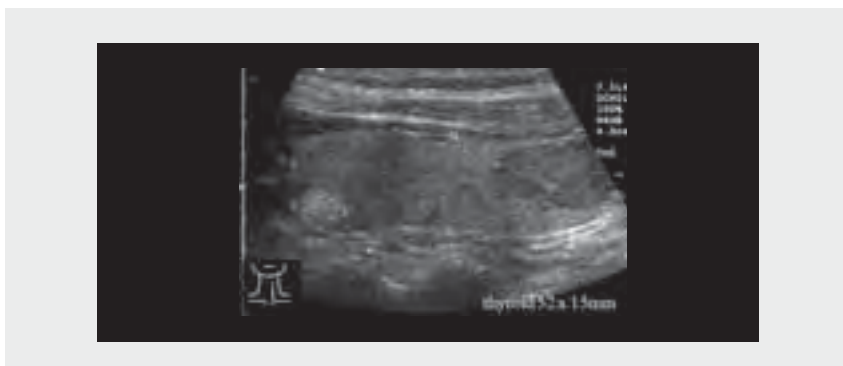


Fig. 4.16. Nodule with a moderately echo-poor pattern surrounding tissue



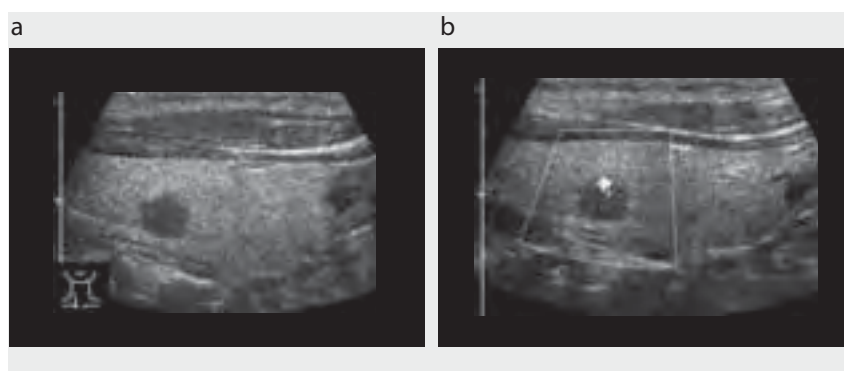
Fig. 4.17. Echo-rich nodule (8 mm) and echo-poor nodule with halo (19 mm)



Malignant tumours

Papillary and **follicular carcinomas** are the commonest thyroid carcinomas (ca. 70% and 15%, respectively). They are highly differentiated and grow slowly. **Anaplastic carcinoma** is less common, especially in areas with no iodine deficiency (ca. 5–10%), and is a carcinoma of older patients (> 65 years). **Medullary carcinoma** arises from the C cells. It occurs sporadically or as part of multiple endocrine neoplasia (IIa or IIb) (Fig. 4.18, Fig. 4.19, Fig. 4.20, Fig. 4.21, Fig. 4.22, Fig. 4.23). **Metastases**, mainly from lung cancer and malignant lymphomas, may involve the thyroid gland.

Fig. 4.18. Small papillary carcinoma (9 mm). (a) B-scan shows an echo-poor lesion with a slightly irregular contour, partially blurred halo-free outline and without a halo. (b) Power Doppler shows a feeding vessel but no vascular halo



The malignant tumours are echo poor and slightly inhomogeneous, although an inhomogeneous pattern is difficult to recognize in smaller lesions. An extremely echo-poor pattern is found in malignant lymphomas and anaplastic carcinomas. Lack of a halo is typical. The contour is irregular and may show pseudopods or spicula. Interruption of the thyroid capsule and infiltration of the surrounding tissue can be visualized. When the sagittal diameter is greater than the transverse diameter, the finding is usually suspect.

Fig. 4.19. Papillary carcinoma (between arrow, 19 mm) of the thyroid with dispersed stronger echoes indicating microcalcification causing an incomplete shadow

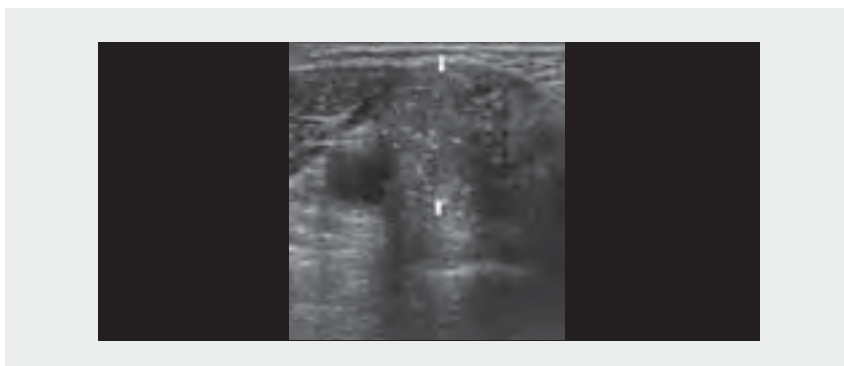


Fig. 4.20. Follicular carcinoma (19 mm). Note the irregular contour, the penetration through the capsule (arrow) and the complex echo pattern with spotted calcifications (shadows)



Fig. 4.21. Large anaplastic carcinoma (diameter, 67 mm) arising in a nodular endemic goitre. The carcinoma in the left lobe is echo poor; the pattern in the right lobe and the isthmus is echo rich. TR, trachea (see Fig. 4.7)

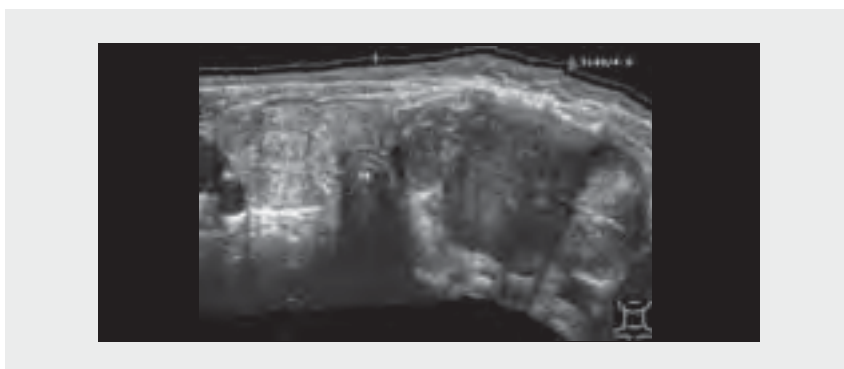


Fig. 4.22. Metastasis (57 mm × 34 mm) from lung cancer in the right thyroid lobe: inhomogeneous, moderately echo-poor pattern, irregular outline

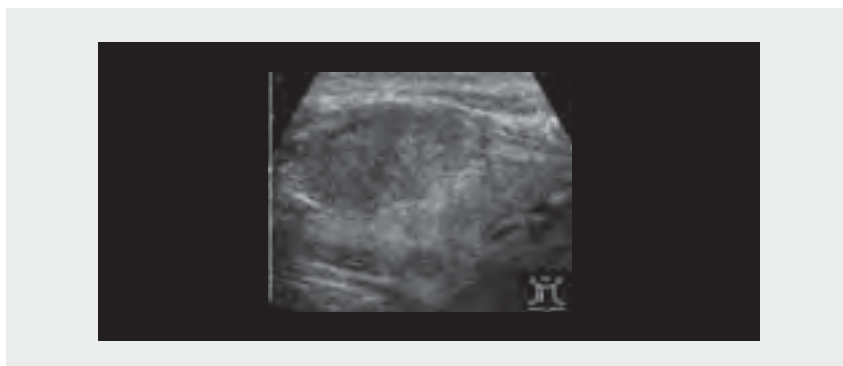
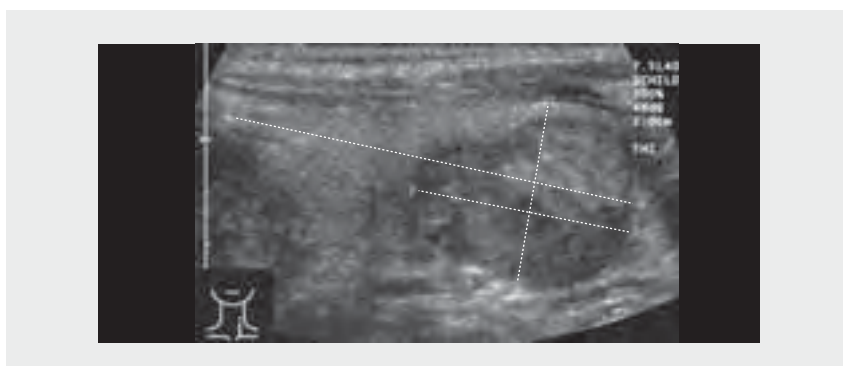


Fig. 4.23. Malignant lymphoma (secondary) in the left thyroid lobe (18 mm × 22 mm)



Dispersed strong echoes arising from microcalcifications are characteristic in papillary carcinoma. Spotted calcifications also occur in medullary and anaplastic carcinomas. Occasionally, small echo or cystic parts are seen in papillary carcinomas.

The Doppler technique shows hypervascularity in highly differentiated carcinomas, but without a vascular halo. Anaplastic carcinomas, most of the metastases and the lymphomas are hypovascular when compared to the thyroid.

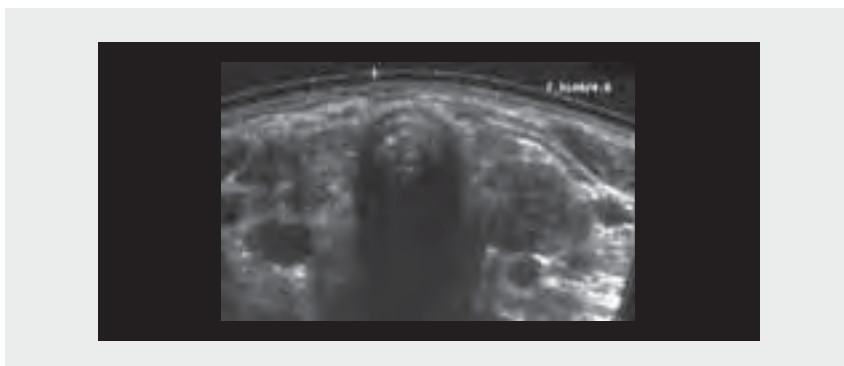
Post-treatment thyroid

Providing the patient with information about the treatment (disease and method) is a prerequisite for post-treatment check-ups. This is especially important after surgery.

After resection of an endemic goitre, relatively large nodular relapses (Fig. 4.24) with inhomogeneous echo patterns on both sides of the trachea may be seen. Lack of the isthmus is typical of the post-operative situation. After subtotal resection, it is sometimes difficult to identify small thyroid remnants, especially if they are not echo rich.

Examination of the lymph nodes is the main objective of follow-up checks after surgical treatment of carcinomas. Enlarged, rounded lymph nodes are suspect (see

Fig. 4.24. Relapse of a nodular endemic goitre (no isthmus) with large nodules with inhomogeneous echotexture



below). It is interesting that lymph node metastases of highly differentiated carcinomas show a hypervascularity similar to that of the primary tumours.

In Grave-Basedow disease, the typical echo-poor pattern disappears with functional remission after treatment. A reduction in the elevated flow velocity in the feeding arteries appears to be an early sign of successful treatment. In contrast, the echo-poor pattern of Hashimoto thyroiditis is seen in all phases, independent of function.

Radioiodine ablation of the thyroid or radiation of the neck (lymphomas) causes a reduction of thyroid tissue and ultimately leads to a small thyroid.

Warm or toxic adenomas treated successfully with alcohol instillation (see below) not only become smaller and more echo rich, but their hypervascularity disappears.

Parathyroid glands

Ultrasound is the first-line method for preoperative localization of orthotopic adenomas of the parathyroid glands in primary hyperthyroidism and for diagnosis of hyperplasia of the parathyroid glands in patients with renal failure.

Orthotopic adenomas are more or less echo poor, smooth nodules at the dorsal border of the thyroid. Their shape is variable, mostly oval, but sometimes moderately long, triangular or lobed. The pattern is more echo poor than that of the normal thyroid but may become complex, with more echo-rich and echo-free areas due to regressive alterations.

Colour Doppler enables identification of the feeding vessels (Fig. 4.25, Fig. 4.26).

Branchial cervical cysts

Medial thyroglossal cysts are located in the midline below the hyoid, above the thyroid. They are usually diagnosed in childhood.

Lateral cervical cysts are located at the anterior margin of the sternocleidomastoid muscle. They grow slowly and sometimes become visible or symptomatic in young adults. Ultrasound demonstrates a lesion with the typical signs of a cyst (round or oval, smooth outline, echo free). In some symptomatic cases, a cervical cyst shows a more or less echo-rich, homogeneous pattern, caused by a secondary infection (Fig. 4.27). A cystic cutaneous fistula may develop.

Fig. 4.25. Adenoma of the parathyroid (p, 12 mm × 4 mm), echo-poor pattern, lobulated shape

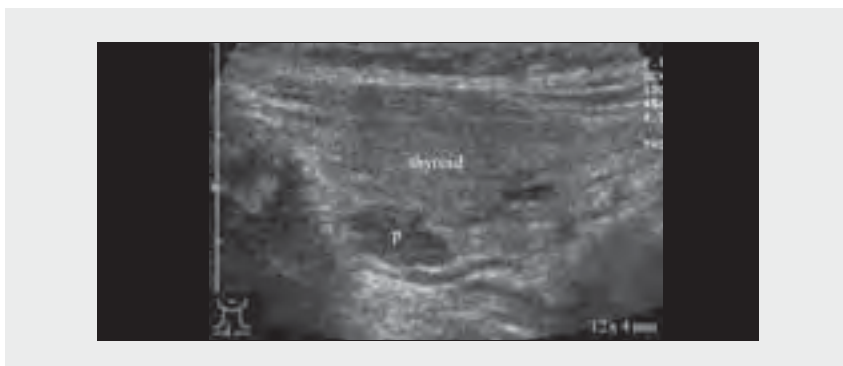


Fig. 4.26. Adenoma of the parathyroid. Echo-poor pattern showing irregular outline. Power Doppler shows the vessels inside the adenoma. Oe, oesophagus

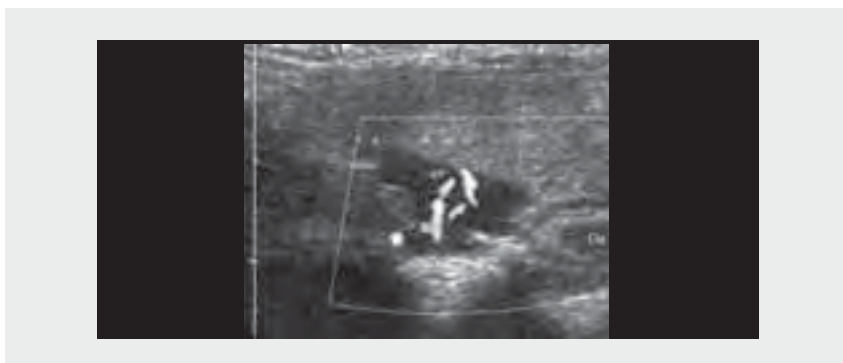
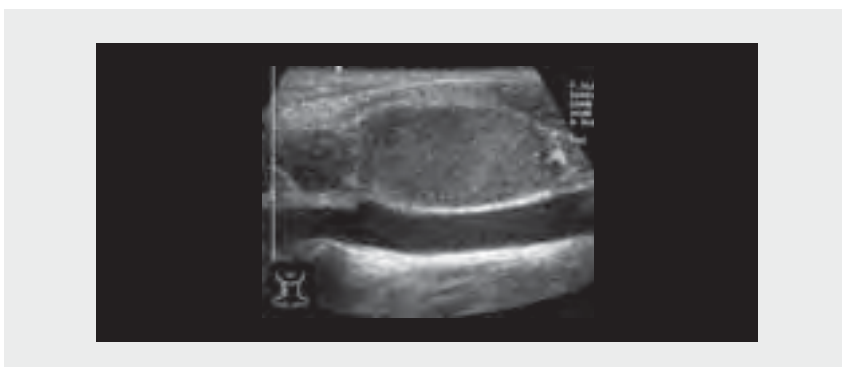


Fig. 4.27. Lateral cervical cyst (diameter, 33 mm). The homogeneous echoes within the cyst are caused by a secondary inflammation. Cranially, note an enlarged, echo-poor inflammatory lymph node



Primary tumours in the neck

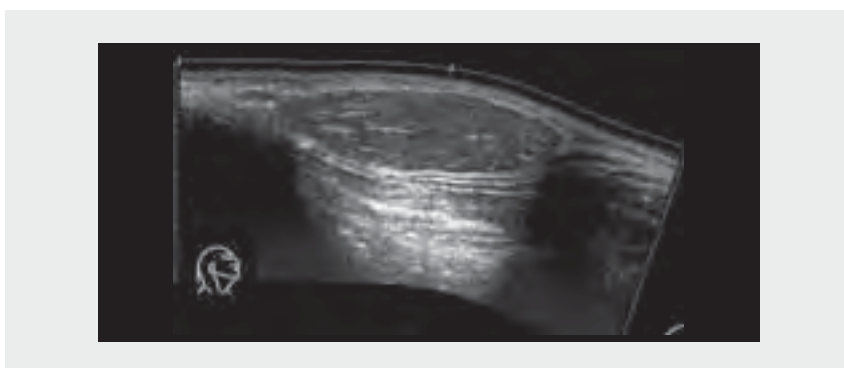
Primary tumours in the neck are rare in adults.

Lipomas and lipofibromas originating from the skin are situated in the nucha. Their pattern is echo rich, and the margins are smooth (Fig. 4.28).

Glomangioma arising from the carotid glomus is demonstrated in the carotid bifurcation as a homogeneous, echo-poor, hypervascular tumour.

Malignant tumours of the deeper layers arise in the oesophagus, the larynx or the hypopharynx. They are visualized as echo-poor, inhomogeneous masses with irregular outlines, often infiltrating the surrounding structures (e.g. the thyroid).

Fig. 4.28. Fibrolipoma (diameter, 54 mm) in the neck. The location, the oval shape and the echo pattern are characteristic



Inflammation of the soft tissue

Inflammation of the cervical soft tissue usually originates from a neighbouring structure, such as the tonsils, or lymphogenously or iatrogenically. The echo pattern may be very poor (abscess) or complex and echo rich with strong echoes (gas) (Fig. 4.29). The distension depends on the fascias and anatomical structures. Structures such as muscles or the thyroid are swollen. In the jugular vein, thrombosis may occur as a complication or, in some cases, as the initial focus (Fig. 4.30). In these cases, the vein is no longer compressible and the wall is thickened. The thrombus itself is echo poor.

Colour Doppler demonstrates hyperaemia of inflamed tissue or avascular abscesses.

Typical peritonsillar abscesses can be demonstrated as echo-poor lesions medial to the large vessels by using the air echoes inside the larynx and the moving echoes of the tongue as anatomical landmarks.

Lymph node diseases

Enlarged lymph nodes are often found in the neck. Reactive hyperplasia may be the commonest cause of lymphadenopathy, but malignant lymphomas and metastases of tumours of the head, the neck or the lung and even distant metastases (e.g. stomach cancer) are also common. Diagnosis is usually made by palpation, often by patients themselves. Several studies have shown, however, that ultrasound is useful in detecting nonpalpable 'occult' metastases and for the staging and follow-up of lymphomas.

Fig. 4.29. Abscess behind the (displaced) left thyroid lobe. B-scan shows an inhomogeneous, echo-poor area with some gas echoes (arrow). A line of strong air echoes indicates the trachea. Ca, common carotids artery; Jv, jugular vein



Fig. 4.30. Inflammatory thrombosis of the left jugular vein. The vein is dilated (compared with the carotid artery) and filled with echo-rich thrombotic material. The wall is echo poor (arrow). Ca, common carotid artery



Lymph nodes involved in **inflammatory diseases** are usually enlarged, but their architecture is not destroyed (Fig. 4.31, Fig. 4.32). Ultrasound therefore visualizes enlarged, oval lymph nodes with smooth contours. The long (longitudinal) diameter is greater than 5–10 mm. The ratio of the long to the short axis remains greater than 1.5. The pattern is more or less echo poor, and the echo-rich hilus is discernible. Colour Doppler shows hyperaemia but normal vascular architecture, with vessels branching out from the hilus ('hilar vascularity') (Fig. 4.32 (a)). The resistance index in inflammatory lymph nodes is less than 0.65.

Abscess formation may cause echo-free areas, and they may break through the capsule into the surrounding tissue.

Granulomatous inflammation (*Boeck disease*), tuberculosis or *Mycobacterium avium-intracellulare* complex infection often result in atypical sonographic findings of the lymph nodes involved, similar to the findings for malignant lymph nodes. The enlarged lymph nodes are rounder, and the patterns become inhomogeneous

Fig. 4.31. Enlarged inflammatory lymph nodes (LK). B-scan shows an echo-poor pattern but an echo-rich hilus (transverse scan through the short axis of the lymph node). Ca, common carotid artery

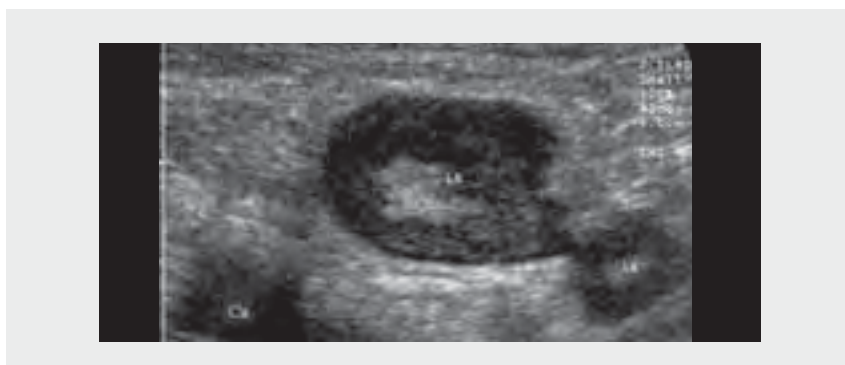
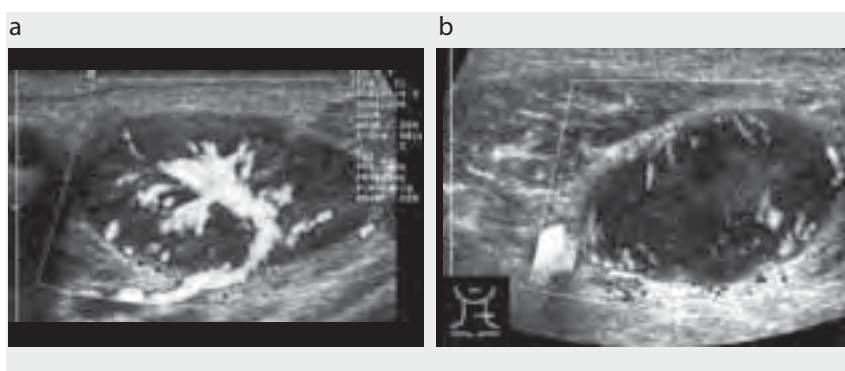


Fig. 4.32. Power Doppler view of cervical lymph nodes. (a) Inflammatory lymph node shows hilar vascularity. (b) Lymph node metastasis (diameter, 28 mm) with peripheral vascularity



with echo-poor granulomas or echo-free caseation. Atypical vessel architecture, displacement of vessels due to caseation and a higher resistance index (up to 0.72) are described in cases of **tuberculosis**.

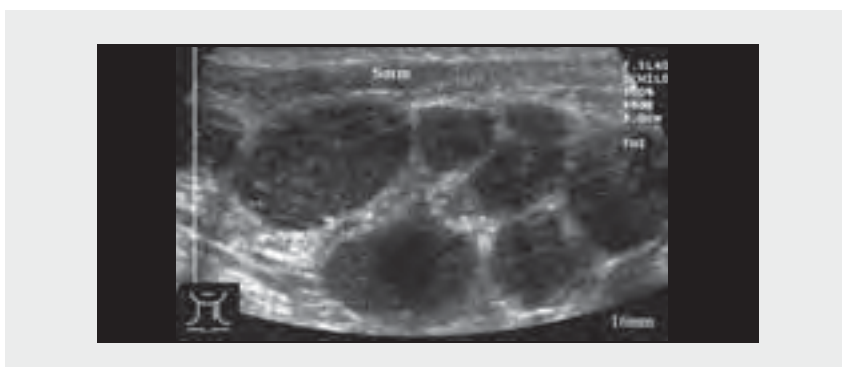
Metastatic lymph nodes are moderately or considerably enlarged, with a more rounded shape. The pattern is less echo poor and inhomogeneous, and the hilus sign is often missing. The contour is irregular, with short pseudopods, indicating infiltration through the capsule (Fig. 4.33). The vascular pattern is irregular, with vessels penetrating the capsule ('peripheral vascularity') (Fig. 4.32b) and the resistance index is high (> 0.8 – 0.9).

The lymph nodes involved in **malignant lymphomas** are extremely echo poor. They are oval, round or polygonal if arranged in a conglomerate. The margin is smooth (Fig. 4.34). The vascular pattern is variable and often regular, as in inflammatory hyperplasia, and the resistance index is less elevated (around 0.65–0.75).

Fig. 4.33. Lymph node metastasis (24 mm × 18 mm) from lung cancer: inhomogeneous, echo-poor pattern compared with the pattern of the thyroid. The jugular vein (Jv) is displaced. Ca, common carotid artery



Fig. 4.34. Conglomerate of enlarged cervical lymph nodes, non-Hodgkin lymphoma: echo-poor pattern, oval or polygonal shape, no hilus sign. Smm, sternocleidomastoid muscle



Differential diagnosis

Goitre

Generally, differentiation of an enlarged thyroid is not difficult.

An endemic goitre shows an echo-rich, homogeneous or mostly inhomogeneous echo pattern, with echo-rich macrofollicular nodules and regressive alterations. Echo-poor sections in endemic goitre, especially if connected with fast growth, are suspect and may indicate malignancy.

Large malignant tumours cause asymmetric enlargement of the thyroid and show an echo-poor, heterogeneous pattern. Dispersed stronger echoes in the mass are caused by calcifications (microcalcification). They should not be misinterpreted as an echo-rich pattern.

In Grave-Basedow disease, the thyroid is symmetrically enlarged and echo poor, with a smooth margin and a regular shape. Hypervascularity is striking and nearly pathognomonic. The similar Hashimoto thyroiditis, with a slight echo-poor enlargement, can be differentiated by less rapid flow in the feeding arteries or more easily by clinical aspects (no ophthalmopathy) and the analysis of antibodies (Table 4.2).

Table 4.2. Differentiation of the enlarged thyroid (goitre)

Ultrasound B-scan	Doppler	Other aspects/function	Diagnosis
Symmetric or asymmetric goitre, echo-rich, mostly inhomogeneous, regressive alterations	–	Normal function, late-stage hypothyroidism and hyperthyroidism (toxic adenoma(s) possible)	Endemic goitre
Asymmetric, echo-poor, irregular outline	Sometimes hypervascular	Fast-growing goitre	Malignant tumour
Symmetric, echo-poor, smooth margin	Hypervascular, high flow	Hyperthyroidism (ophthalmopathy), TSH antibodies	Grave-Basedow disease
Symmetric, echo-poor moderate enlargement	Hypervascular	Hyperthyroidism or normal function, TPO antibodies	Hashimoto thyroiditis, initial stage

TSH, thyroid-stimulating hormone; TPO, thyroid peroxidase.

Small thyroid

Small thyroids (< 10 ml) in adults are consequences of inflammatory disease or therapy. Any previous surgical reduction or radioiodine treatment should be established from the case history. A small thyroid with a regular echo pattern, associated with hypothyroidism, can also be due to previous radiation therapy (e.g. for malignant lymphoma). An echo-poor pattern is typical in the atrophic stage of Hashimoto thyroiditis.

Echo-poor nodule

Differentiation of focal lesions in the thyroid gland is the most challenging aspect of sonographic diagnosis of the thyroid. Nodules are very common and mostly asymptomatic. Malignant tumours are rare and, in the early stage, are also asymptomatic.

Echo-rich lesions are hyperplastic nodules or benign adenomas. Echo-poor nodules are a problem, as many adenomas and malignant tumours show this ultrasonic feature. Additionally, warm and toxic adenomas as well as highly differentiated carcinomas are hypervascular. In many cases, a fine-needle biopsy is required to establish a final diagnosis, although there are several sonographic signs that should raise suspicions of malignancy (Table 4.3). The presence of only one of these symptoms should be investigated by puncture; if three or more of these signs are present, malignancy is likely. The sonographic criteria for malignant focal lesions of the thyroid are:

- echo-poor, inhomogeneous pattern
- microcalcifications
- no halo (B-scan)
- greater sagittal diameter
- size > 3 cm

- blurred margin
- irregular contour
- infiltration of surrounding structures
- high attenuation
- hypervascularity within the nodule but with no vascular halo (Doppler) and
- enlarged lymph nodes.

It is also useful to look at other symptoms and findings. A history of radiation therapy of the neck, a family history of thyroid nodules, fast growth of the nodule or enlarged lymph nodes are suspect. Proof of a warm, toxic nodule by scintigraphy or a low level of thyroid-stimulating hormone (but not hyperthyroidism itself) exclude a carcinoma. The differential diagnoses of echo-poor lesions is illustrated in Table 4.3.

Table 4.3. Differential diagnoses of echo-poor focal lesions of the thyroid

Disorder	Echo pattern	Contour	Doppler
Follicular adenoma	Halo	Smooth	Hypervascular
Carcinoma, highly differentiated	Heterogeneous, no halo, microcalcifications	Irregular, blurred	Hypervascular, no vascular halo
Carcinoma, poorly differentiated	Heterogeneous	Irregular, blurred	Hypovascular
De Quervain thyroiditis	Homogeneous	Blurred	Hypovascular
Abscess (acute thyroiditis)	Echo free	Blurred	Avascular
Parathyroid adenoma	Heterogeneous	Smooth, variable shape	Feeding vessels

Other lesions and masses in the neck

It is generally not difficult to differentiate between thyroid tumours and tumours of other structures. Tumours of the lymph nodes are situated lateral to the great vessels. Carcinomas of the hypopharynx, larynx or cervical oesophagus are situated behind the thyroid, but may infiltrate the gland from the dorsal surface. Rare tumours and masses, such as glomangiomas or cervical cysts, are also characterized by a typical location.

Ultrasound-guided fine-needle biopsy

Fine-needle biopsy is a good complement to ultrasonography of the thyroid and the neck. If the general recommendations and rules discussed in Chapter 3 are followed, biopsy of lesions in the neck is particularly easy, almost without risk and can be carried out on outpatients.

Fine-needle biopsy of thyroid nodules is done mainly by aspiration, as described above. A second biopsy is recommended for less experienced operators to avoid false or insufficient results. A complementary biopsy with a cutting needle may be useful for the diagnosis of lymphomas and anaplastic carcinomas.

All suspect lesions should be investigated by fine-needle biopsy of the thyroid, if a diagnosis cannot be made with non-invasive tests. De Quervain thyroiditis can be diagnosed with cytological proof of the characteristic giant cells.

In the same way, lesions and masses outside the thyroid, especially unclear tumours, abscesses and suspicious lymph nodes, can be punctured. To avoid fistulas, if an atypical, possibly tuberculous, lymph node is punctured, it is useful to shift the skin over the lesion before inserting the needle.

Finally, an ultrasound-guided puncture can be used to treat hot adenomas of the thyroid or of the parathyroid gland by percutaneous injection of 96% ethanol. The position of the needle has to be controlled precisely to avoid injury to the recurrent nerve. Colour Doppler demonstrates a decrease in hypervascularity after successful treatment, while a B-scan shows regression in the size of the nodule and a less echo-poor pattern.



Chapter 5

Chest

Indications	93
Examination technique	93
	93 Equipment, transducer
	94 Preparation
	94 Position of the patient
	94 Scanning technique
Normal findings	94
Pathological findings	95
	95 Chest wall
	97 Bone
	99 Pleura
	103 Diaphragm
	103 Peripheral pulmonary consolidation
	109 Mediastinum

Chest

Indications

The fact that ultrasound is reflected completely by the bony thorax and by the air-filled lungs led to the mistaken notion that sonography is not a helpful diagnostic tool for the chest. In recent years, however, technical advances and new scientific evidence have led to a steadily broadening spectrum of applications of sonography to diseases of the chest: chest-wall lesions can be depicted, and pleural effusion and peripheral lung consolidation have become useful sonic windows. Although the sonographic image does not provide a complete overview of the chest, it is useful for certain indications:

Symptoms:

- chest pain
- dyspnoea
- fever
- inflow congestion.

Physical examination:

- palpable mass
- percussion dullness or damping
- rale.

In addition to X-ray, CT and magnetic resonance imaging (MRI):

- differentiation of solids and liquids
- infiltration of the pleura or chest wall
- vascularization
- breathing dynamics.

Examination technique

Equipment, transducer

Any equipment used for sonographic examination of the abdomen and small parts may also be used to examine the thorax. Ultrasound examination of the chest wall and the axilla and supraclavicular regions generally requires a linear probe with frequencies of 5–8 MHz. Recently introduced probes of 10–13 MHz are excellent for evaluating lymph nodes. For investigating the lung, a convex or sector probe of 3–5 MHz provides adequate depth of penetration.

Preparation

No specific preparation is necessary.

Position of the patient

Usually, the dorsal and lateral images are obtained with the patient sitting, whereas the supine position is used for visualizing the ventral side. When the arms are raised and crossed behind the head, the intercostal spaces are extended.

Scanning technique

The transducer is moved along the intercostal spaces in the dorsal-to-ventral direction and in longitudinal and transverse positions. Bedridden and intensive-care patients are examined by turning them to the oblique position on the bed. During every stage of the examination, the user should determine the breath-related movement of the pleura, the so-called 'gliding sign', in combination with respiratory manoeuvres, such as coughing or sniffing. The diaphragm is examined from the abdomen, in the subcostal section by the transhepatic route on the right side and, to a lesser extent, through the spleen on the left side.

Normal findings

Fig. 5.1, Fig. 5.2 and Fig. 5.3 show the normal aspect of the chest.

Fig. 5.1. Chest wall in the third intercostal space. Ultrasound imaging is limited by total reflection from the aerated lung, so-called visceral pleura (arrows): an echogenic, breathing-dependent, sliding line. M, pectoralis muscle

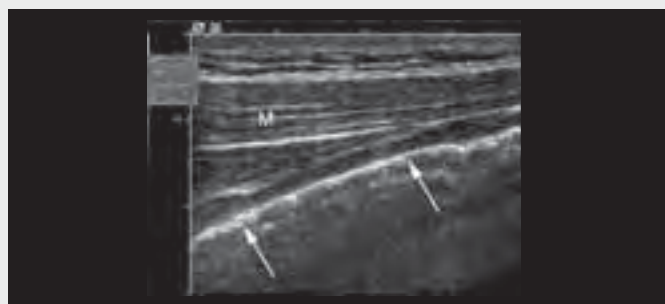


Fig. 5.2. (a) The visceral pleura (arrow) dorsal to the rib cartilage (C) is shifted ventrally towards the transducer as a result of various ultrasound beam rates in cartilage and soft tissue of the chest wall: velocity artefact. (b) The rib (R) absorbs the ultrasound beam and leads to an acoustic shadow

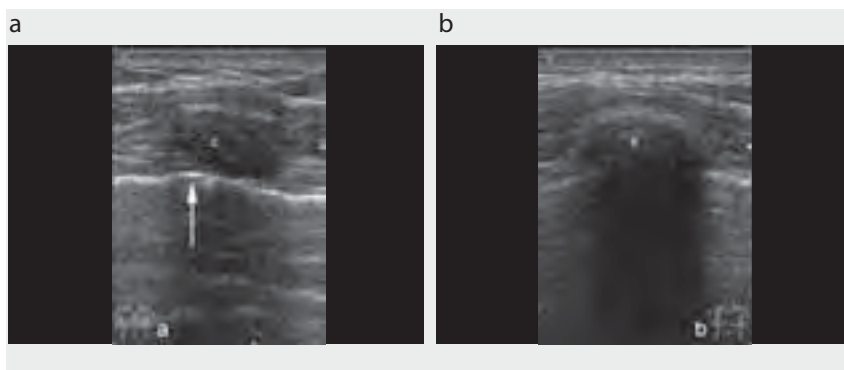


Fig. 5.3. Pleura. The sliding, wide visceral pleura (1) is an artefact caused by total reflection at the air-filled lung. Between the pleural sheets (2), echo-free fluid in the pleural space can be seen. (3) The echogenic parietal pleura



Pathological findings

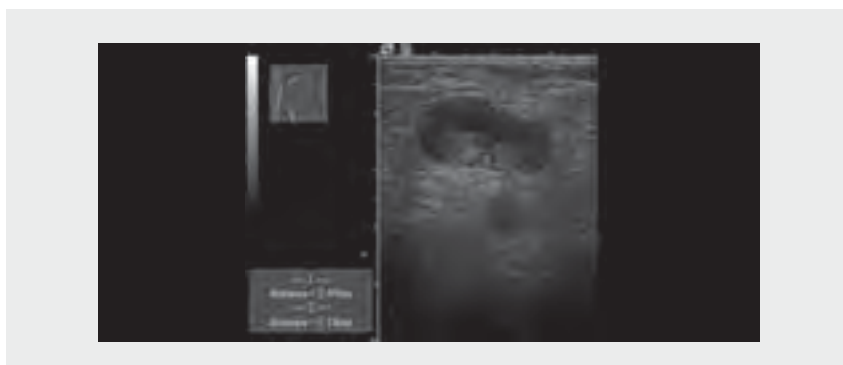
Chest wall

Soft-tissue lesions

Suspect or unclear findings found during palpation of the chest wall should initially be examined by ultrasound. In most cases, the examiner will find lymph nodes, which are the most clinically relevant finding.

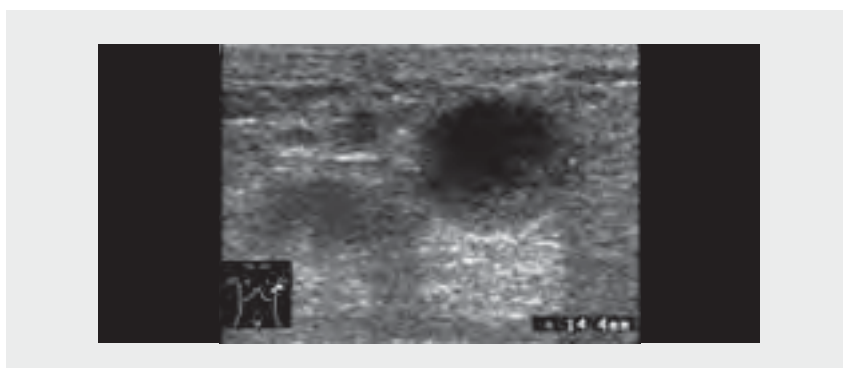
Reactive and inflammatory lymph nodes are seldom larger than 20 mm. Their form is oval or elongated, and the margin is smooth, sharply demarcated and arranged in a string-of-pearls fashion. Depending on the anatomical structure, there is often an echogenic central zone, a so-called 'hilar fat sign' (Fig. 5.4). This echogenic centre becomes larger during the healing phase of inflammatory lymph nodes. Vascularization is regular.

Fig. 5.4. Inflammatory lymph node: oval, smooth, and clearly demarcated. Echo-rich central zone is called the 'hilar fat sign', corresponding to the fatty connective tissue in the central region of the lymph node



Lymph node metastases appear as round-to-oval inhomogeneous structures, usually with well defined borders. They typically show extracapsular growth with irregular borders and diffused infiltrating growth into vessels and the surrounding tissue (Fig. 5.5). Vascularization is irregular, mostly at the margin and corkscrew-like.

Fig. 5.5. Lymph node metastasis of an epidermoid lung cancer. Rounded, invasive growth into the surrounding tissue, sometimes echo inhomogeneous, with reduced mobility



Axillary, supraclavicular and cervical nonpalpable lymph nodes are more easily detected by ultrasound than by CT. This is important for the staging of lung and breast cancers.

A homogeneous, echo-poor, sharply demarcated shape is typical of **malignant lymphomas**. Lymph nodes in centrocytic malignant lymphomas or Hodgkin lymphomas can present as almost echo free and cyst-like. Lymphomatous lymph nodes are round and oval but seldom triangular. Vascularization is enhanced or irregular (Fig. 5.6).

Note: Acute inflammatory lymph nodes are similar to lymphomatous lymph nodes.

Fig. 5.6. Malignant B-cell lymphoma. Smooth margin, sharply demarcated, hypoechoic with enhanced irregular vascularization



Haematomas can present with varying echo patterns as a result of the number of erythrocytes and the grade of organization. They can first be echo rich, then echo poor and later inhomogeneous.

The echogenicity of **lipomas** depends on their cellular fat content and differences in impedance in the interstitial tissue. The sonographic texture can vary from echo poor to relatively echo rich. The borderline of the surrounding tissue can be incomplete.

Bone

Rib and sternum fractures: it is surprising that rib fractures are diagnosed twice as frequently by sonography than by chest radiography. Conventional X-rays provide an overall view of the chest but have the disadvantage of occasional superimposition. On ultrasonic examination, the patient indicates the site of the pain and the examiner obtains an image by closely following the course of the ribs, looking for typical signs of fracture at the corticalis reflection (see below and Fig. 5.7). Minute dislocations and fissures are visible as a reverberation artefact at the traumatized point, referred to as a 'chimney phenomenon'.

Fig. 5.7. Rib fracture. Step-and-gap formation of 1 mm (arrow), not seen on X-ray. M, intercostal muscle; F, subcutaneous fat



The sonographic signs of rib and sternum fractures, at the site of pain, are:

Direct signs:

- gap
- step
- dislocation.

Indirect signs:

- haematoma
- chimney phenomenon
- pleural effusion
- lung contusion
- skin emphysema.

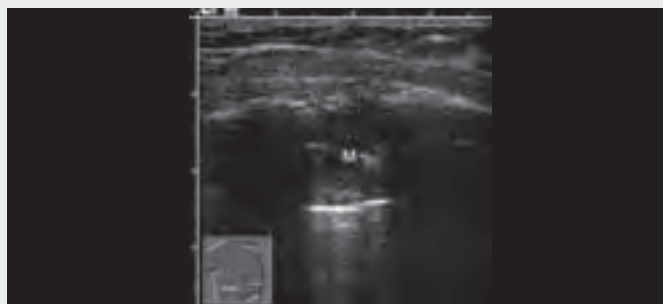
Note: At the sternum, the synchondrosis of the manubrium should not be misinterpreted as a fracture (Fig. 5.8).

Fig. 5.8. Sternum fracture (F) with dislocation of 5 mm. The hump and cortical interruption of the manubrium (M) should not be misinterpreted as a fracture



Osteolytic metastases in the bony thorax cause disruption of the corticalis reflex with pathological ultrasound transmission. The echo texture is sometimes poor and hazy (Fig. 5.9). With colour Doppler, corkscrew-like vessel neoformations can be found. During therapy, the size, shape and structure of metastatic osteolysis can be used as follow-up parameters.

Fig. 5.9. Osteolytic rib metastasis (M). The cortical reflection of the rib is disrupted. The ultrasound beam passes through the inhomogeneous metastatic formation to the visceral pleura



Pleura

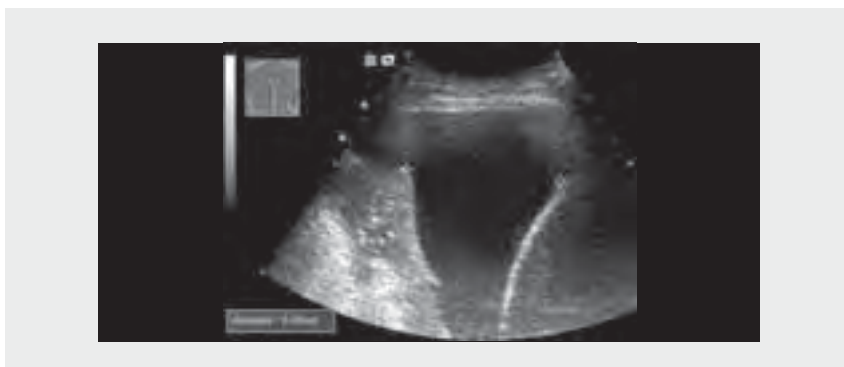
The normal pleura is only 0.2–0.4 mm thick and, hence, at the limit of resolution of current ultrasound systems. It is not always possible to visualize sonographically both the pleural blades and the hypoechoic space between them. The finer visceral pleura is submerged in the thick line of total reflection of the ultrasound at the air-filled lung (Fig. 5.3). As soon as the peripheral lung is free of air because of a pathological process, the actual visceral pleura can be marked off as a fine echogenic line.

Pleural effusion

In contrast to X-ray, ultrasound can detect pleural effusions of as little as 5 ml laterodorsally to the angle between the chest wall and the diaphragm, with patients in either a standing or sitting position. By turning the supine patient slightly sideways, small dorsal effusions can also be identified.

Pleural effusions are echo free as they are liquid formations (Fig. 5.10). Similarly, pleural scars and thickening are also visualized as hypoechoic structures. However, pleural effusion changes its shape with respiration and shows the fluid colour sign, which originates from the lung pulse and respiration shifting of the fluid.

Fig. 5.10. Large, almost echo-free pleural effusion caused by congestive heart failure. The echoes at the margin and in the depth are artefacts



Transudates are almost always echo free, whereas about half of **exudates** are echogenic. The echogenicity of exudates often increases during illness, while transudates become slightly echogenic after puncture. Diffusely distributed, swirling or floating, slight echoes indicate reflecting particles in the fluid, e.g. cells, protein, fibrin or blood. Echoes that swirl with the respiratory or cardiac rhythm clearly indicate fluid collection. Movable strands, fibrinous strings and septations are typical of inflammatory effusions (Fig. 5.11). **Malignant effusions** can also appear to be echo free or septated. Only nodules indicate malignancy (Fig. 5.12).

Volumetry of pleural effusion

Anatomical differences and the various shapes of the chest make pleural effusions highly variable. Thus, the exact volume of an effusion cannot be measured.

Fig. 5.11. Pleural empyema with several cavities, septations and fibrinous bands

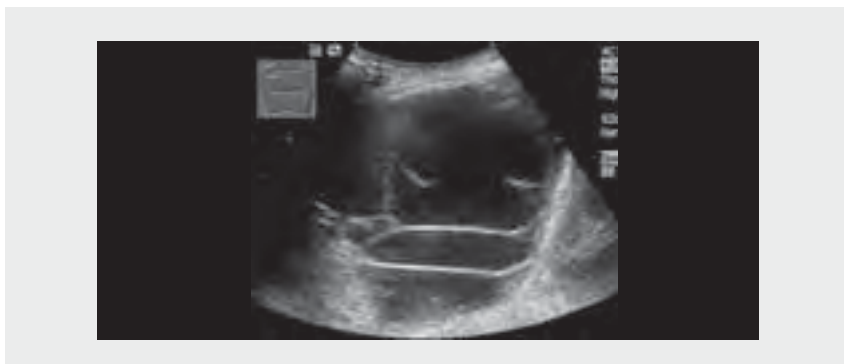


Fig. 5.12. Metastatic (M) nodules of an adenocarcinoma on the thickened and destroyed diaphragm

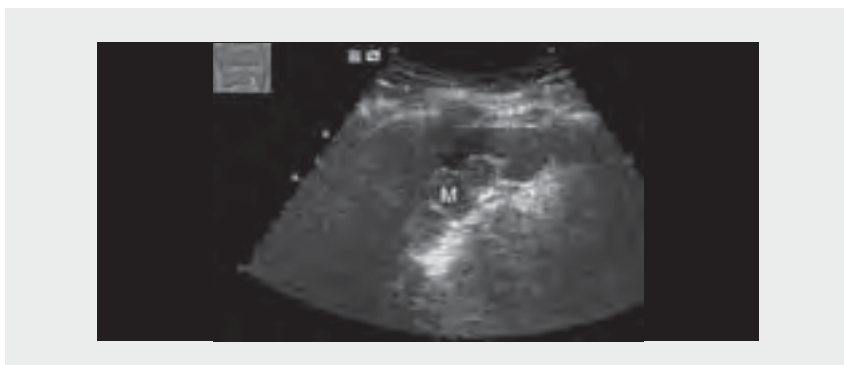


Fig. 5.13. Estimate of the volume of a pleural effusion: lateral plus median subpulmonary height of effusion $\times 70$: corresponds to about 800 ml



With the patient in the sitting position, the sum of the basal lung–diaphragm distance (in cm) and the lateral height of the effusion (in cm) multiplied by 70 will result in an acceptable estimate of the volume of pleural effusion (Fig. 5.13). In routine clinical follow-up, it is sufficient to measure the subpulmonary and lateral ‘water level’.

For bedridden patients, the planimetric square dimension of an effusion in a transverse section multiplied by the maximum craniocaudal length times an empirical factor of 2/3 is a good correlation of real effusion volume. Similar results have been reported by multiplying the maximum thickness of the pleural fluid layer (in cm) by 50 and then taking 800 from the result.

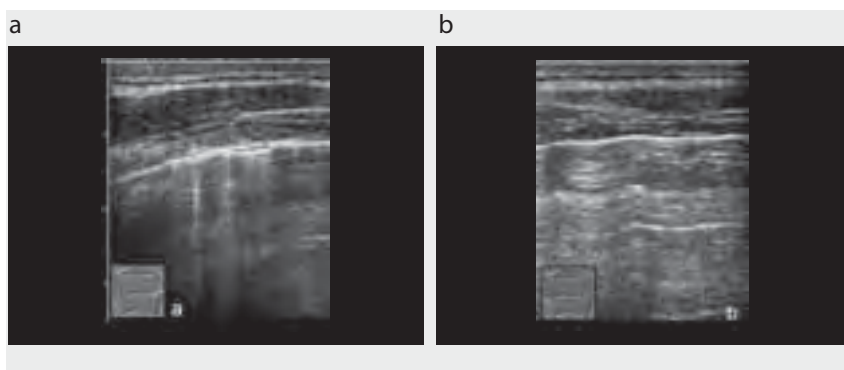
Pneumothorax

The major criterion of pneumothorax is absence of breath-related movement of the visceral pleura, referred to as the ‘sliding sign’. Further signs, in comparison with the healthy side, are:

- absence of sliding sign
- broadening of visceral pleura band
- absence of comet-tail artefacts
- horizontal reverberation artefacts and
- lung point.

The extent of the lung collapse and the breadth of major pneumothorax cannot be seen by sonography. The fleeting appearance of lung sliding replacing a pneumothorax pattern is termed the ‘lung point’ (Fig. 5.14).

Fig. 5.14. Pneumothorax. (a) Healthy side; sliding visceral pleura band; some vertical comet-tail artefacts. (b) Side of pneumothorax; loss of sliding sign; enhanced horizontal reverberation artefacts in the lung



Pleuritis

Pleuritis is most frequently caused by viral infections or tuberculosis. Clinically, pleuritis is difficult to diagnose and often the diagnosis can be made only by excluding other diseases that cause chest pain. A chest X-ray sometimes shows a blurred or even absent contour of the diaphragm; it can also demonstrate an effusion. Pleural alterations, which can be missed by X-ray, are detectable by ultrasonography in up to 90% of cases (Fig. 5.15, Fig. 5.16).

Fig. 5.15. Pleuritis. Rough appearance and interruption of the normally smooth pleura visceralis. Small subpleural echo-poor consolidations

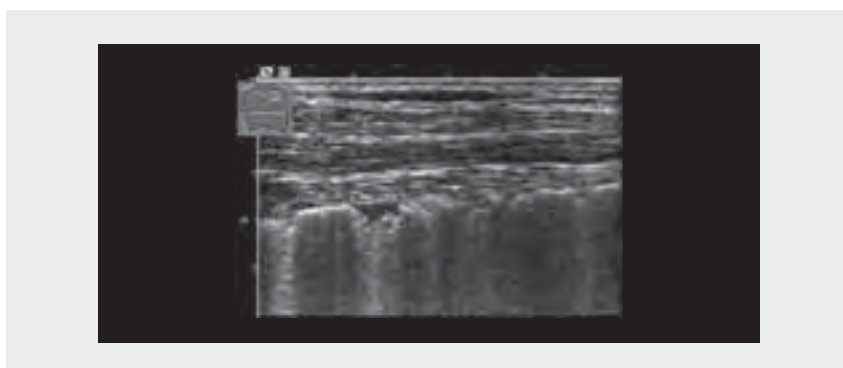
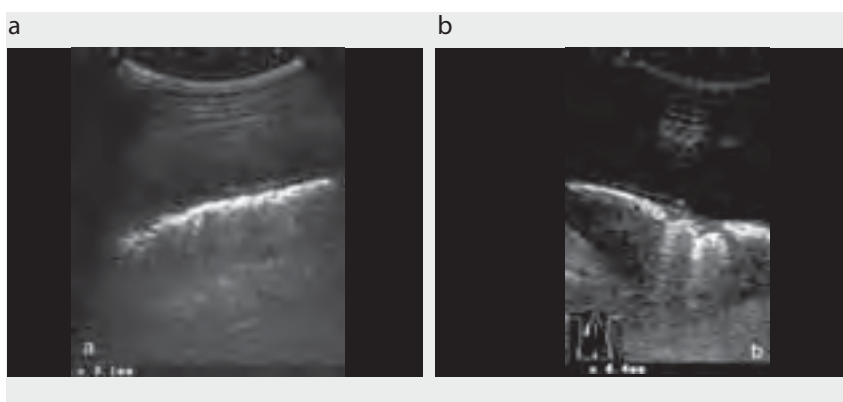


Fig. 5.16. Tuberculous pleuritis. (a) Echo-poor thickening of the pleura visceralis up to 3 mm. (b) Nodular subpleural consolidations. Diagnosis is confirmed by ultrasound-guided biopsy



The sonographic findings in pleuritis are:

- rough appearance of pleura visceralis
- interruptions of pleura visceralis
- small subpleural consolidations and
- small effusion.

Pleural mesothelioma

Mesotheliomas are usually visualized as diffuse, irregular thickenings of the pleura. They have very irregular, partly angular, unclear borders. In addition to tumour-like formations, mesotheliomas can also present as extensive, tapestry-like growths with nodules. Large pleural effusions frequently occur with mesotheliomas (Fig. 5.17).

Fig. 5.17. Pleural mesothelioma. Nodular and plate-formed broadening of the pleura. Echo-poor and irregular vascularization

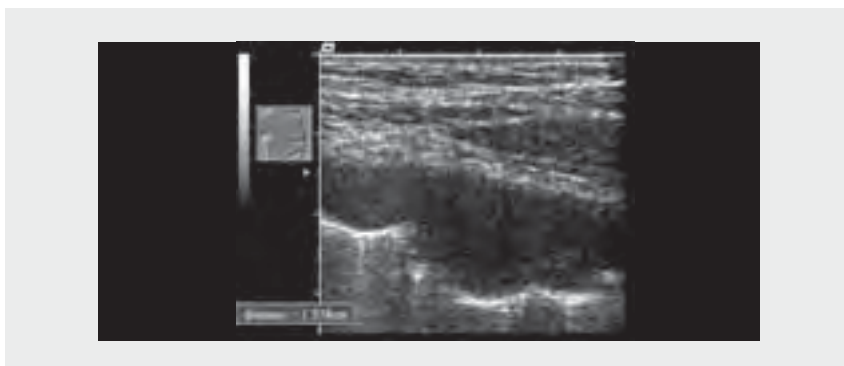
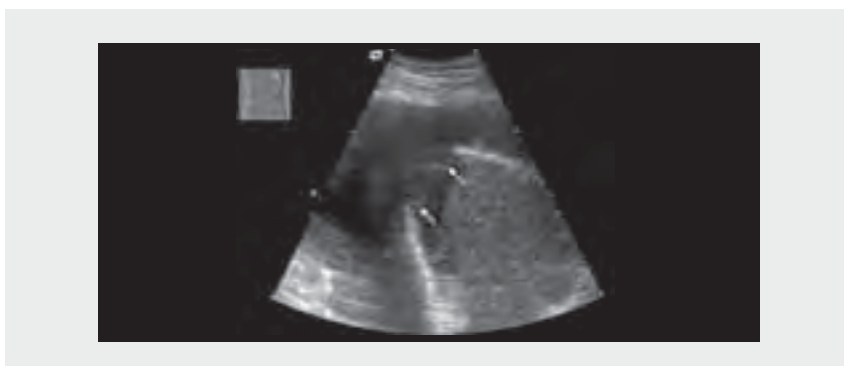


Fig. 5.18. Rupture of the diaphragm (arrows) after a serious blunt-abdominal trauma



Diaphragm

Real-time sonographic examination is the most suitable method for functional examination of the diaphragm. Normal equilateral up-and-down movement of the diaphragm in harmony with respiration can be observed. Paralysis of the diaphragm attracts the examiner's attention because of absent or paradoxical movement. Ruptures of the diaphragm can also be recognized (Fig. 5.18). One should not be misled by an apparent diaphragm hiatus originating at an artefact corresponding to the outline shadow.

Peripheral pulmonary consolidation

Ultrasound imaging of the lung is not possible in healthy people, because the ultrasound beam is reflected totally at the surface. The prerequisite for lung sonography is that the consolidation extends to the pleura.

Pneumonia

In the early congestive stage of pneumonia, the echo texture of the lung is similar to that of the liver. A marked tree-shaped bronchoaerogram and a large number of

lenticular echo reflections measuring a few millimetres are frequently observed up to the pleura (Fig. 5.19, Fig. 5.20). In a densely subpleural location, one finds a broad, highly hypoechoic strip, which is a superficial fluid alveologram. In viral or fungal pneumonia, less marked air bronchograms are obtained.

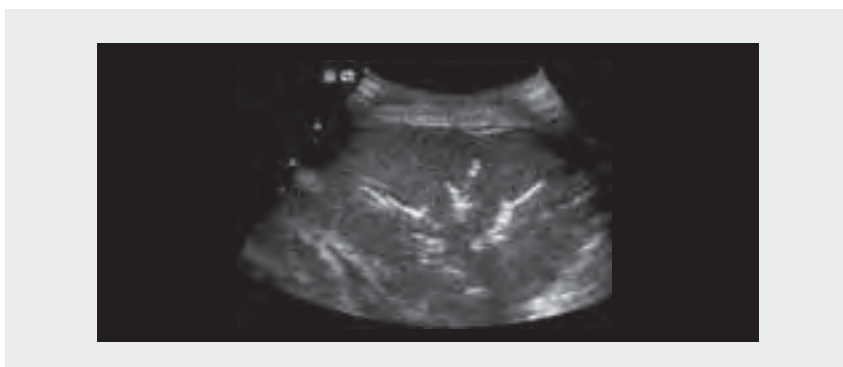
Ultrasound images of pneumonia are characterized by an irregular, serrated, somewhat blurred margin. The fluid bronchogram is characterized by anechoic tubular structures in the bronchial tree. A persistent fluid bronchogram arouses suspicion of post-stenotic pneumonitis and should be followed by suitable bronchoscopic clarification. On colour-coded duplex sonography, pneumonia has a typical appearance: circulation is uniformly increased and branched, while the vessels have a normal course. The sonographic findings in pneumonia are:

- hepatoid in the early stage
- air bronchogram
- lenticular air trappings

Fig. 5.19. Lobar pneumonia. Liver-like consolidation of the left upper-lobe with lenticular air trappings and an air bronchogram



Fig. 5.20. Tree-like air bronchogram in pneumonia



- fluid bronchogram (post-stenotic)
- blurred and serrated margins
- reverberation echoes in the margin and
- hypoechoic abscess formation.

Bacterial pneumonias tend to fuse and form abscesses seen as round or oval, largely anechoic foci (Fig. 5.21). Depending on the formation of a capsule, the margin is smooth and echo dense. In cases of complicated pneumonia, it is useful to obtain a specimen for the detection of pathogens by means of ultrasound-guided aspiration.

When pneumonia is in the healing phase, the infiltrated lung tissue is increasingly ventilated, and the air gives rise to reflection and reverberation artefacts in ultrasonograms. The pneumonia recedes on the ultrasound image and appears smaller than on a chest radiograph, which is consistent with the clinical course (Fig. 5.22).

Fig. 5.21. Small abscess formation (+ — +) in lobar pneumonia. Nearly echo free and rounded. An air inlet indicates the connection to the bronchial system

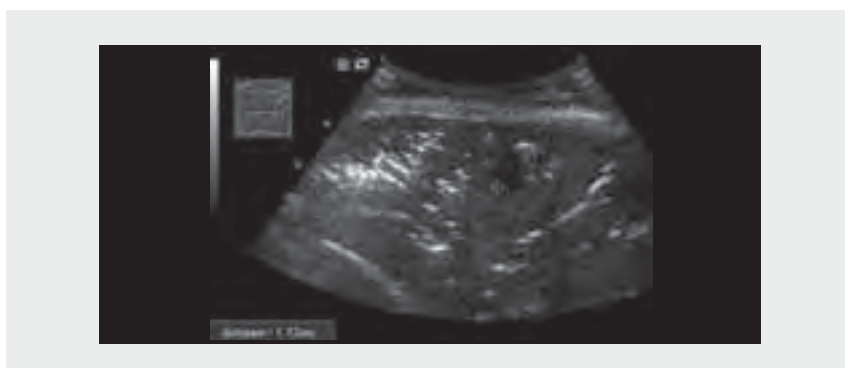
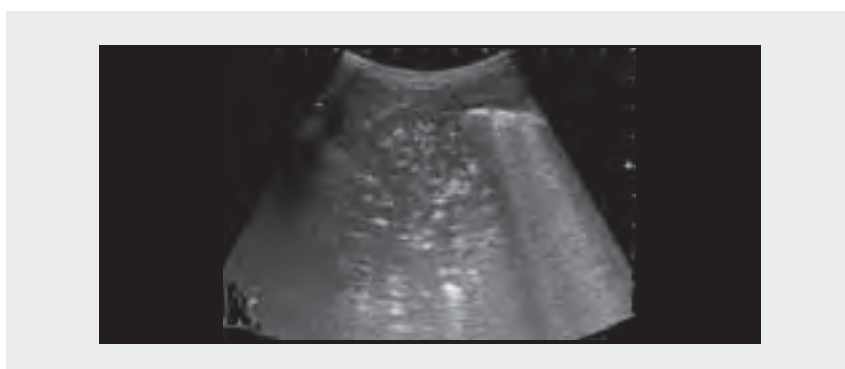


Fig. 5.22. Healing phase of pneumonia. The consolidation is receding and resolving, the air bronchogram is disappearing, air trappings and reverberation artefacts are increasing, all of which are consistent with clinical management



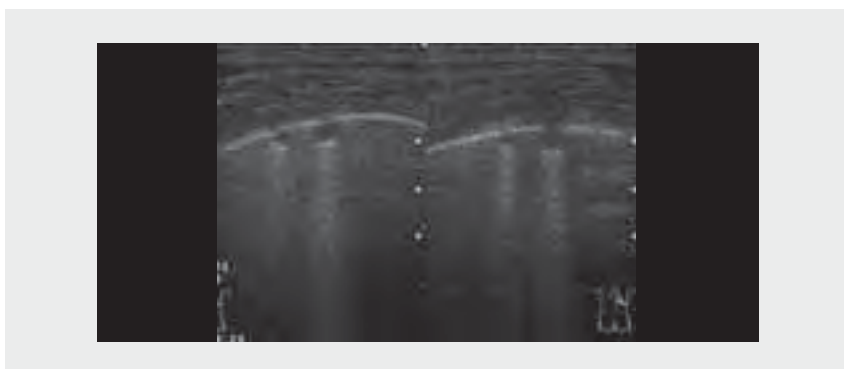
Tuberculosis

Pulmonary tuberculosis is polymorphic on X-ray as well as on chest sonography. The sonogram reveals isolated or numerous subpleural nodular hypoechoic lesions (Fig. 5.16, Fig. 5.17, Fig. 5.18, Fig. 5.19, Fig. 5.20, Fig. 5.21, Fig. 5.22, Fig. 5.23). Imaging of these lesions may be facilitated by the presence of a pleural effusion. Miliary tuberculosis is characterized by nodular dissemination occurring as multiple subpleural nodules measuring a few millimetres. Liquefaction is well demonstrated in the sonogram, although the presence of air in the tuberculous cavern may limit visualization. The patient's response to tuberculostatic treatment can be monitored well by sonography, especially in cases of pleural and subpleural tuberculosis.

The sonographic findings in tuberculosis are:

- pleural effusion
- fragmentation of visceral pleura
- subpleural infiltrations of various forms
- air bronchogram in cases of larger infiltrations and
- broad reflection artefact in cavities

Fig. 5.23. Miliary tuberculosis. Multiple rounded subpleural consolidations up to 5 mm



Interstitial lung disease

Diseases of the framework lung cannot be imaged by sonography, and the technique is of little use for their primary diagnosis. Here, the value of sonography lies in the detection of minimal pleural effusions and subpleural infiltrations during follow-up.

Pulmonary embolism

A few minutes after a secondary pulmonary artery has become occluded, the surfactant collapses, and interstitial fluid and erythrocytes flow into the alveolar space. Haemorrhagic congestion offers ideal conditions for ultrasound imaging. These consolidations are open at the periphery along with their base, which creates good conditions for transthoracic sonography. According to the results of new imaging procedures, the frequency of haemorrhagic reperfusionable pulmonary infarction is much higher than previously reported (Fig. 5.24, Fig. 5.25).

Fig. 5.24. Pulmonary embolism: two pleural-based infiltrations

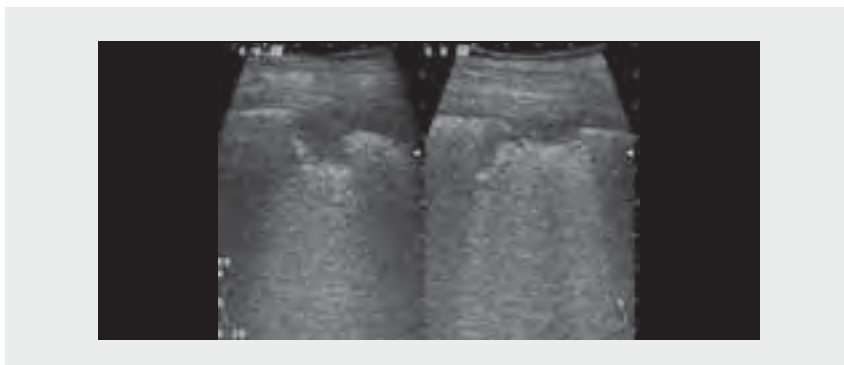
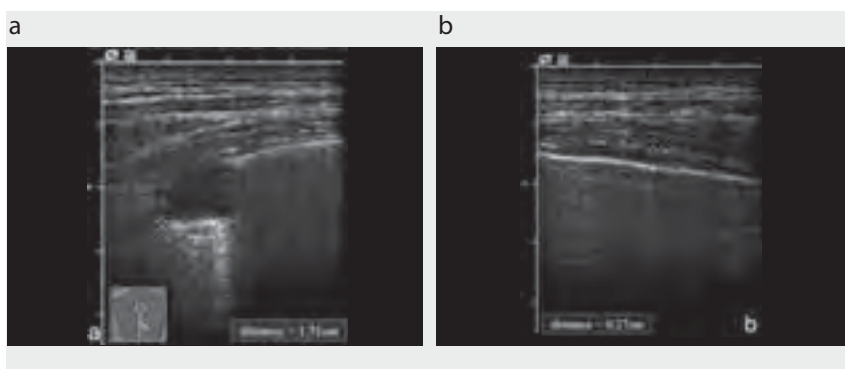


Fig. 5.25. Pulmonary embolism. (a) Triangular pleural-based, homogeneous airless inlets. (b) Concomitant small pleural effusion



The sonomorphological criteria for a peripheral pulmonary embolism are:

- echo poor
- size, average 16 mm × 12 mm (range, 5–70 mm)
- pleural-based
- triangular > rounded
- central bronchial reflexion
- vascularization stop
- 2.5 lesions per patient
- in two thirds of cases, the location is dorsobasal and
- small pleural effusion.

The overall sensitivity of chest sonography in pulmonary embolism is 80% and the specificity 93% (accuracy 95%). In thromboembolism, chest sonography should be performed in the context of echocardiography and leg vein sonography. Ultrasound can provide three kinds of information: the source in deep veins, the haemodynamic relevance on the way through the heart and the outcome as pulmonary embolism: ‘killing three birds with one stone’ results in a sensitivity of 92%.

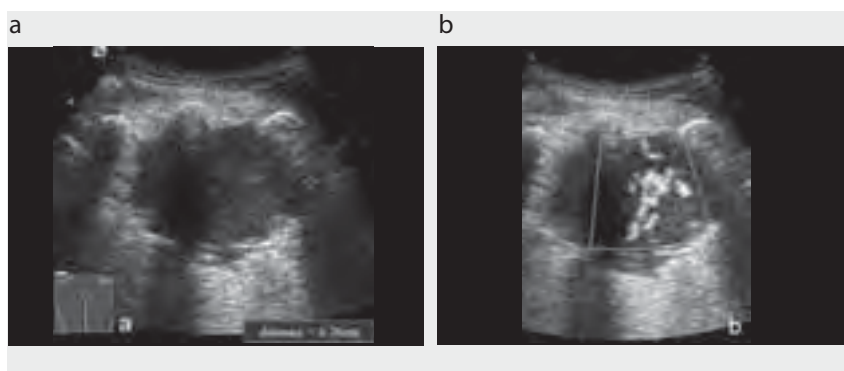
Pulmonary carcinomas and metastases

In sonograms, lung carcinomas and metastases are, for the most part, rounded or polycyclic. Pulmonary malignancies can have a variable echo texture; they are usually hypoechoic, moderately echo dense or very inhomogeneously structured. They frequently have sharp margins and fringed or finger-shaped ramifications into the ventilated lung (Fig. 5.26). The tumour vessels are irregular and shaped like a corkscrew. Dynamic ultrasound examination is better than CT or MRI for depicting malignant invasion of the chest wall or subclavian vessels. The advantages of ultrasound-guided biopsy are manifold: fast availability, low complication rate, absence of electromagnetic radiation and low cost.

The sonographic features of pulmonary carcinomas are:

- hypoechoic, inhomogeneous
- rounded, polycyclic
- sharp, serrated margins
- ramifications and fringes
- infiltration of chest wall and
- irregular vascularization.

Fig. 5.26. (a) Epidermoid lung cancer infiltrating the chest wall, destroying the ribs and intercostal space. Fringes and ramifications. (b) Irregular neovascularization of cancer



Atelectasis

Lung atelectases are characterized by partial or complete absence of ventilation. **Compression atelectasis** is caused by voluminous pleural effusion. The patient may develop triangular, homogeneous, hypoechoic consolidations shaped like a wedge or a pointed cap and have blurred margins to ventilated lung parenchyma (Fig. 5.27). These are partially reventilated during inspiration and after puncture of the effusion.

A sonographic image of **obstructive atelectasis** is marked by a largely homogeneous, hypoechoic presentation of lung tissue in terms of hepatization. Effusion is absent or very small. Depending on the duration of atelectasis, intraparenchymatous structures may also be seen, including hypoechoic vascular lines and echogenic bronchial reflexes. Secretory congestion of the bronchi presents a fluid bronchogram. On colour Doppler sonography, regular vessels along the bronchi are seen.

In cases of chest trauma, especially serial rib fractures, **pulmonary contusions** are seen better in sonography than in radiographs. Alveolar oedema and alveolar haemorrhage caused by trauma are visualized as hypoechoic, plate-like, blurred lesions with indistinct margins (Fig. 5.28). These are more pronounced in the presence of concomitant pleural effusion.

Fig. 5.27. Compression atelectasis. Triangular, hypoechoic, pointed cap-like transformation of lung parenchyma, surrounded by fluid. Partial reventilation during inspiration

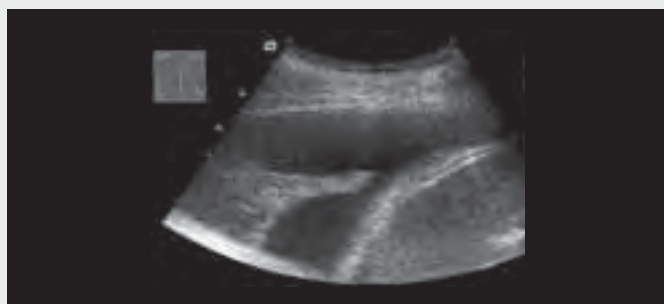


Fig. 5.28. Lung contusion. Plate-formed subpleural haemorrhage (arrows), irregular and blurred demarcation



Mediastinum

Most of the clinically relevant space-occupying masses in the adult mediastinum are located in the anterior and mid-mediastinum and are, therefore, readily accessible for sonographic assessment. Sonographic access to the mediastinum is obtained supra- or parasternally; occasionally, the infrasternal path is chosen. A good understanding of anatomy is absolutely essential. Lesions of the anterior superior mediastinum can be identified clearly as solid or cystic. Tumours that appear at the margin of the sternum are easily localized and biopsied. Ultrasound examination may demonstrate regression

Fig. 5.29. Mediastinal lymph node metastases from a small-cell lung cancer (LC) by the suprasternal approach. AO, aorta; BT, branchiocephalic trunk

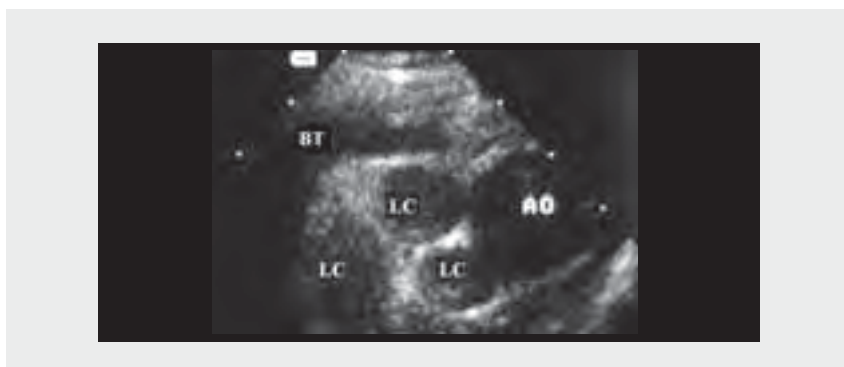
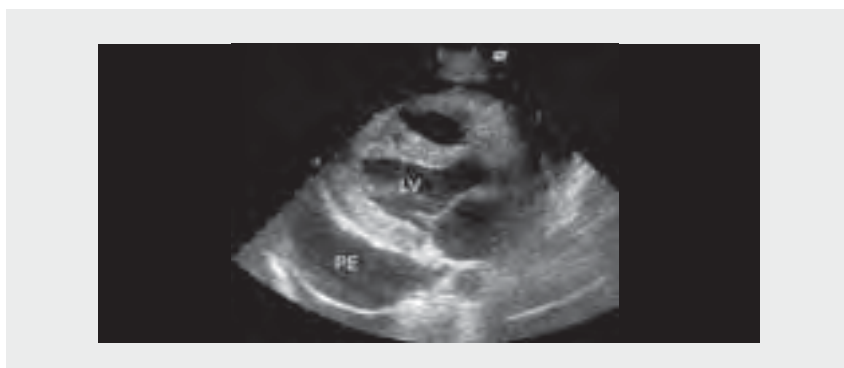


Fig. 5.30. Pericardial effusion (PE) in the parasternal longitudinal approach, caused by viral pericarditis. LV, left ventricle



after the treatment of mediastinal lymphoma or metastases (Fig. 5.29). Inflow congestion and superior vena cava syndrome can be cleared by sonography. Colour Doppler may detect collateral vessels. The development of endoscopic ultrasound has opened up new diagnostic possibilities for the detection and analysis of mediastinal lymph nodes.

Pericardium

Pericardial effusion is easily diagnosed, as a left sternal or subcostal approach shows the fluid surrounding the myocardium. Echogenic layers on the myocardium and fibrinous bands may indicate chronic inflammation caused by infection or rheumatic disease (Fig. 5.30). Malignant pericardial effusions sometimes show swirling echoes. Pericardial tamponade is marked sonographically by the collapse of the right atrial and/or ventricular walls during diastole. When the clinical situation is critical, ultrasound allows an immediate, safe pericardial tap. Sometimes, it is difficult to distinguish between epicardial fat pads and true pericardial effusions.

Abdominal cavity and retroperitoneum

Indications	113
Examination technique	113
	113 Equipment, transducer
	113 Preparation
	113 Position of the patient
	114 Scanning technique
Normal findings	114
	114 Abdominal wall, abdominal cavity and retroperitoneal space
	117 Aorta and vena cava
Pathological findings	118
	118 Abdominal wall
	122 Abdominal cavity
	127 Retroperitoneal space
	131 Aorta and vena cava
Differential diagnosis	135
Supplementary methods	138

Abdominal cavity and retroperitoneum

Indications

The indications of ultrasonography of the abdominal cavity and retroperitoneum are:

- palpable mass
- pain
- fistulas
- ascites
- suspected perforation (free air demonstrable?)
- hernia
- malignant lymphomas (staging, follow-up)
- aortic aneurysm
- venous congestion
- blunt trauma
- suspected postoperative complications

Examination technique

Equipment, transducer

Abdominal scanners, curved array or sector transducer, 3–5 MHz are used for general examinations. Linear array transducers, 5–10 MHz, are best suited for abdominal wall and superficial structures.

Preparation

No specific preparation is required.

Position of the patient

Supine is generally the best, in the left or right oblique or lateral position, with head held high or low, if needed.

Scanning technique

The abdominal wall is examined systematically in longitudinal and transverse scans, starting in the cranial part below the ribs from the midline. The corresponding left and right sides are used for comparison.

The abdominal cavity is usually visualized in examinations of the abdominal organs. For the detection of ascites, the splenic bed, Morison's pouch and the retrovesical space in the small pelvis have to be scanned. For determination of the presence of free air, the region between the surface of the right liver lobe and the abdominal wall must be scanned, with the patient in a slightly left oblique position (the area before the right liver lobe should be the highest point of the cavity).

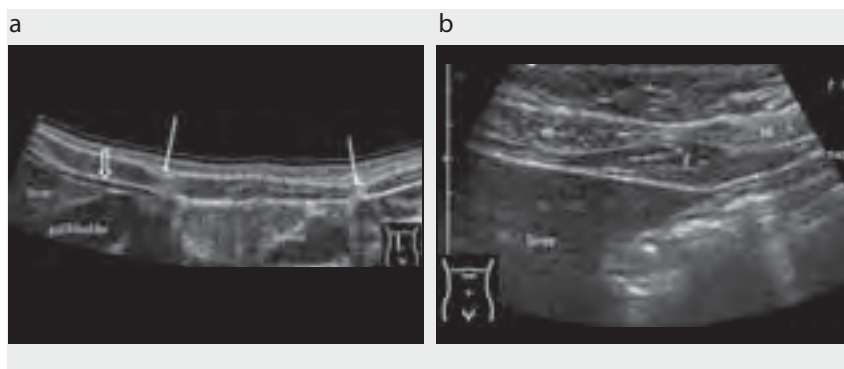
In the retroperitoneal space, the large vessels and the kidneys (see Chapter 13, Kidneys and ureters) are the anatomical landmarks for orientation. The large vessels should always be visualized in longitudinal and transverse scans from the diaphragm to the bifurcation. To overcome the problem of meteorism, an examination from the flanks (coronal scans) or with the patient in an upright position is recommended. Another method is to displace the gas in the intestinal loops by graded compression of the transducer in the area to be scanned.

Normal findings

Abdominal wall, abdominal cavity and retroperitoneal space

Skin, subcutaneous tissue, muscles and the parietal peritoneum form the anterolateral abdominal wall. On both sides of the linea alba, the rectus abdominis muscles are visualized as echo-poor structures with transverse lines of stronger echoes corresponding to the characteristic inscriptions. The fascial sheath cannot be seen. The three thin muscles (external and internal oblique and transversus abdominis) forming the lateral wall are easily differentiated in younger and muscular individuals. In obese persons, the image consists of a heterogeneous, not clearly structured echo-poor wall (Fig. 6.1, Fig. 6.2). The extraperitoneal fascia forms a thicker structure behind the linea

Fig. 6.1. (a) Abdominal wall Rectus abdominis with inscriptions (arrows). Athlete. Thin layer of extra-abdominal fatty tissue in front of the liver (broad arrow). (b) Abdominal wall. Extra-abdominal fatty tissue behind the wall (m, rectus abdominis) and in front of the liver (f, fatty tissue)



alba cranial to the umbilicus. It appears triangular in a longitudinal scan and rhomboid in transverse scans. It should not be misinterpreted as a mass (Fig. 6.1).

The posterior wall is marked by the strong echoes of the ventral surface of the vertebrae, which absorb all the energy and cause an acoustic shadow. The intervertebral discs also cause strong borderline echoes but do not absorb all the energy, so that echoes behind them are seen. On both sides, echo-poor muscles (psoas muscle and quadratus lumborum) are observable. Depending on age and condition, their diameter and shape differ from person to person (see Fig. 6.3, Fig. 6.4, Fig. 6.5, Fig. 13.9).

The diaphragm forms the 'roof' of the abdomen and appears as a thin, echo-poor layer or structure, but only in those parts that do not border the air-containing lung, e.g. dorsal to the liver or the pillar in front of the aorta (see Fig. 6.5). In the other sections, a line of bright borderline echoes marks the interface between the diaphragm and the lung and hides the thin echo-poor diaphragm (see Fig. 1.26, Fig. 7.5b).

Fig. 6.2. Abdominal wall. Transverse scan shows subcutaneous fat and thin rectus abdominis. The linea alba is marked by an arrow

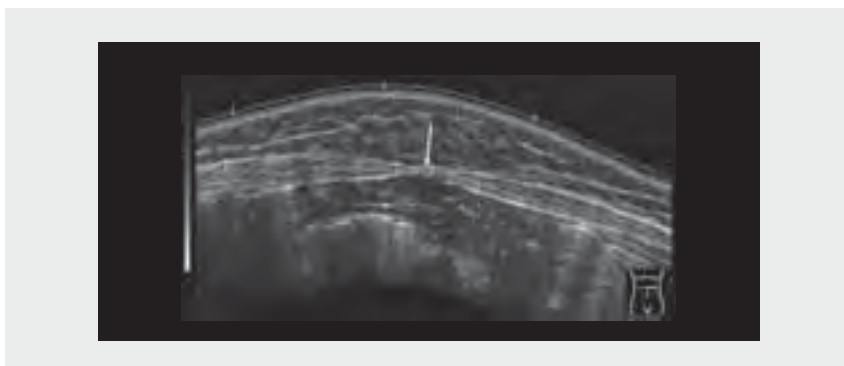


Fig. 6.3. Topography of the abdomen, transverse (a) and longitudinal (b) scan. Abdominal cavity (grey) and retroperitoneal space (white). In (a) k, kidney. (b) The tumour (T) is localized in the retroperitoneal space (axis of the kidney, dotted line) despite its short distance from the ventral abdominal wall.

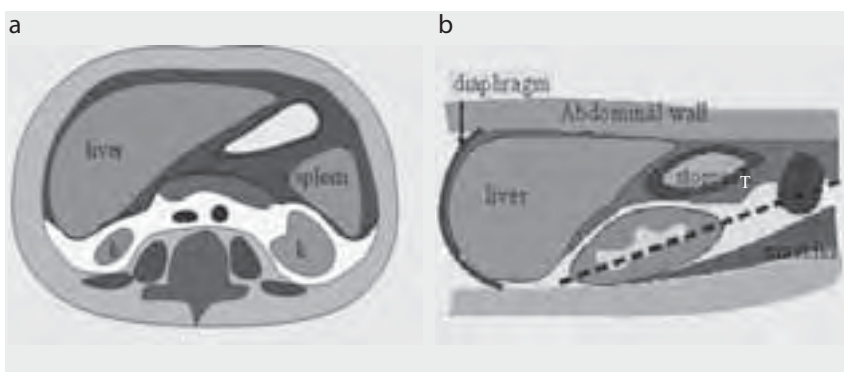


Fig. 6.4. Abdominal and retroperitoneal space. The borderline echoes between the liver and the kidney (arrow) mark the border between the abdomen and the retroperitoneal space, but are not caused by the parietal peritoneum. (p, psoas muscle; s, shadow behind the vertebral column; vc, vena cava; ao, aorta.)

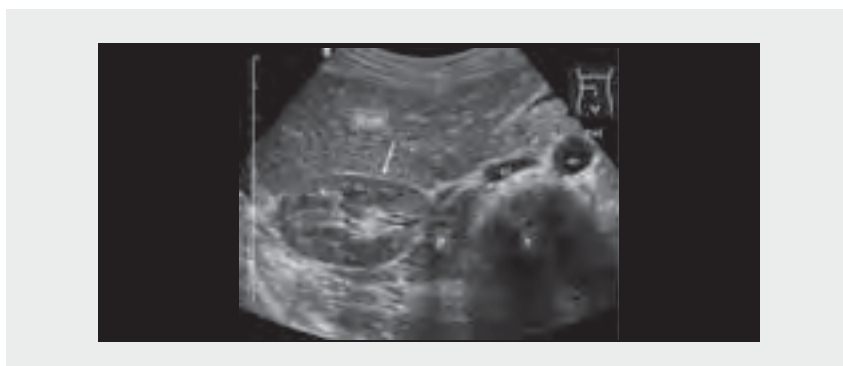
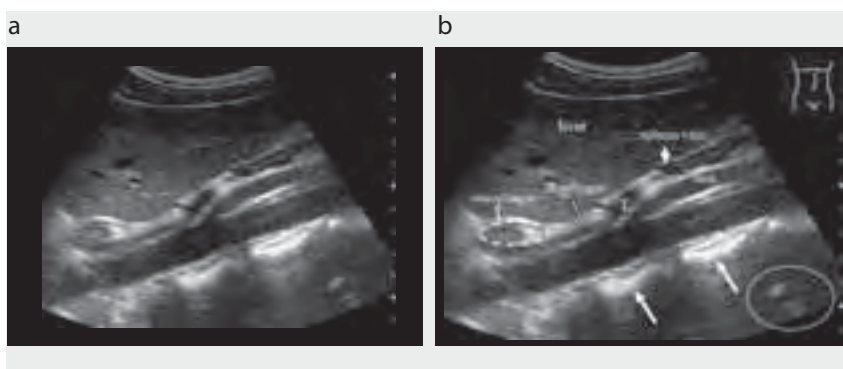


Fig. 6.5. (a, b) Abdominal aorta, coeliac trunk (T) and superior mesenteric artery (sma). The arrows mark the strong echoes of the vertebral bodies. Real echoes arising from the vertebral canal are seen behind a disc (in the bottom right-hand circle)



The retroperitoneal space is separated from the abdominal space by the parietal peritoneum, but ultrasound does not generally allow visualization of this thin serous lining. Thin echo lines between intra-abdominal organs and retroperitoneal organs and structures are mostly borderline echoes. The retroperitoneal or intra-abdominal localization of a mass or fluid can be estimated from the proximity of their relation to the retroperitoneal organs, especially the kidneys and the aorta (Fig. 6.3).

The abdominal cavity is separated by ligaments into different but communicating spaces and recesses, which are important for diagnosis and therapy. The mesentery and the retroperitoneal connective tissue appear echo rich and coarse, particularly in obese patients. The medium-size vessels in the ligaments can be seen, if the image is not impaired by meteorism.

Aorta and vena cava

The abdominal **aorta** is easily visualized as a nearly echo-free structure, with strong wall echoes running in front of the vertebral column (distance < 6 mm) from the aortic hiatus to the bifurcation. The internal diameter varies with the patient's age, from 11 mm to 19 mm in the upper part and from 10 mm to 15 mm in the lower part. The coeliac trunk and its branches, the superior and inferior mesenteric artery and the renal arteries can be visualized with ultrasound as well, if meteorism does not impede the examination (Fig. 6.5).

Spectral Doppler shows a relatively high diastolic flow above the renal arteries (low resistance profile) and a low diastolic flow (high resistance) in the lower part. The peak velocity (V_{\max}) lies in the range 70–180 cm/s and the mean velocity (V_{mean}) in the range 40–70 cm/s (Fig. 6.6).

Fig. 6.6. Abdominal aorta. Spectral Doppler shows a low-resistance flow (high diastolic flow) in the upper part (a) and a high-resistance flow in the lower part (b)

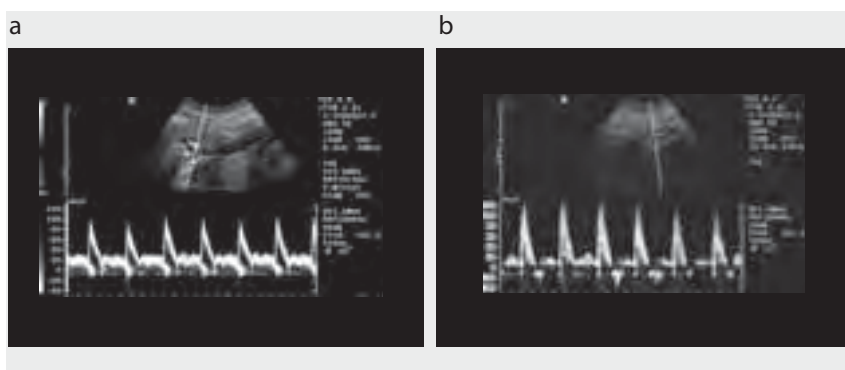
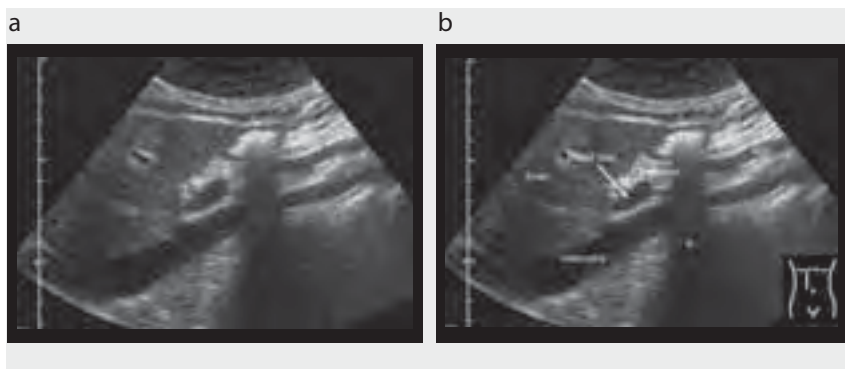


Fig. 6.7. Vena cava. The body of the pancreas is partially covered by shadow(S) arising from air in the distal stomach (smv, superior mesenteric vein)



The inferior vena cava runs up the right side, slightly curved in the sagittal plane, with a greater distance from the aorta in the upper part. Its cross-section is oval with a distinctly smaller sagittal diameter, especially in the lower part (Fig. 6.4). The calibre varies with the actual thoracic pressure. The echoes of the wall are weaker (Fig. 6.7). In

front, behind and on both sides of the vessels, large groups of lymph nodes are arranged with long axes of up to 20 mm.

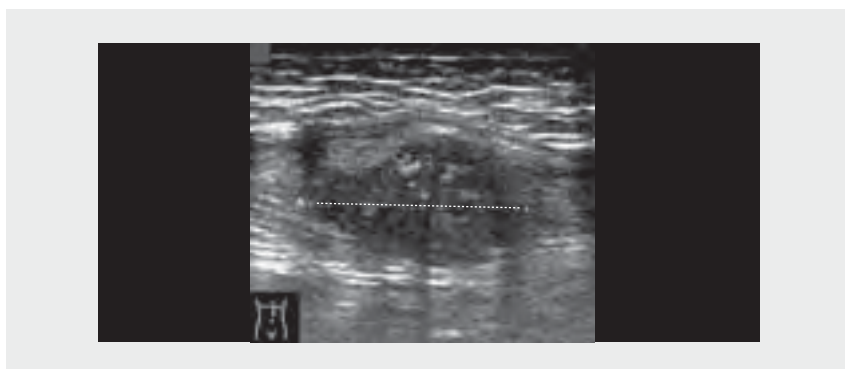
Pathological findings

Abdominal wall

Tumours

Primary tumours of the abdomen wall are rare. Benign **lipomas** and **fibrolipomas** are more or less echo rich, with sharp margins. They do not contrast well with the surrounding fat tissue (see Fig. 4.28). **Desmoid tumours** are associated with a recent pregnancy. Ultrasound demonstrates echo-poor lesions, most with sharp margins. A blurred border indicates infiltration into surrounding tissues. **Metastases** are usually echo poor or heterogeneous with irregular, ill-defined margins (Fig. 6.8).

Fig. 6.8. Metastasis (diameter, 24 mm). The irregular, blurred boundary and the heterogeneous echo-poor structure are characteristic



Foreign-body granulomas are characterized by a strong echo in the centre and, often, an annular echo-poor or average structure. Colour Doppler shows a hypervascular zone around the small lesion (small-parts scanner).

Inflammation, fluid collections

An **inflammation** of the wall may occur as a complication of an operation or a trauma. The inflamed area appears more echo dense, with a blurred structure, than the normal wall.

Abscesses are associated with a trauma, a laparotomy or, rarely, an enterocutaneous fistula. Abscesses are oval or irregular, depending on the structures of the wall. The pattern is echo poor or even echo free (Fig. 6.9). Strong echoes indicate gas in the abscess. The margin is often ill defined. Colour Doppler shows no signals in the lesion but a hyperaemic zone around it.

Seromas are also associated with laparotomy. They are echo free or very echo poor, with a sharp margin (Fig. 6.10). It is difficult to distinguish a post-operative seroma from a post-operative abscess if the latter does not show typical symptoms. If the clinical examination is also ambiguous, a guided puncture may identify the nature of the lesion.

Fig. 6.9. Abscess (post-operative). Note the thin, echo-poor fistula (arrow). The sonographic feature is similar to that of a metastasis (see Fig. 6.8), but the history and clinical symptoms are different

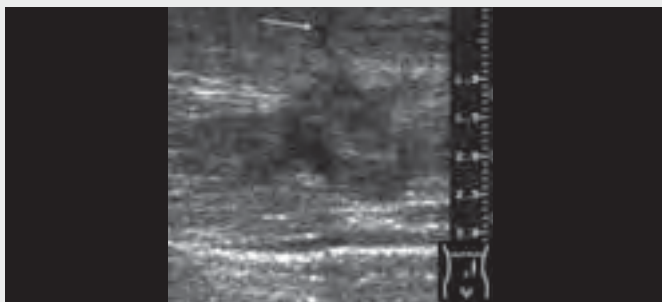
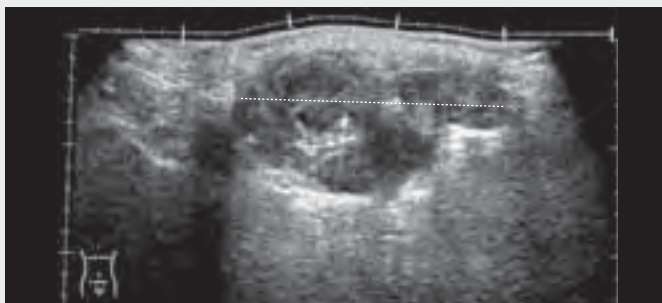


Fig. 6.10. Seroma. Note the sharp margins. The fluid is echo free, apart from some artefacts



Fig. 6.11. Haematoma (diameter, 131 mm). The echo pattern of the older haematoma is relatively heterogeneous; the margin is irregular but sharp



The echo pattern of **haematomas** depends on their stage: bleeding into the tissue initially causes an echo-rich, 'cloud-like' pattern, with irregular, blurred margins. Later, the blood forms a circumscribed echo-poor lesion (Fig. 6.11). Finally, this lesion becomes increasingly echo rich, indicating the organization of the haematoma.

Subcutaneous emphysema

A subcutaneous emphysema of the abdominal wall can be due to a perforating trauma. Ultrasound demonstrates a line of strong echoes within the wall (but not behind the wall, which indicates meteorism). The acoustic shadow covers the deeper layers of the wall and the abdomen.

Hernias

Hernias arise at typically weak parts of the linea alba, mainly above the umbilicus (epigastric hernia), the umbilicus itself (umbilical hernia), the linea semilunaris (Spigelian hernia), the inguinal canal (inguinal hernias) and the femoral ring (femoral hernia). Incisional hernias are late complications of operative wounds. The point of pain or palpation guides the ultrasound examination.

The ultrasound features of a hernia are variable, depending on the content of the hernial sac. The echo pattern of the visceral peritoneum (fat tissue) is echo rich, and intestinal loops can be identified. Lack of movement, a swollen, echo-poor wall of the bowel and fluid (but not ascites) in the sac indicate an incarcerated hernia. The sonographic signs of bowel obstruction (see Chapter 11, Gastrointestinal tract) indicate strangulation. The hernial orifice can be visualized by ultrasound as a gap in the linea alba (epigastric hernia) or at the border of the abdomen, which sometimes allows repositioning (Fig. 6.12, Fig. 6.13, Fig. 6.14, Fig. 6.15).

Fig. 6.12. Incisional hernia (40 mm, larger measure), through the gap in the fascia (indicated by the arrow, 9 mm). The hernia contains fatty tissue only

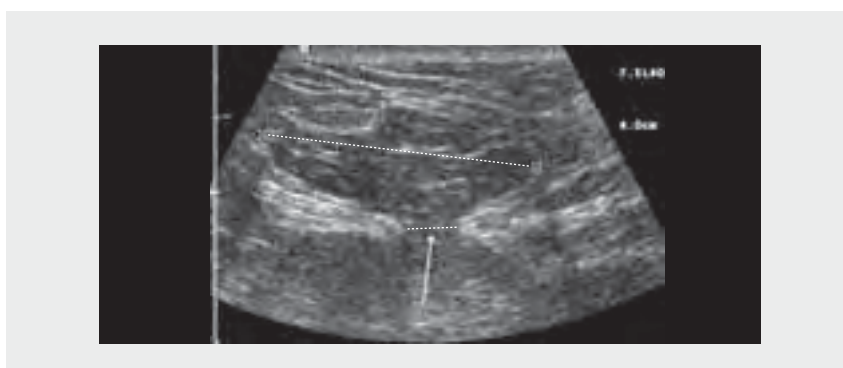


Fig. 6.13. Incisional hernia. The fluid and the swollen wall of the small bowel in the sac indicate an alteration in torsion and obstruction of the blood supply



Fig. 6.14. Incarcerated Spigelian hernia (arrows). The hernia causes mechanical obstruction of the small bowel (dilated fluid-filled loops with a swollen wall)

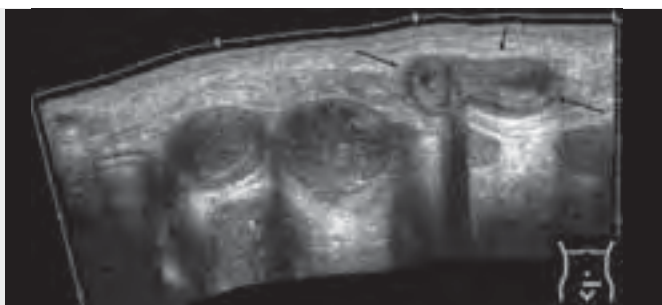


Fig. 6.15. Inguinal hernia (diameter, 18 mm). Fluid in the sac (arrow) and the echo-poor, thickened wall indicate alteration of the bowel (see also Fig. 15.49)



Abdominal cavity

Ascites

The presence of ascites is a common symptom in many types of disorder (Table 6.1).

Small amounts of ascites should be sought in typical recesses, Morison's pouch or Douglas's pouch. Amounts of fluid greater than 10 ml can be demonstrated with ultrasound. The fluid is echo free or very echo poor, which does not exclude an exudate. Fine, dispersed echoes in the fluid suggest haemorrhagic (malignant) ascites or exudates. At a later stage, they are often characterized by filiform echoes. Purulent ascites is less echo poor. Diagnosis of the type and cause of ascites are often more reliable if additional signs are found (Table 6.1, Fig. 6.16, Fig. 6.17, Fig. 6.18, Fig. 6.19, Fig. 6.20, Fig. 6.21, Fig. 6.22, Fig. 6.23, Fig. 6.24, Fig. 6.25).

Table 6.1. Types of ascites

Disorder	Type	Ultrasound findings	Additional findings
Portal hypertension	Transudate	Echo free	Liver, spleen, gallbladder
Venous congestion (heart failure)	Transudate	Echo free	Dilated vena cava, pleural effusion
Nephritic syndrome	Transudate	Echo free	Kidneys
Inflammatory disorder (peritonitis)	Serofibrinous exudates	Echo free or echo poor, filiform echoes (fibrin)	Thickened bowel wall, abscess, gas echoes (perforation)
Tuberculosis	Exudates	Echo poor	Echo-poor lymph nodes, thickened mesentery, complex inflammatory masses (HIV infection)
Pancreatogenic ascites	Exudates	Echo free or echo poor	Pancreatitis
Malignant tumours	Variable, haemorrhagic, chylous	Echo free, fine dispersed echoes	Retracted bowel loops, thickened mesentery, metastases (liver)
Trauma, anticoagulation	Blood	Echo poor or even echo free	Trauma, anticoagulation

Fig. 6.16. Small amount of ascites in Morison's pouch (arrow) and in front of the right liver lobe position 'a'. The small line of ascites in front of the liver 'a' is 'masked' by reverberation echoes



Fig. 6.17. A trace of fluid in Douglas's pouch (arrow). Nearly echo-free blood after a fall



Fig. 6.18. Fluid (bleeding) in the rectouterine space. The uterus and the adnexa (follicles in the right ovary, arrow) are surrounded by the fluid. Note the different appearance of the echo-poor blood and the echo-free fluid in the bladder



Fig. 6.19. Inflammatory ascites (exudates) with filiform echo lines in the stage of organization (adhesions)



Fig. 6.20. Haemorrhagic, malignant ascites (ovarian cancer), showing faint echoes



Fig. 6.21. Ascites (transudate) with floating small bowel loops

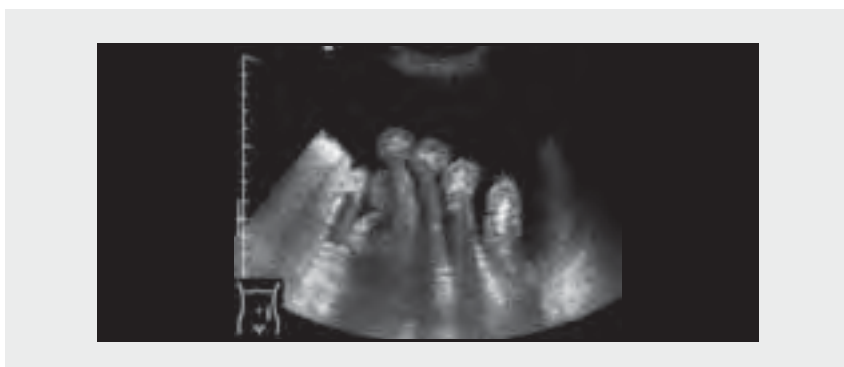


Fig. 6.22. Mesothelioma. The visceral serous lining of the loops and the parietal serosa are thickened (arrow). Close to the abdominal wall, note typical reverberation artefacts. A, ascites



Fig. 6.23. Small amount of ascites between small bowel loops. The ascites does not flow up because of post-operative adhesions. Note the oedema of the small bowel



Fig. 6.24. Abscess (localized peritonitis; diameters, 26 mm and 11 mm). Note the inflamed, thickened wall of the small bowel (D)



Fig. 6.25. Postoperative haematoma, showing similar sonographic features as abscesses (see also Fig. 6.24, Fig. 6.26)

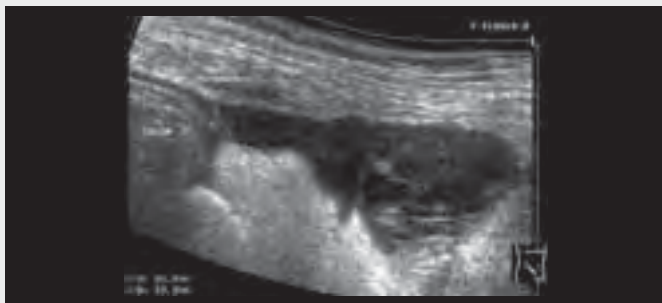


Fig. 6.26. Intra-abdominal abscess. Note that it is difficult to decide whether all the strong gas echoes are within the lumen of the bowel



The thickness of the gallbladder wall is a reliable symptom for distinguishing benign ascites caused by portal hypertension or hypalbuminaemia (thickened wall) from malignant ascites (normal wall). Floating small-bowel loops are characteristic of extensive ascites (transudates and some exudates). The loops are often retracted in inflammatory disease or in malignant infiltration of the mesentery. In cases of localized peritonitis or (postoperative) adhesions, the fluid may be more localized and not flow up when the position of the patient changes.

Whenever ascites is seen, all parts and all organs of the abdomen must be examined carefully to find the underlying disorder (see Table 6.1)

Pseudomyxoma peritonei

This term describes a special type of gelatinous ascites, often caused by an ovarian cancer. Ultrasound demonstrates extended ascites with septa.

Quincke oedema

This disorder is caused by a lack of the C1-esterase inhibitor. It may affect the abdomen, causing ascites and oedema of the gastric and intestinal walls. The echo-free ascites and the very echo-poor swelling of the walls disappear within hours or 2–3 days.

Peritonitis

Peritonitis may arise from an infectious disease of an abdominal organ (e.g. appendicitis, diverticulitis) or be caused by a (bowel) perforation. Initially, the peritonitis remains localized. Ultrasound can visualize echo-poor fluid collection surrounded by adhered intestinal loops, often with a thickened, echo-poor wall. Strong gas echoes within the fluid are highly symptomatic of bowel perforation. The sonographic indications of bowel obstruction (see Chapter 11, Gastrointestinal tract) may also be seen. If the peritonitis remains localized, an abscess or a complex inflammatory tumour is visualized by ultrasound. If diffuse peritonitis develops, ascites and unmoving bowel loops (paralytic ileus) are seen.

A special type of ascites is secondary infection of an initially sterile ascites caused by portal hypertension.

Peritoneal tuberculosis

Peritoneal tuberculosis is a common extrapulmonary manifestation that is seen in advanced stages of HIV infection. Usually, ascites occurs secondary to an affection of the small bowel. The course is usually chronic, and two types, 'wet' and 'dry', are differentiated.

The ultrasound findings are not specific but indicative of the clinical background. Ascites, echo free or with filiform echoes, is the leading symptom of the 'wet' type. In the 'dry' form, irregular thickening of the mesentery with a complex echo pattern is seen, but ultrasound usually cannot visualize the small tubercles in the peritoneum. The affected lymph nodes are rounded and echo poor, with small echo-free lesions (caseous degeneration). Only small, localized portions of less echo-poor fluid are found. The affected intestinal loops are matted, and the thickened wall is echo poor. The adhesions of the intestine, the mesentery, small abscesses and enlarged lymph nodes may form large pseudotumours with a complex echo pattern.

Adhesions

Post-operative adhesions between the bowel and the abdominal wall are a common problem. Ultrasound is usually not useful for visualizing these thin bridges directly, but real-time examination of the movement of the intestine gives an indirect indication. The upper and lower parts of the abdomen are scanned with the transducer positioned in the midline and midclavicular line. An easily discernible structure is examined during deep inspiration and expiration. Normally, it shifts more than 6 cm in the upper and less than 4 cm in the lower abdomen. A shift of more than 3 cm is suspect, and no shift confirms the diagnosis.

Retroperitoneal space

Retroperitoneal fluid collections are either haemorrhagic (trauma, anticoagulation therapy, neoplasms, aneurysm) or inflammatory. Additionally, urinomas may occur around the kidney (see Chapter 13, Kidneys and ureters). The fluid is mostly limited to the original site by the various ligaments, which makes it easier to find the causative disorder. Fluid in the anterior pararenal space may be caused by acute necrotizing pancreatitis. Fluid in the medial part is caused by disorders of the large vessels (see section on Aorta and vena cava in this chapter). Fluid in the perirenal space is caused mainly by diseases of the kidneys (see Chapter 13, Kidneys and ureters). Fluid is found behind the kidneys in infections of the psoas muscle, which is due to abscesses or haemorrhage (see Fig. 6.27, Fig. 6.28, see also Fig. 13.63, Fig. 13.64). The latter may occur spontaneously if the patient is on anticoagulant therapy. Abscesses are secondary to inflammatory disorders of the vertebral column (e.g. spondylodiscitis, tuberculous spondylitis) or of the abdomen (appendicitis, fistulas, postoperative complications). The psoas itself may be thickened, with a partially echo-free, irregular pattern, which is best visualized by comparison with the psoas muscle on the other side.

Retroperitoneal fluid collections are mostly echo poor, corresponding to their characteristics (blood, inflammatory exudates).

Cystic lesions

Echo-free and smoothly delineated **mesenteric cysts** are very rare. In endemic areas, parasitic disorders (*Echinococcus granulosus* infections, hydatid disease) have to be taken into consideration if cystic or complex partially cystic lesions are found in the

Fig. 6.27. Psoas haematoma (fresh, anticoagulation therapy). The haematoma localized in front of the muscle appears rather inhomogeneous, with ill-defined borders (arrows)



Fig. 6.28. Old haematoma (19 mm × 33 mm) in front of the psoas muscle, 6 weeks after an accident. The rounded haematoma is homogeneous and echo poor with sharp margins. It has the appearance of a tumour



abdominal cavity. **Seromas**, **biliomas** or **lymphoceles** are echo free and smooth, like serous cysts. They are diagnosed from the clinical background.

Tumours

Primary tumours of the peritoneum and the retroperitoneum are rare. Benign **lymphangiomas** show a complex pattern, with echo-free areas.

Malignant mesotheliomas cause thickening of the parietal and visceral peritoneum, which is visualized as a relatively echo-rich lining of the bowel, organs and the inner surface of the wall, connected by ascites (see Fig. 6.22).

Liposarcomas are echo rich and show poor contrast with fat tissue. Other malignant tumours, such as **leiomyosarcoma**, show a more complex, inhomogeneous pattern. Malignant tumours frequently become large, as they may cause no symptoms for a long time. Their size, an inhomogeneous pattern, an irregular shape and a blurred outline indicate malignancy (Fig. 6.29, Fig. 13.65), whereas small, more homogeneous tumours with sharp, smooth borders may be benign. Generally, reliable differentiation is not possible.

Fig. 6.29. Retroperitoneal sarcoma (diameter, 104 mm). Note the inhomogeneous, relatively echo-rich pattern. The aorta (ao) is discernible but not the vena cava

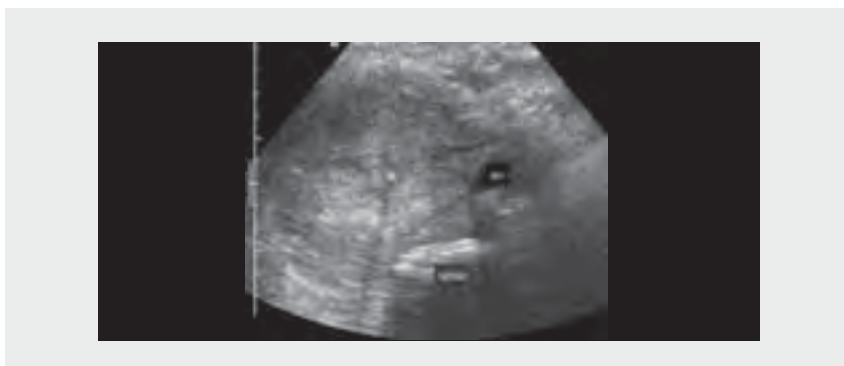
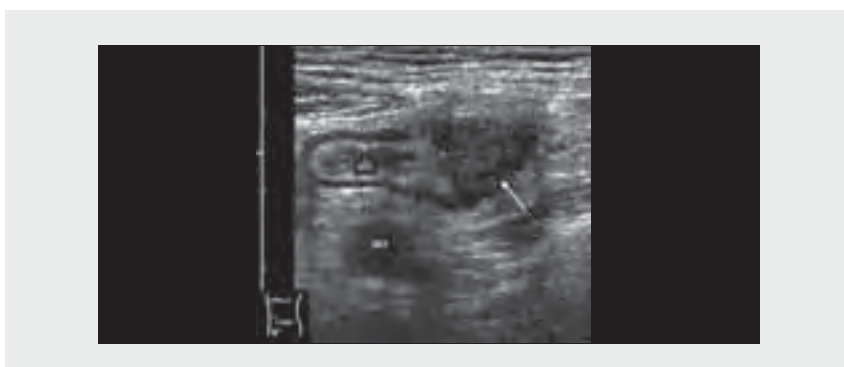


Fig. 6.30. Metastasis (13 mm) in the visceral mesentery of a small bowel loop (arrow), (sb, small bowel; ao, aorta)



Metastases are commoner in the mesentery and the retroperitoneal lymph nodes (Fig. 6.30, see also Fig. 6.32). Usually, they are echo poor and associated with ascites (Fig. 6.20). Diffuse infiltration of the mesentery causes shrinking and retraction of the intestine. Carcinomatous lymph nodes are enlarged, moderately echo poor and often show an irregular, ill-defined outline. Colour Doppler permits visualization of irregular 'peripheral' vascularity.

Malignant lymphomas

Advanced malignant lymphomas usually involve the retroperitoneal, para-aortic lymph nodes. Not infrequently, they also involve the mesenteric lymph nodes.

The lymph nodes are enlarged, more rounded and echo poor, the hilus sign is missing, the nodes are conglomerated or, less frequently, isolated, and they surround the large vessels. Compression of these vessels, especially of the vena cava, should be diagnosed only if the vessel is dilated distally (Fig. 6.30, Fig. 6.31, Fig. 6.32, Fig. 6.33, Fig. 6.34, Fig. 6.35).

Fig. 6.31. (a) Non-Hodgkin lymphoma with multiple enlarged, echo-poor lymph nodes around the coeliac trunk. (b) Lymphadenitis mesenterica. The slightly enlarged mesenteric lymph nodes are relatively echo rich (hilus sign) and oval

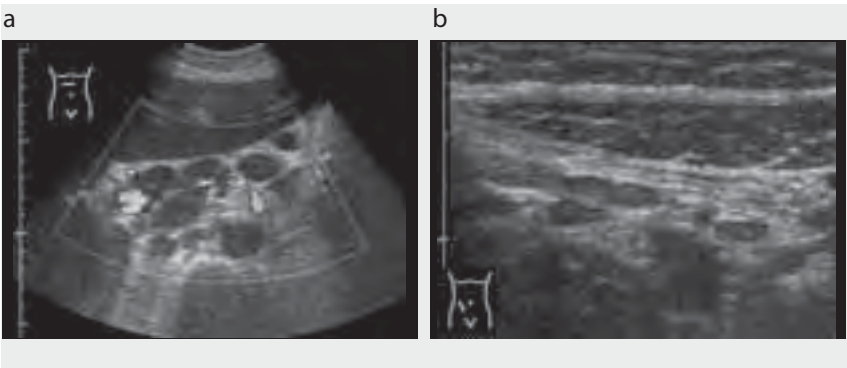


Fig. 6.32. Lymph node metastasis (gastric cancer; diameter, 45 mm) behind the (compressed) vena cava (vc); pv, portal vein

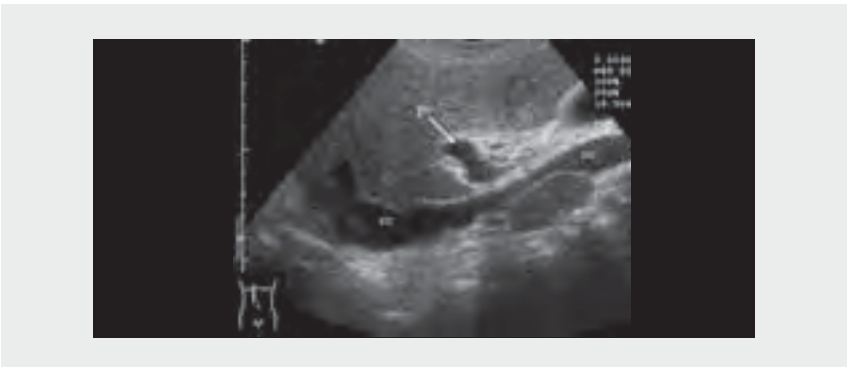


Fig. 6.33. Malignant lymphoma (arrows, 37 mm). The distance between the aorta and the spine is increased. A diagnosis of compression of the vena cava (vc) should not be based on the oval cross-section shown, but only if the section distal to the tumour is dilated (ao, aorta; pv, portal vein)



Fig. 6.34. Immunocytoma. Enlarged lymph nodes (arrows) in front of the aorta in the angle of the superior mesenteric artery (sma); t, coeliac trunk

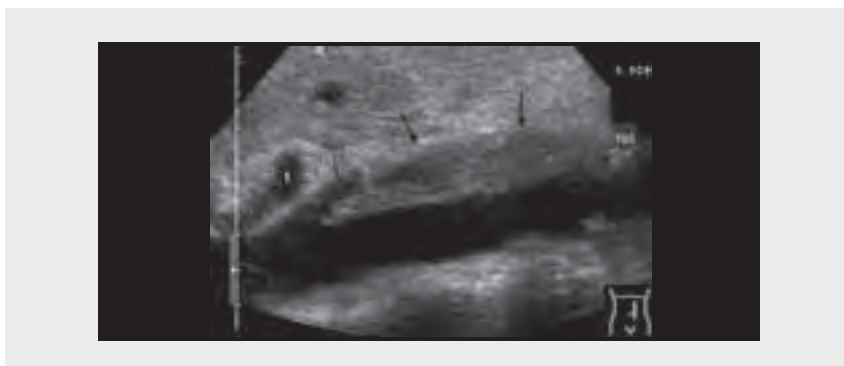
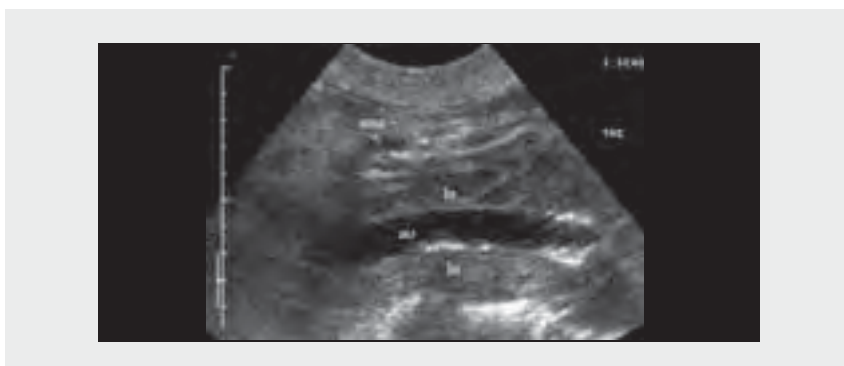


Fig. 6.35. Low-grade non-Hodgkin lymphoma (ln). The enlarged retroperitoneal lymph nodes coat the aorta (ao); sma, superior mesenteric artery; see also Fig. 6.46)



The lymph nodes are hypervascular, as shown by the colour or power Doppler technique. The vascularity varies and may be regular ('hilar' vascularity) or pathological (peripheral vascularity).

Retroperitoneal fibrosis

This disorder is characterized by augmented connective tissue between the renal pelvis and the promontory of the sacrum. The etiology is unknown but, in some cases, the disease occurs as a reaction to aortic aneurysms, retroperitoneal surgery or drugs.

Ultrasound shows an echo-poor mass around the large vessels, sometimes with ill-defined borders. A compression of one or both ureters simultaneously is characteristic (Fig. 6.46 and Fig. 13.61 in Chapter 13, Kidneys and ureters).

Aorta and vena cava

Situs inversus of the great vessels is rare; however, **variations** of the coeliac trunk and of the superior mesenteric artery are common, e.g. a common trunk for the two vessels or origination of the hepatic artery from the superior mesenteric artery.

Arteriosclerosis is characterized by irregular thickening of the wall and elongation of the aorta, evident from the fact that the aorta is curved like an S and cannot be depicted in one scanning plane. The inner surface of the irregular wall can be depicted especially well with B-flow technique (see Fig. 6.36, Fig. 1.17). **Stenosis** can also be visualized with B-scan; however, an exact estimate is possible only with the spectral Doppler technique.

Aneurysms are typical, significant complications and consist of spindle-shaped, focal dilatations with a transverse diameter greater than 3.5 cm. B-scan shows the size and shape of an aneurysm and partial thrombosis. The latter is echo poor and can be clearly distinguished from the residual lumen. A large transverse diameter and an asymmetric thrombosis are regarded as risk factors for perforation. An echo-poor mass around the aneurysm is strongly indicative of perforation into the retroperitoneal space (Fig. 6.37, Fig. 6.38, Fig. 6.39, Fig. 6.40).

Colour Doppler shows the sometimes turbulent or rotating flow and is useful for identifying the vessels branching off. The distance between the aneurysm and the renal arteries is particularly important. In suprarenal aneurysms, the left renal vein should also be identified.

Fig. 6.36. Aortosclerosis (diameter, 16 mm). Localized calcifications cause strong echoes and acoustic shadows (see Fig. 1.17); sma, superior mesenteric artery

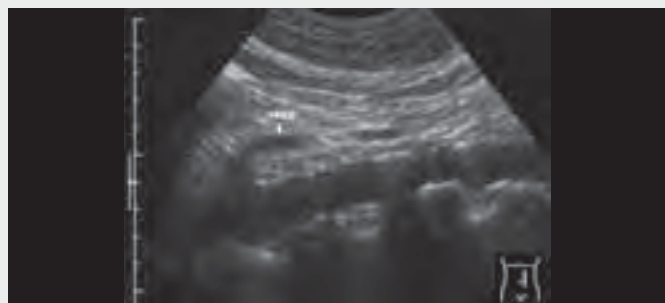


Fig. 6.37. Small aortic aneurysm (diameter, 24 mm; aorta, 15 mm) without thrombosis



Fig. 6.38. Infrarenal aortic aneurysm (diameter, 47 mm) without thrombosis. Note the natural 'contrast' of the blood (turbulent flow)

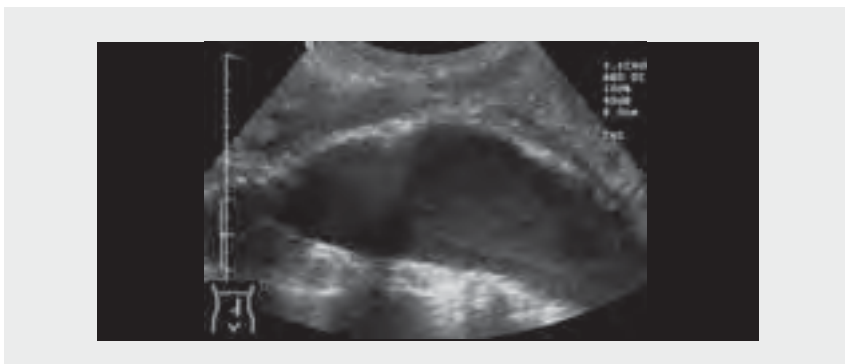


Fig. 6.39. Aortic aneurysm (75 mm \times 63 mm). Asymmetric thrombosis

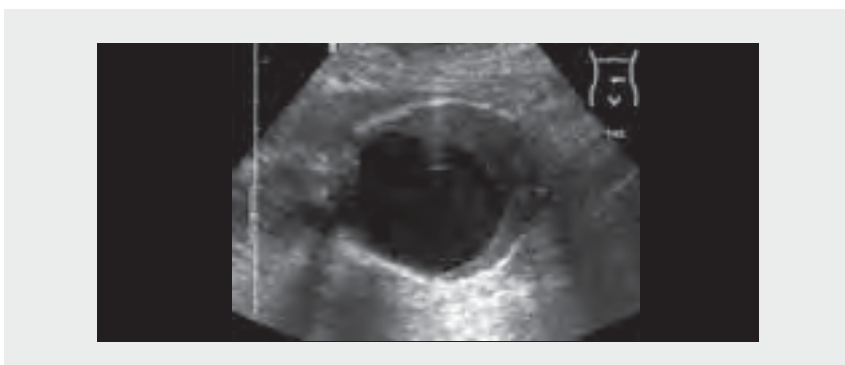


Fig. 6.40. Aortic aneurysm (53 \times 49 mm). Circular thrombosis. Colour Doppler shows rotating flow (bright pixels correspond to red and dark pixels to blue)



Ultrasound is useful for postoperative check-ups of prostheses, to measure their diameter and detect complications, such as stenosis, obstruction or inflammatory reactions.

Special types of aneurysm are sack-shaped, inflammatory and dissecting aneurysms. Sack-shaped (false) aneurysms of the aorta are rarely seen and are characteristic of medium-size arteries in systemic vasculitis. The term '**inflammatory aneurysm**' refers to a strong inflammatory reaction of surrounding tissue, especially in front of the aorta. The lymph nodes in the region are enlarged. It is related to retroperitoneal fibrosis.

Dissecting aneurysms cause only slight dilatation of the aorta. Careful B-scan examination may show flapping intimal lamellae. Colour Doppler differentiates true and false lumina more clearly, the flow direction in systole and diastole and the connection between the two lumina (Fig. 6.41).

Fig. 6.41. Dissecting aneurysm. (a) B-scan shows slight dilatation and a membrane in the middle of the lumen. (b) Colour Doppler shows different flows in the true (red = bright) and the false lumina (blue = dark)

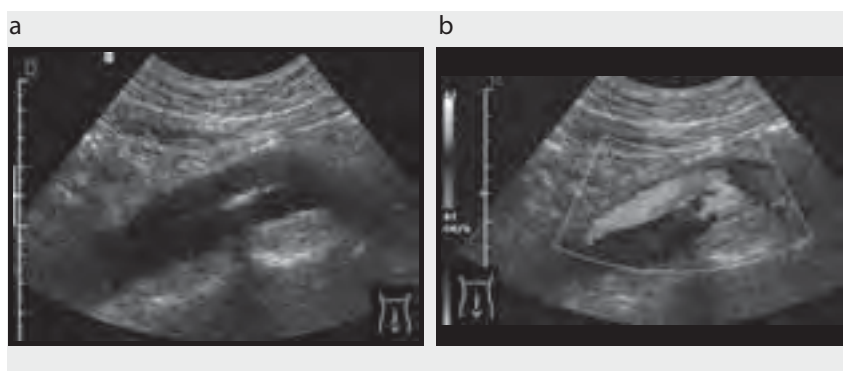
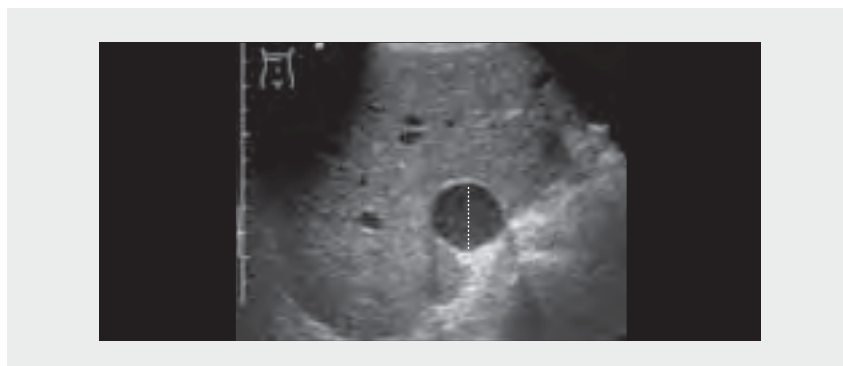


Fig. 6.42. Venous congestion (heart failure). The vena cava is dilated (30 mm), the cross-section round (see Fig. 6.4)



Venous congestion is easily visualized with B-scan: the cross-section of the vein becomes round, the vessel is dilated, and respiratory movements are missing. The feeding vessels, particularly the hepatic veins, are dilated (Fig. 6.42, Fig. 2.2).

A **thrombus** in the vena cava usually originates from a thrombosis of a feeding vein. A thrombus protruding into the lumen of the vena cava is echo poor and easy to detect. The vena cava is not dilated. A fresh thrombosis originating in the vena cava itself may sometimes appear nearly echo free and is, therefore, difficult to detect (Fig. 6.43, Fig. 6.44).

Differentiation between a simple thrombosis and a **tumour thrombosis** is difficult or even impossible with B-scan and colour Doppler. The thin tumour vessels can often be visualized only with contrast agents. Examination of the organ, drained by the vein, permits detection of the nature of the thrombus (see Chapter 13, Kidneys and ureters).

Colour Doppler permits detection of the flow in a thrombotic vein. It is particularly useful for follow-up control of cava filters.

Fig. 6.43. Thrombosis of the vena cava. The vessel is dilated (between calipers, 28 mm) and shows few echoes inside (fresh thrombosis); ao, aorta



Fig. 6.44. Thrombosis of the left renal vein, protruding into the vena cava (vc)



Differential diagnosis

The differential diagnosis of focal lesions in the abdominal wall does not pose problems if the clinical background is taken into account. Differentiation between a more harmless seroma and an abscess after laparotomy is sometimes difficult if there are no clear clinical or sonographic signs of an abscess. Ultrasonic-guided puncture is the

method of choice for clarifying the difference. Benign tumours, such as lipofibromas, and malignant lesions, mainly metastases, can usually be differentiated on the basis of the different echo patterns and the definition of the outline, as described in section on Abdominal wall in this chapter.

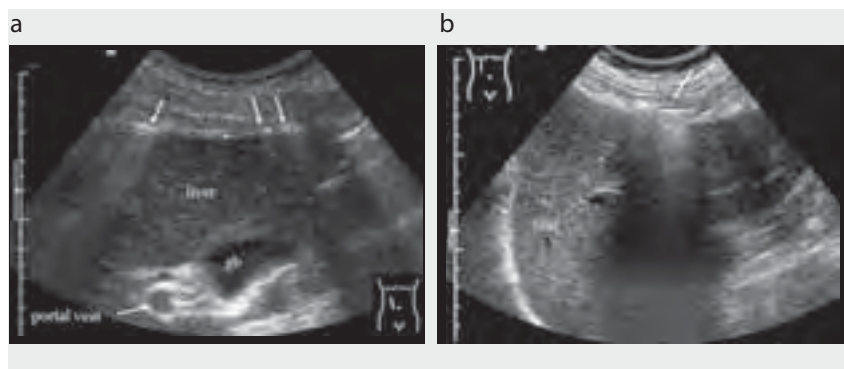
Ascites is a common ambiguous symptom of many diseases. Misdiagnosis of a large (ovarian) cyst as an ascites can be avoided, as a giant cyst will displace the intestine, whereas floating small bowel loops are always seen in ascites.

The main clinical problem in differentiation is between benign and malignant ascites. This can be resolved by examining the gallbladder wall: a thickened wall is a reliable sign of benign ascites, especially that caused by portal hypertension. The nature of the fluid itself does not help, as exudates or malignant ascites may appear to be echo-free transudates. In contrast, echoes within the fluid are not seen in transudates but indicate inhomogeneous fluid, exudates, purulent, haemorrhagic or chylous ascites. Generally, examination of the abdominal organs enables diagnosis of the causal disorder, as shown in Table 6.1.

In certain situations it is difficult to decide whether typical gas echoes are caused by gas bubbles in the bowel or from outside it due to perforation or abscess. Therefore, a diagnosis of free air or gas in the abdomen should be made only if gas echoes are detected in front of the right liver. The possibility of interposition of gas-containing colon sections (Chilaiditi syndrome) should be considered (Fig. 6.45).

Tumours in the abdomen pose some difficulties for differential diagnosis. It is not easy to identify the origin of the tumour, which may be an abdominal organ or, more

Fig. 6.45. Gas echoes in front of the right liver lobe. (a) Free gas (arrows) caused by perforation of a duodenal ulcer. (b) Gas inside the colon in Chilaiditi syndrome (colon interposition); gb, gallbladder. The thin wall (arrow) is difficult to see (3.5 MHz)



rarely, the connective tissue of the abdominal cavity or retroperitoneal space. Careful examination in different scanning planes, including guided palpation, may establish a connection with a certain organ or structure. Association with clear anatomical structures, such as the kidney or the aorta, can help in identifying the location. It should be noted that a tumour's close connection to the abdominal wall does not exclude a retroperitoneal origin (see Fig. 6.3a).

Differentiation between neoplastic lesions and pseudotumours is also difficult. Pancreatic pseudocysts are typical examples. They may be seen months or years after a

trauma or as an asymptomatic relict of a previous pancreatitis and are not infrequently localized some distance from the pancreas. Aneurysms of medium-size vessels pose a similar problem. They may be thrombosed and have the appearance of a tumour but not associated with an organ if the connection to an artery is not seen initially. Inflammatory pseudotumours consisting of small abscesses, fistulas, intestinal loops, lymph nodes and inflamed connective tissue show a complex pattern. Sometimes, a malignant tumour may cause an inflammatory reaction and have similar sonographic features. Large malignant tumours show a complex pattern, with echo-rich, echo-poor or even cystic sections. Consequently, a mass with cystic parts should not be misinterpreted as a (harmless) cyst.

The retroperitoneal lymph nodes, which are affected by malignant lymphomas or metastasizing carcinomas, represent a special problem for differential diagnosis, as the sonographic features of a partially thrombotic aortic aneurysm and of retroperitoneal fibrosis are similar. A horseshoe kidney also imitates a mass in front of the aorta. The relation of the 'mass' to the vena cava and its outline should resolve the situation, as shown in Table 6.2 and Fig. 6.46.

Table 6.2. Differential diagnoses of echo-poor masses around the aorta

Disorder	Ultrasound findings	Additional findings
Malignant lymphoma	Echo-poor, enlarged lymph nodes on both sides of both vessels. Aorta marked by strong wall echoes. Increased distance between aorta and vertebral column	Mesenteric lymph nodes, enlarged spleen
Retroperitoneal fibrosis	Echo-poor tissue around both vessels, ill-defined border	Hydronephrosis
Aneurysm	Echo-poor thrombosis, strong wall echoes at the surface of the mass	Vena cava not included
Horseshoe kidney	Echo-poor mass in front of the vessels. Smooth, sharp contour, connection to the kidneys	–
Abdominal tumour (colon)	Echo-poor or target-like lesion ('pseudokidney sign') distant to the aorta	–

Fig. 6.46. Differential diagnosis of echo-poor masses and structures around the aorta (see also Table 6.2)



Supplementary methods

Ultrasound-guided puncture is the simplest, most reliable method for establishing a final diagnosis in various situations, such as solid tumours of unclear origin and nature, ascites and other fluid collections (see Chapter 3, Interventional ultrasound).



Chapter 7

Liver

Indications	141
Examination technique	141
141	Equipment transducer
141	Preparation
141	Position of the patient
141	Scanning technique
Normal findings	142
142	Echo texture
142	Echogenicity
142	Size
142	Normal anatomy
Pathological findings	145
145	Infectious diseases
152	Metabolic disorders
153	Vascular diseases
156	Focal hepatic lesions
Trauma	165

Liver

Indications

The indications for ultrasonography of the liver are:

- enlarged liver (hepatomegaly)
- suspected liver abscess
- jaundice
- abdominal trauma
- ascites
- suspected metastases in the liver
- suspected liver mass
- right upper abdominal pain
- screening for endemic echinococcosis.

Examination technique

Equipment transducer

The examination should be carried out with the highest frequency transducer possible, usually 3.5 MHz or 5.0 MHz. Doppler techniques are needed for precise analysis of the vessels.

Preparation

The patient should take nothing by mouth for 8 h before the examination. If fluid is essential to prevent dehydration, only water should be given. If the symptoms are acute, the examination should be undertaken immediately. In the case of infants, if the clinical condition of the patient permits, they should be given nothing by mouth for 3 h before the examination.

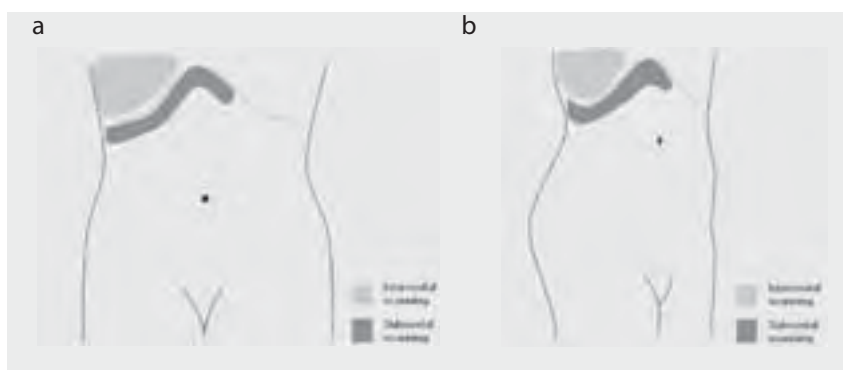
Position of the patient

Real-time imaging of the liver is performed with the patient in the supine, left-oblique and left-lateral decubitus positions.

Scanning technique

Scanning should be in the sagittal, transverse and oblique planes, including scans through the intercostal and subcostal spaces (Fig. 7.1).

Fig. 7.1. Scanning area for evaluation of the liver in (a) supine position and (b) left posterior oblique position



Normal findings

Echo texture

The normal liver parenchyma is homogeneous. Within the homogeneous parenchyma lie the thin-walled hepatic veins, the brightly reflective portal veins, the hepatic arteries and the hepatic duct. The liver texture is comparable to that of the renal parenchyma. The normal liver parenchyma should have a softer, more homogeneous texture than the dense medulla and hypoechoic renal cortex.

Echogenicity

The liver can be as or more echogenic than the kidney (Fig. 7.2); however, it can be less echogenic than the kidney, as the echogenicity of the renal cortex can be increased in some renal diseases (Fig. 7.3). The spleen has about the same echogenicity and the pancreas about the same or slightly greater echogenicity than the liver.

Size

Size is measured as shown in Fig. 7.4. Generally, the liver measures less than 15 cm, with 20 cm representing the upper limit of normal. Hepatomegaly is present when the liver exceeds 20 cm. There is, however, considerable variation.

Normal anatomy

Liver anatomy is based on its vasculature. The right, middle and left hepatic veins course between lobes and segments, and eight segments are distinguished in the Couinaud classification (Fig. 7.5). The middle hepatic vein separates the anterior segment of the right lobe from the medial segment of the left lobe. The right hepatic vein divides the right lobe into anterior and posterior segments, and the left hepatic vein divides the left lobe into medial and lateral segments. The ascending segment of the left portal vein and the fissure for the ligamentum teres also separate the medial segment of the left lobe from the lateral segment.

Fig. 7.2. Normal echo texture and echogenicity of the liver. The liver is isoechoic to the cortex of the right kidney (RK)

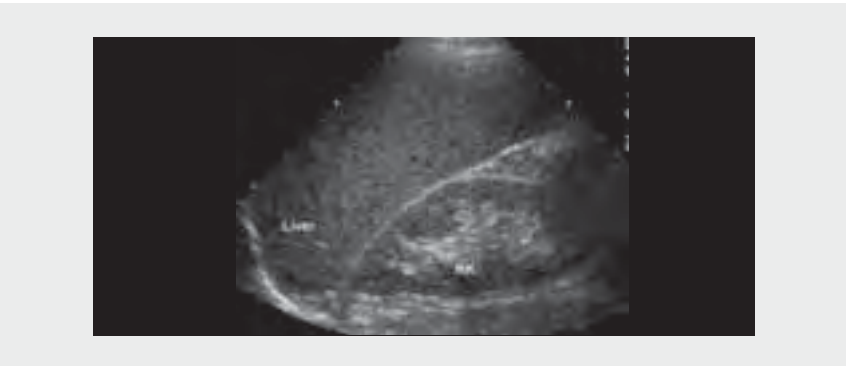


Fig. 7.3. Echogenicity of normal liver and in chronic renal parenchymal disease. Owing to increased renal cortical echo, that of the liver appears to be lower



Fig. 7.4. Measurement of the liver, from the inferior tip to the dome on real ultrasonography (a) and diagrammatically (b)

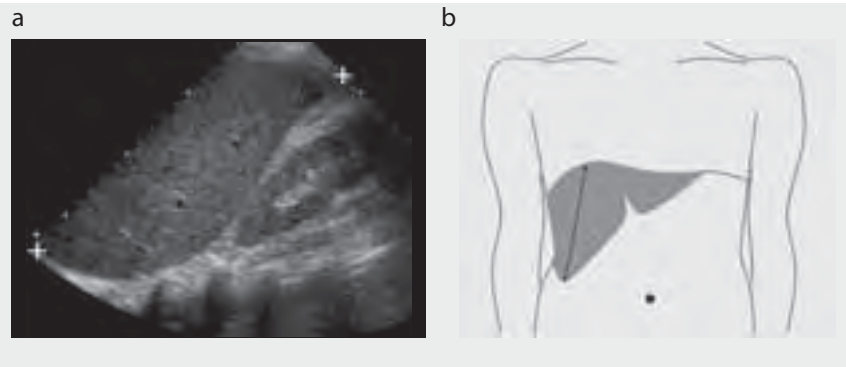


Fig. 7.5. Normal anatomy of the liver. (a) The right hepatic vein (RHV) divides the right anterior segment (RAS) and the right posterior segment (RPS) of the liver. The middle hepatic vein (MHV) (arrow) divides the right lobe and the left lobe, and the left hepatic vein (LHV) divides the left medial segment (LMS) and the left lateral segment (LLS); (IVC, inferior vena cava). (b) The open arrow shows the left hepatic vein, and the long solid arrow indicates the middle hepatic vein (RL, right lobe). (c) The main interlobar fissure (open arrow) divides the right and left lobes of the liver. The umbilical segment (solid arrows) of the left portal vein divides the LMS and the LLS. (d) Open arrow indicates the main interlobar fissure. The fissure for the ligamentum teres (solid arrow) divides the LMS and the LLS. (e–h) The segments are numbered 1–8 according to the Couinaud classification: (e) longitudinal scan at the epigastrium; (f) subcostal oblique ascending scan; (g) subcostal right transverse scan (GB, gallbladder; PV, portal vein); (h) right hypochondrium, longitudinal scan

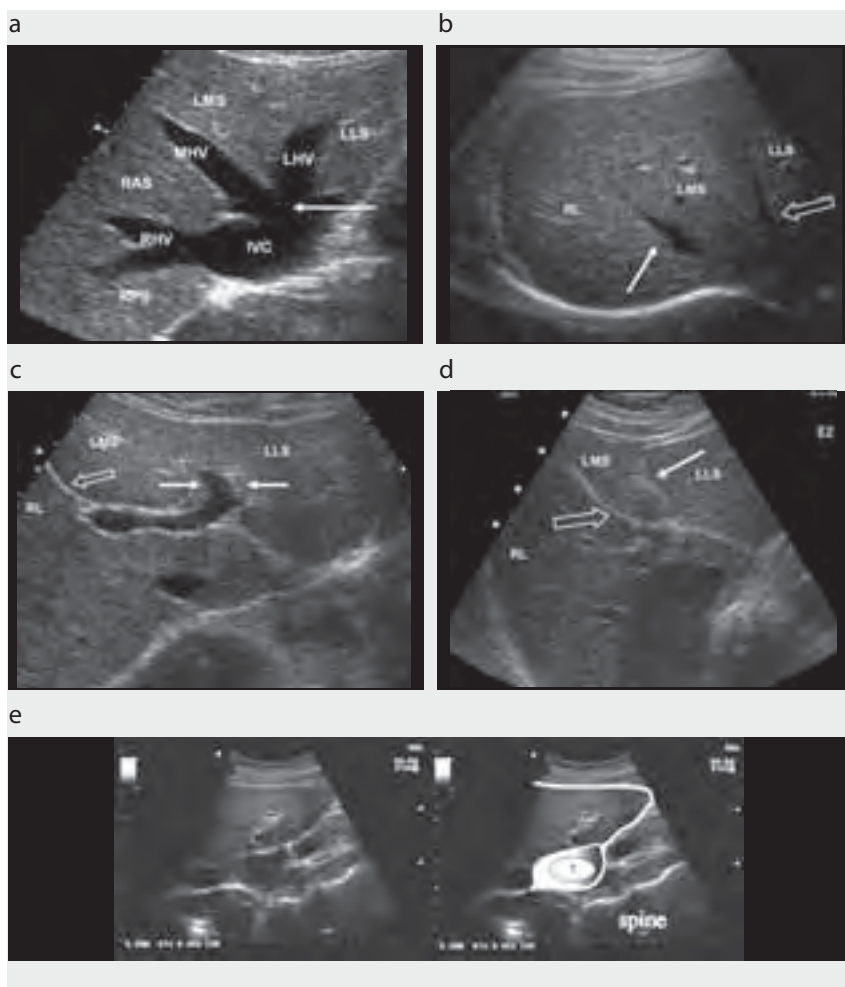
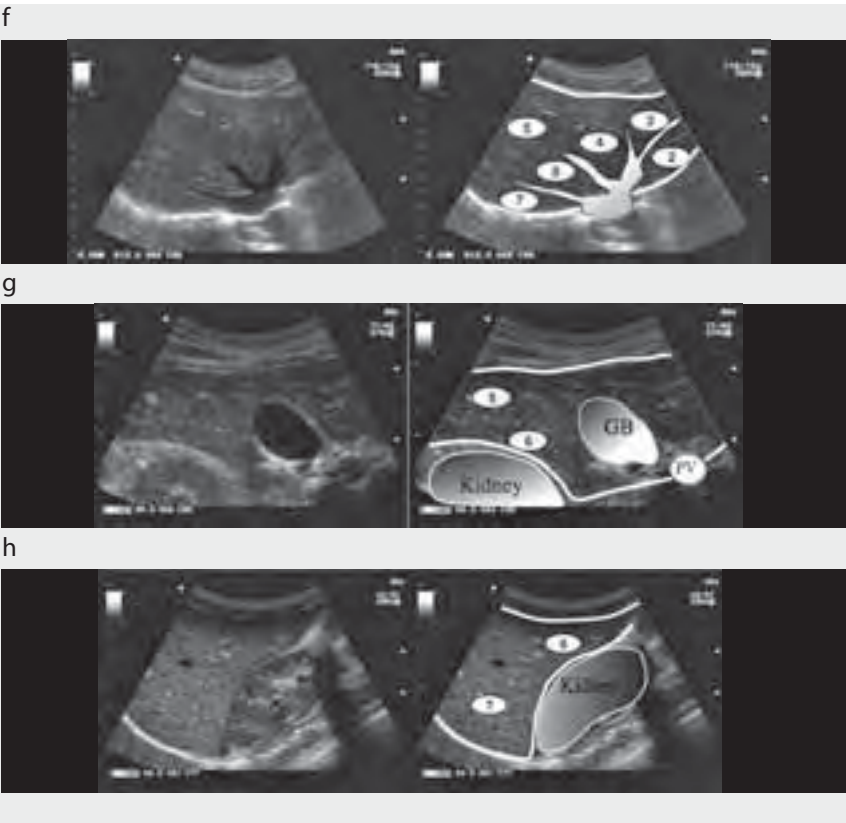


Fig. 7.5. continued



Pathological findings

Infectious diseases

Hepatitis

‘Hepatitis’ is the general term for inflammatory and infectious disease of the liver, of which there are many causes. Patients with acute and chronic hepatitis may initially present with flu-like and gastrointestinal symptoms, including loss of appetite, nausea, vomiting and fatigue.

In **acute hepatitis**, the liver parenchyma may have diffusely decreased echogenicity, with accentuated brightness of the portal triads, known as ‘periportal cuffing’ (Fig. 7.6). Hepatomegaly and thickening of the gallbladder wall are associated findings. In most cases, the liver appears normal.

In most cases of **chronic hepatitis**, the liver appears normal. The liver parenchyma may be coarse, with decreased brightness of the portal triads, but the degree of attenuation is not as great as in fatty infiltration (Fig. 7.7). The liver does not increase in size.

Fig. 7.6. Acute hepatitis. (a) The right hepatic lobe shows normal echo texture and normal echogenicity (arrow indicates right pleural effusion). (b) Diffuse thickening (arrows) of the gallbladder is revealed, suggesting gallbladder oedema

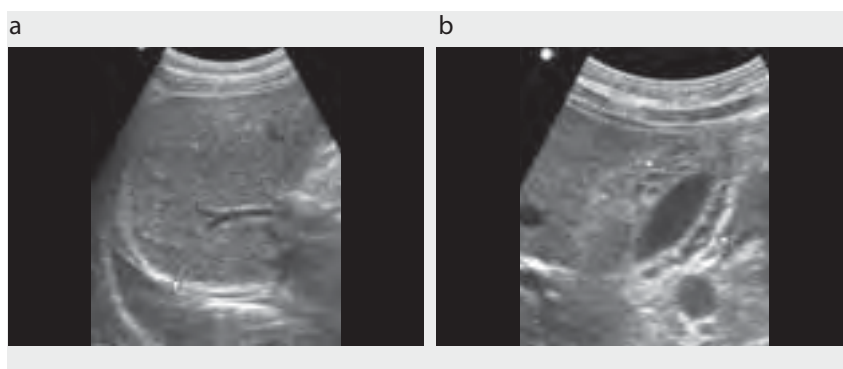
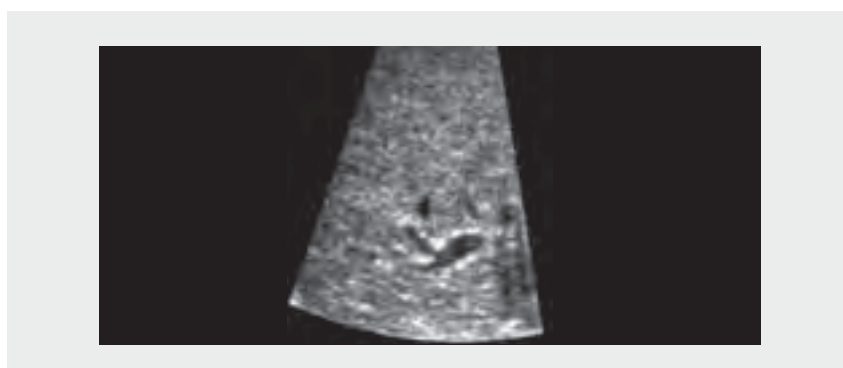


Fig. 7.7. Chronic hepatitis. Note the coarse echo texture of the liver, with increased echogenicity



Cirrhosis

Sonographic diagnosis of cirrhosis may be difficult. The specific findings include a coarse liver pattern secondary to fibrosis and nodularity (Fig. 7.8); increased attenuation may be present, with decreased vascular markings. Diffuse steatosis can also manifest as increased attenuation with decreased vascular markings. Hepatosplenomegaly may be present, with ascites surrounding the liver in the early stages of cirrhosis, whereas in advanced stages the liver is often small, with enlargement of the caudate, left lobe or both relative to the right lobe. Isoechoic or hypoechoic regenerative nodules may be seen throughout the liver parenchyma, most of which are less than 1 cm in diameter. Dysplastic nodules are larger than regenerative nodules and can have variable echogenicity. As cirrhosis is considered premalignant, further examination and follow-up are needed.

Fig. 7.8. Liver cirrhosis. (a) Very coarse liver echo texture and surface nodularity (arrows), either gross or micronodular, are demonstrated by ultrasound (a, ascites). (b) The portal vein is dilated by > 1.3 cm in diameter. (c) Recanalization of the umbilical vein (uv) can create a spontaneous portosystemic shunt (g, gallbladder). (d, e) Volumetric changes in cirrhosis, either segmental, caudate (segment 1) hypertrophy (arrows in (d)) or regional right lobe atrophy (arrow in (e)) (a, ascites). (f) Splenomegaly of different degrees can be associated with cirrhosis (s, spleen; k, kidney). (g) Cirrhosis decompensation: ascites and gallbladder wall oedema (arrows) are noted

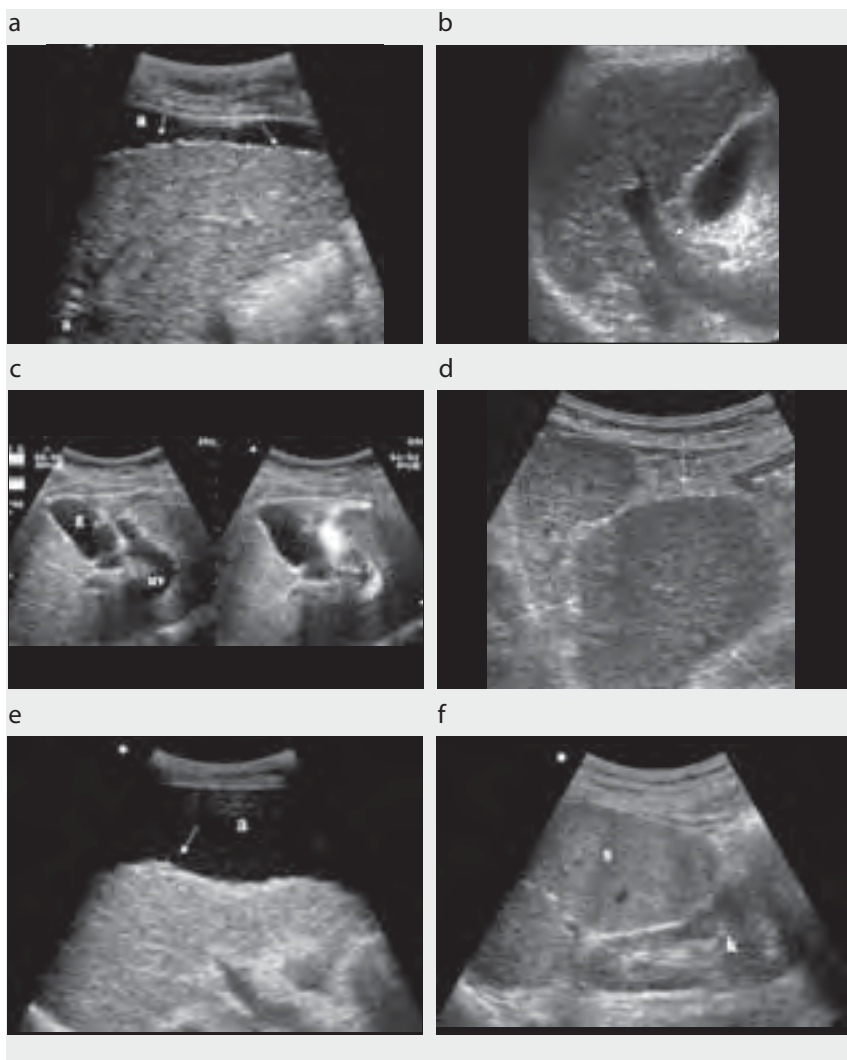
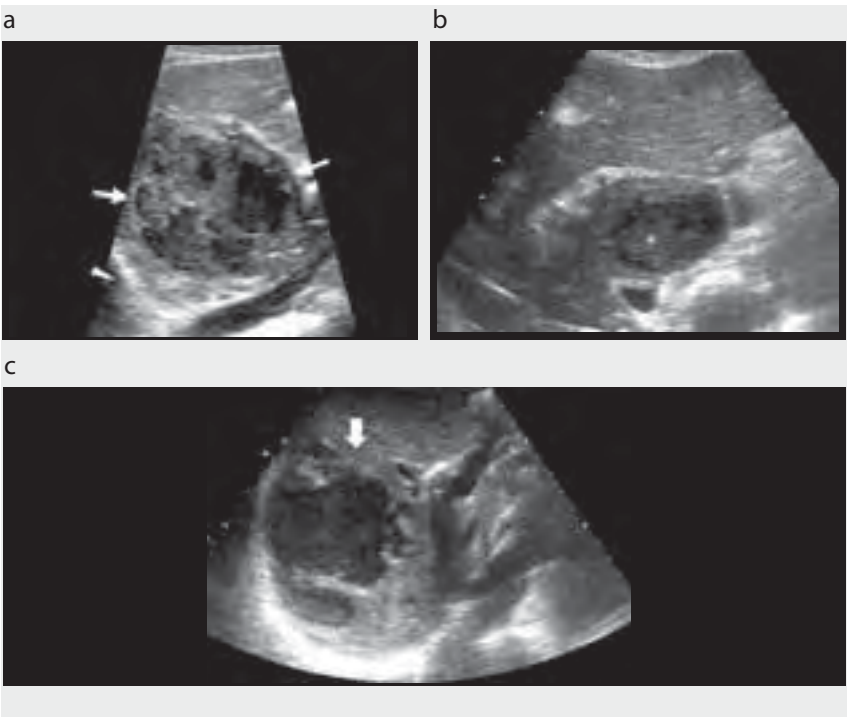


Fig. 7.8. continued



Fig. 7.9. (a, b, c) Mature liver abscesses (arrows): these are complex lesions with irregular, thick walls and septa and inhomogeneous echoes on the inside (arrowhead, diaphragm; asterisk, necrotic debris)



Pyogenic liver abscess

Sonographic identification of a pyogenic abscess depends on the maturity and internal consistency of the lesion. Mature purulent abscesses appear cystic, the fluid ranging from anechoic to highly echogenic (Fig. 7.9). Immature abscesses may appear solid, with altered echogenicity, and are usually hypoechoic (Fig. 7.10). The abscess may have echogenic foci, with a posterior reverberation artefact if gas is present. Fluid-filled interfaces, internal

septations and some debris are found along the posterior margin. The abscess wall can vary from well defined to irregular and thick (Fig. 7.11).

Fig. 7.10. Immature liver abscesses (arrows). Both hypoechoic (a) and isoechoic (b) abscesses appear solid

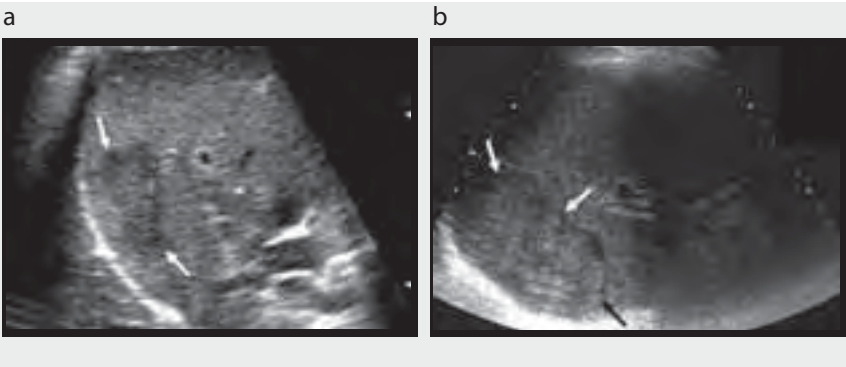
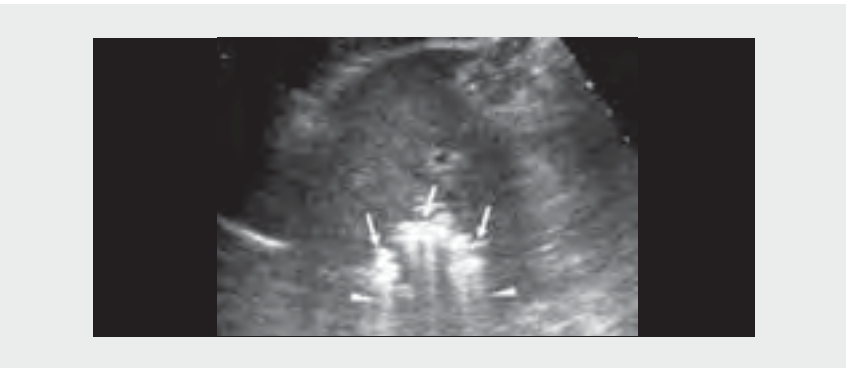


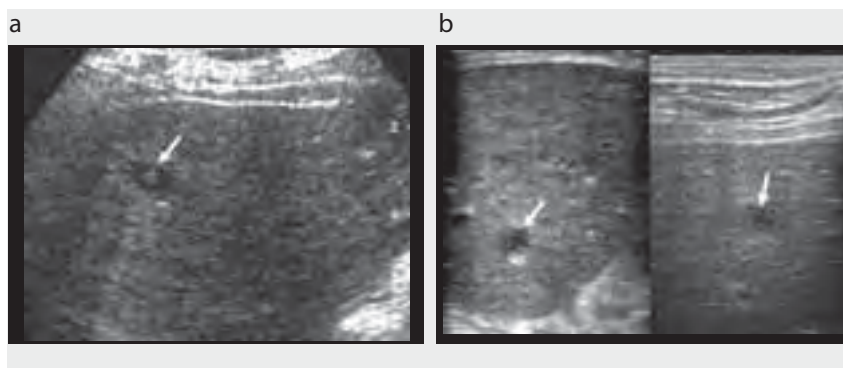
Fig. 7.11. Air-containing liver abscess (arrows). Multiple ring-down artefacts (arrowheads) arise from the abscess



Fungal diseases

Hepatic candidiasis usually occurs in immunocompromised hosts and is transmitted via the bloodstream. The commonest finding is multiple hypoechoic nodules with discrete margins. Other sonographic patterns are ‘wheel-within-a-wheel’ patterns, multiple small hypoechoic lesions with echogenic central foci, referred to as ‘bull’s eye’ or ‘target’ lesions (Fig. 7.12), or multiple hyperechoic nodules with posterior shadowing. Of these, the ‘wheel-within-a-wheel’ and ‘bull’s eye’ patterns suggest that the infection is active, whereas the other two patterns occur later in the course of the disease and suggest that the infection is subsiding.

Fig. 7.12. Hepatic candidiasis. (a) A hypoechoic lesion with an echogenic central focus ('bull's-eye' nodule, arrow) is seen. (b) The typical 'wheel-within-a-wheel' pattern (arrows) seen during the course of the disease consists of a peripheral hypoechoic zone, a second echogenic wheel and a central hypoechoic nidus (arrow)



Amoebic abscess

An amoebic abscess is a collection of pus caused by hepatic infection with the parasite *Entamoeba histolytica*. The sonographic appearance of amoebic abscess is nonspecific and similar to that of pyogenic abscesses.

Echinococcal cysts

These cysts are most prevalent in sheep- and cattle-raising countries, especially Australia, the Mediterranean region and the Middle East. The sonographic features of echinococcal cyst are:

- simple cyst containing no internal architecture, except sand
- 'water lily sign', which are cysts with detached endocyst secondary to rupture
- 'cyst-within-a-cyst', with daughter cysts matrix and
- a densely calcified mass (Fig. 7.13).

Septations are frequent and include a honeycomb appearance with fluid collection. If a 'water lily sign' or 'cyst-within-a-cyst' is found, it is specific for echinococcal cyst.

There are two current classifications of hydatid cysts, one by WHO, consisting of cystic echinococcosis (CE) 1–5, and one by Gharbi, which is annotated simply as 1–5.

Hepatic tuberculosis

Involvement of the liver and spleen is common in patients with miliary tuberculosis. Sonography usually demonstrates only nonspecific hepatomegaly; however, the lesions are too small to be seen sonographically. Sometimes, either small, echo-poor nodules or a large mass called a pseudotumour or tuberculoma can appear over the liver (Fig. 7.14). Tuberculomas are frequently echo poor and must be distinguished from metastasis, abscess and primary liver tumour. As the disease progresses, hepatic tuberculosis may involve calcifications. In an analysis of patients with HIV infection and abnormal abdominal CT findings, 20% had liver cirrhosis.

Fig. 7.13. Hydatid cyst of the liver. (a) Type 1. Note the thick membrane (vc, vena cava). (b) Type 2. The membranes are detached (dotted line). (c) Type 3 (arrows). Multivesicular, with typical honeycomb appearance. (d) Type 4. Note the thick, tangled membrane and daughter vesicles (arrows). (e) Type 5. Ultrasound cannot explore the content of a calcified cyst (arrow)

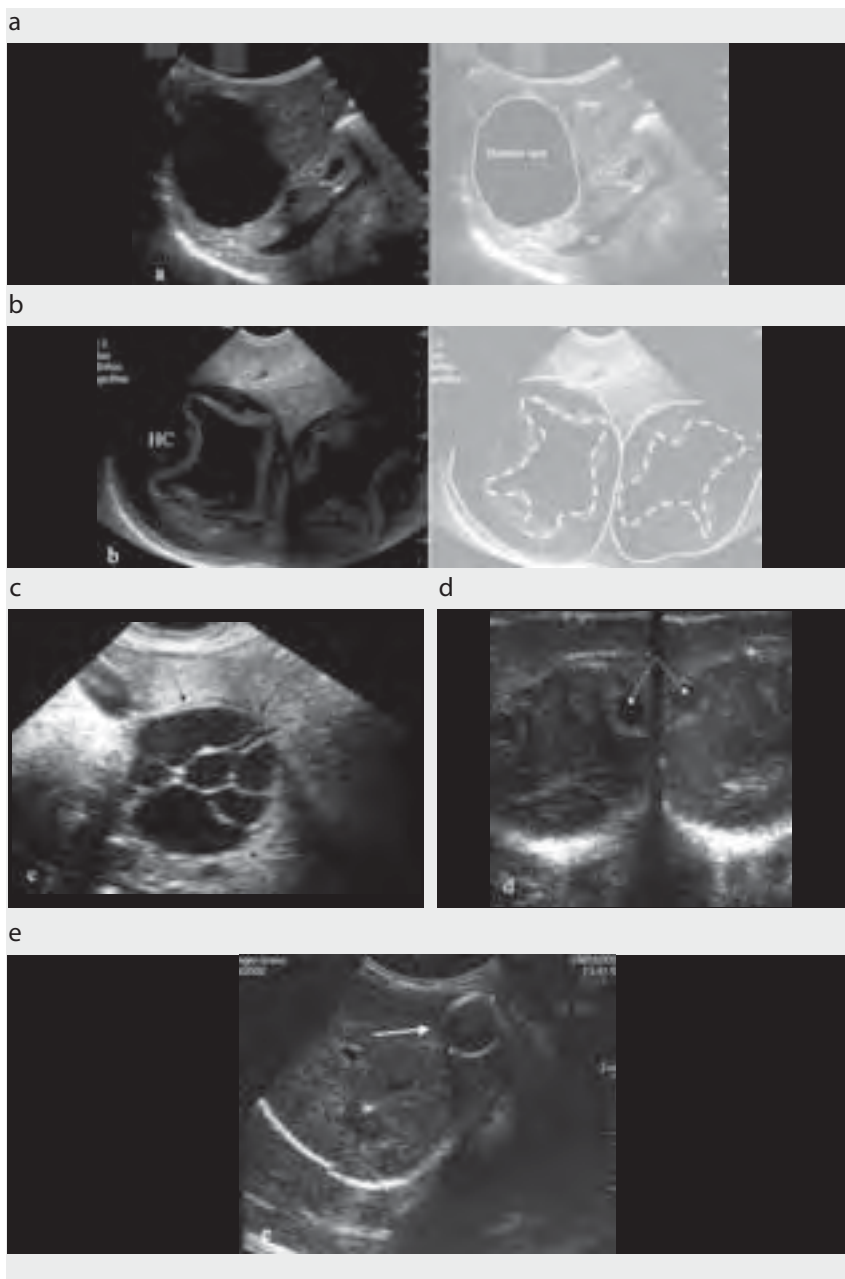
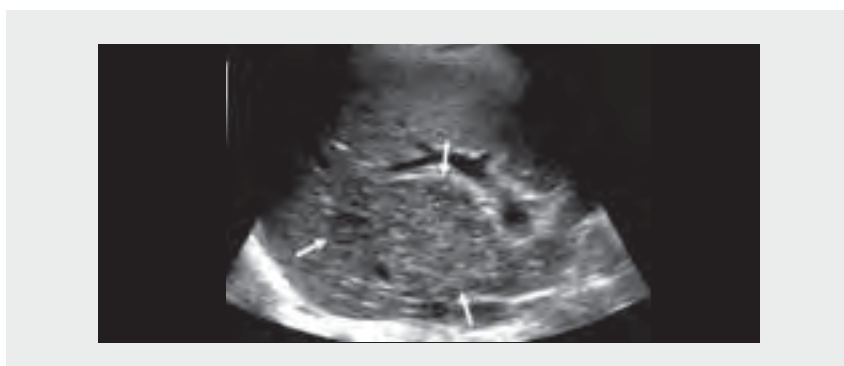


Fig. 7.14. Hepatic tuberculoma. An ill-defined, echo-poor, large mass (arrows) is seen in the right lobe of the liver



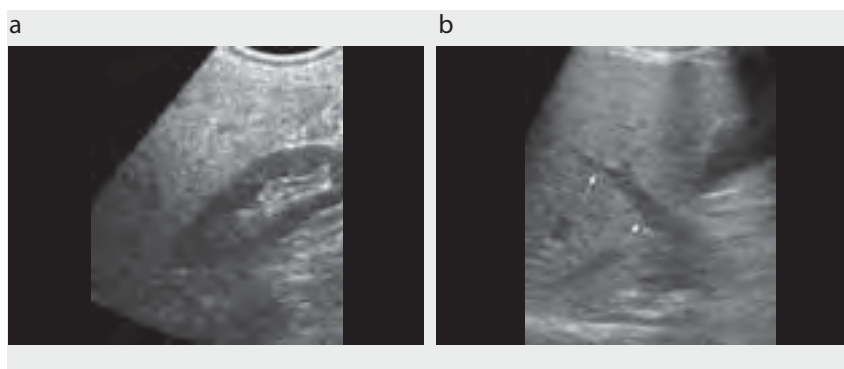
Metabolic disorders

Fatty liver

Sonographically, the liver has increased echogenicity and may be enlarged. Diffuse fatty liver has homogeneously increased echogenicity. The sonographic features of diffuse fatty liver are:

- bright liver, with greater echogenicity than the kidney
- decreased portal vein wall visualization
- poor penetration of the posterior liver and
- hepatomegaly (Fig. 7.15).

Fig. 7.15. Diffuse fatty liver. (a) The liver shows greater echogenicity than the kidney, with poor penetration of the posterior liver. (b) Decreased visualization of the portal vein wall (arrows) is seen



Focal fatty deposits show regions of increased echogenicity on a background of normal liver parenchyma (Fig. 7.16 (a)), whereas focal fatty sparing appears as hypoechoic masses within a dense, fatty-infiltrated liver (Fig. 7.16 (b)). Frequent locations include the region of the porta hepatis, near the falciform ligament, the dorsal

left lobe and the caudate lobe. These deposits tend to be geographically configured, i.e. have a map-like appearance but not nodular or round. The hepatic vessels are usually normal and not displaced in these areas on colour or power Doppler images.

Fig. 7.16. (a) Focal fat deposition (arrow) in the left lobe of the liver (MHV, middle hepatic vein). (b) Focal fatty “sparing” (between calipers) as a hypoechoic mass within a bright liver

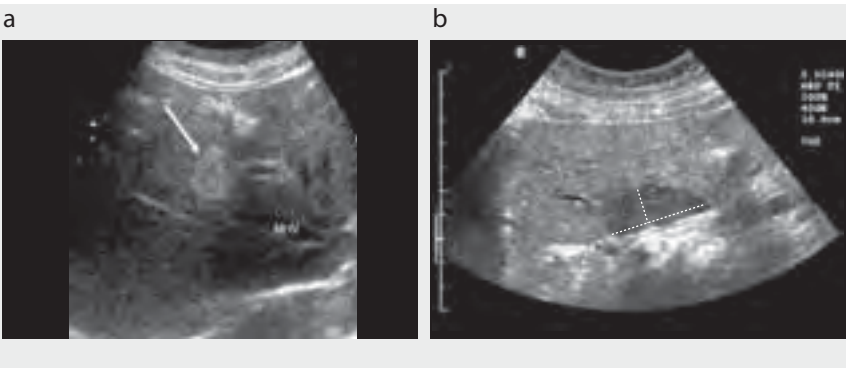
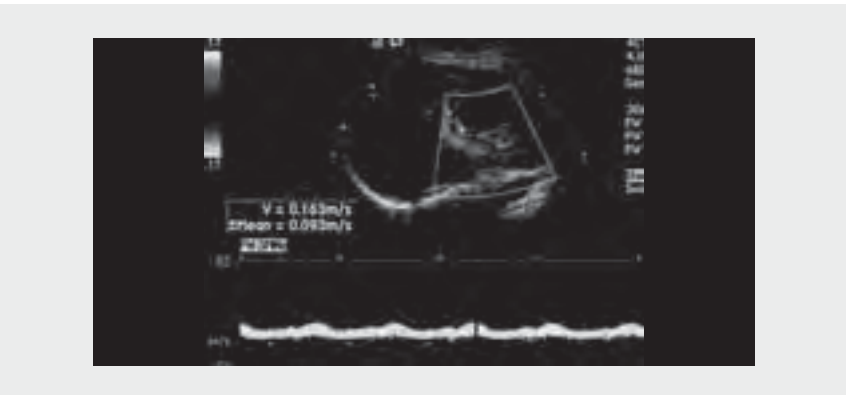


Fig. 7.17. Normal portal vein flow. Note the undulating hepatopetal flow signal



Vascular diseases

Portal hypertension

Sonography can be useful for defining the presence of ascites, hepatosplenomegaly and collateral circulation; the cause of jaundice; and the patency of hepatic vascular channels. The normal portal vein has an undulating hepatopetal flow (Fig. 7.17), whereas the calibre of the portal and splenic veins may be increased by more than 1.3–1.6 cm in portal hypertension. With the development of a porto-systemic shunt, however, the calibre of the veins may decrease. The superior mesenteric and splenic veins are more strongly influenced by respiration and the patient’s position. Thus, any increase in size may not be due to portal hypertension. The main sites of porto-systemic shunt are the gastro-oesophageal junction, for the gastric and para-oesophageal varix;

the fissure of the ligamentum teres, for the recanalized umbilical vein; the splenic and left renal hilum, for spleno-renal and gastro-renal shunts; and the mesentery for mesenteric varix. The mean portal venous flow velocity is approximately 15–18 cm/s but varies with respiration and cardiac pulsation. As portal hypertension develops, the flow becomes monophasic. In advanced portal hypertension, the flow becomes biphasic and finally hepatofugal (Fig. 7.18).

Fig. 7.18. Reversed portal venous flow in portal hypertension. Note the biphasic hepatofugal flow signal



Portal vein thrombosis

Portal vein thrombosis develops secondary to slow flow, hypercoagulable states, inflammation or invasion by a malignancy such as hepatocellular carcinoma, metastatic liver disease, pancreatic carcinoma or primary hepatic vascular leiomyosarcoma of the portal vein. Slow flow is usually secondary to portal hypertension, with shunting of mesenteric and splenic flow away from the liver. Sonography is an accurate means of confirming portal vein thrombosis. In sonography, portal flow is absent, and the vessel may be filled with a hypoechoic thrombus. As an acute thrombus can be hypoechoic or anechoic and may be overlooked, colour Doppler examination is necessary. Doppler sonography is also useful for distinguishing benign from malignant portal vein thrombi in patients with cirrhosis. The following sonographic findings suggest malignant thrombi:

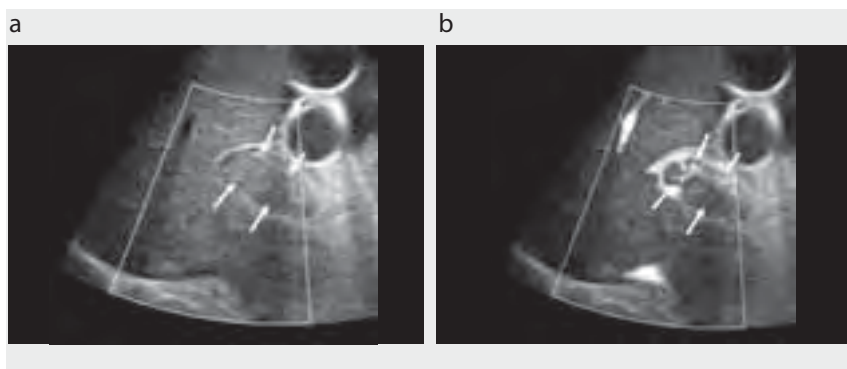
- expansion of involved portal vein
- a periportal tumour connected to the thrombi and
- a pulsatile flow signal within the thrombi (Fig. 7.19).

‘Cavernous transformation’ of the portal vein manifests as numerous wormlike vessels at the porta hepatis, which represent periportal collateral circulation. This is observed in longstanding thrombus or occlusion, i.e. longer than 12 months.

Hepatic venous obstruction and Budd-Chiari syndrome

As the hepatic veins have thin walls and no adventitia, the walls are less echogenic than those of the portal vein. The flow patterns in the hepatic vein are influenced by heart

Fig. 7.19. Malignant portal vein thrombosis. (a) On the grey-scale image, echogenic material (arrows) is seen within the main portal vein, with dilatation of the portal vein. (b) On a power Doppler image, irregular vascular channels with a pulsatile flow signal are seen within the thrombus (arrows)



motion. Normal individuals show two prominent antegrade (hepatofugal) waves and one prominent retrograde (hepatopetal) wave; thus, the hepatic veins have a triphasic wave. The larger of the two antegrade waves occurs during systole and is due to atrial relaxation, whereas the other occurs during diastole after opening of the tricuspid valve. The retrograde wave occurs when the right atrium contracts at the end of diastole.

Obliteration of hepatic vein pulsatility should be considered abnormal. In some cases, it may indicate anatomical obstruction between the right atrium and hepatic veins, such as a tumour or Budd-Chiari syndrome.

Hepatic venous obstruction can be due to obstruction of the suprahepatic portion of the inferior vena cava, thrombosis of the main hepatic veins themselves or obstruction at the level of small hepatic venules. Budd-Chiari syndrome generally involves the first two conditions, while hepatic veno-occlusive disease involves the last.

The sonographic findings in Budd-Chiari syndrome include evidence of hepatic vein occlusion and abnormal intrahepatic collaterals. The findings in hepatic vein occlusion include partial or complete disappearance of the hepatic veins, stenosis, dilatation, thick wall echoes, abnormal course, extrahepatic anastomoses and thrombosis.

In Budd-Chiari syndrome, Doppler sonography may show abnormal blood-flow patterns in the hepatic veins and inferior vena cava. The flow in the inferior vena cava, the hepatic veins or both changes from phasic to absent, reversed, turbulent or continuous. The portal blood flow may also be affected, characteristically being either slowed or reversed. Colour Doppler imaging can reveal hepatic venous occlusion, hepatic-systemic collaterals, hepatic vein–portal vein collaterals and anomalous or accessory hepatic veins of increased calibre.

Hepatic veno-occlusive disease

Hepatic veno-occlusive disease is defined as progressive occlusion of the small hepatic venules. Patients with this disease are clinically indistinguishable from those with Budd-Chiari syndrome. Doppler sonography shows normal calibre, patency and phasic flow in the main hepatic veins and inferior vena cava. The flow in the portal vein may be abnormal, being either reversed or ‘to-and-fro’.

Focal hepatic lesions

Benign cysts

Simple cysts are usually incidental, because most patients who have them are asymptomatic. Simple cysts are anechoic, with a well demarcated, thin wall and posterior acoustic enhancement (Fig. 7.20). Infrequently, these cysts contain fine linear internal septa. Complications such as haemorrhage or infection may occur and cause pain. Calcification may be seen within the cyst wall and may cause shadowing. In adult polycystic liver disease, the cysts are small (< 2–3 cm) and occur throughout the hepatic parenchyma. Histologically, they are similar to simple hepatic cysts.

Peribiliary cysts are small (0.2–2.5 cm) and are usually located centrally within the porta hepatis or at the junction of the main right and left hepatic ducts. Sonographically, peribiliary cysts can be seen as discrete, clustered cysts or as tubular structures with thin septa, paralleling the bile ducts and portal veins (Fig. 7.21).

Fig. 7.20. A simple cyst in the right lobe of the liver, showing a well demarcated, thin-walled, anechoic lesion (long arrow) with posterior acoustic enhancement (short arrows)



Fig. 7.21. Peribiliary cysts. Colour Doppler sonography shows multiple cysts (arrows) clustered around the portal veins (RPV, right portal vein; LPV, left portal vein; IVC, inferior vena cava)



Biliary hamartoma

Bile duct hamartomas are benign liver malformations, which usually show innumerable, well defined, solid nodules less than 1 cm in diameter. The lesions are usually hypoechoic and less commonly hyperechoic. Bright echogenic foci in the liver with distal ring-down artefacts are characteristic (Fig. 7.22).

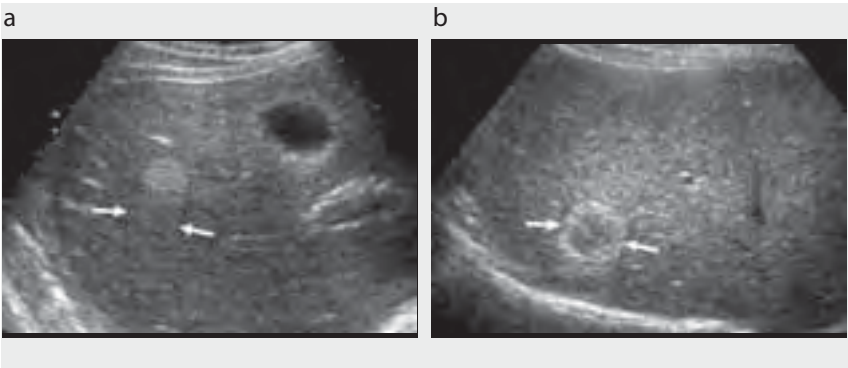
Fig. 7.22. Biliary hamartoma. Multiple echogenic foci with posterior ring-down artefacts (arrows) are seen in the right lobe of the liver



Haemangioma

Haemangiomas are benign congenital tumours consisting of large, blood-filled cystic spaces. They are the commonest benign tumours of the liver. Their sonographic appearance is characteristic: most are less than 3 cm, homogeneous and hyperechoic with acoustic enhancement (Fig. 7.23 (a)). Another typical feature is a heterogeneous central area containing hypoechoic portions with a thin or thick echogenic border (Fig. 7.23 (b)). Haemangiomas are round, oval or lobulated, with well defined borders. Larger haemangiomas may have a mixed pattern, resulting from necrosis. Calcification is rare.

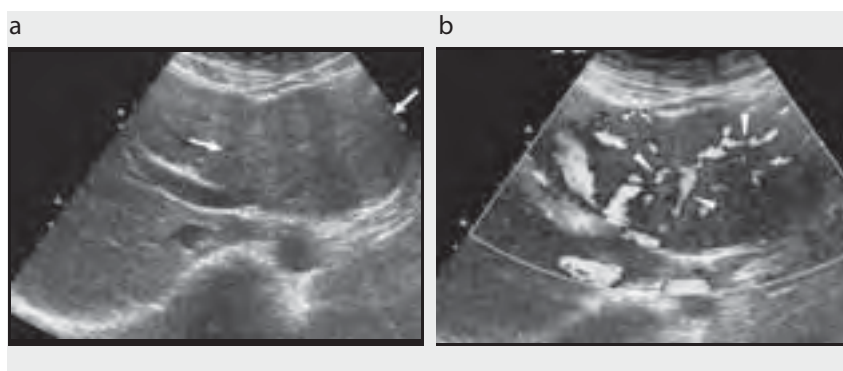
Fig. 7.23. Typical hepatic haemangiomas. (a) A homogeneous hyperechoic nodule with posterior acoustic enhancement (arrows). (b) A hyperechoic nodule (arrows) with a central heterogeneous hypoechoic area



Focal nodular hyperplasia

Focal nodular hyperplasia is the second most common benign liver mass after haemangioma. It is commoner in women than men, particularly among women of childbearing age, and is typically a well circumscribed, usually solitary mass with a central scar. Its excellent blood supply makes haemorrhage, necrosis and calcification rare. On sonography, focal nodular hyperplasia is well defined and hyperechogenic or isoechogenic relative to the liver (Fig. 7.24 (a)). It often manifests as a subtle liver mass that is difficult to differentiate from the adjacent normal liver. Doppler features of focal nodular hyperplasia are highly indicative, in that well developed peripheral and central blood vessels are seen (Fig. 7.24 (b)). The characteristic finding on colour Doppler is intra-tumoral blood vessels within the central scar, with either a linear or a stellate configuration.

Fig. 7.24. Focal nodular hyperplasia. (a) A nearly isoechoic mass (arrows) can be seen in the left lobe of the liver. (b) On colour Doppler sonography, stellate or spoke-wheel-like vascularity (arrowheads) due to centrifugal arterial flow is noted



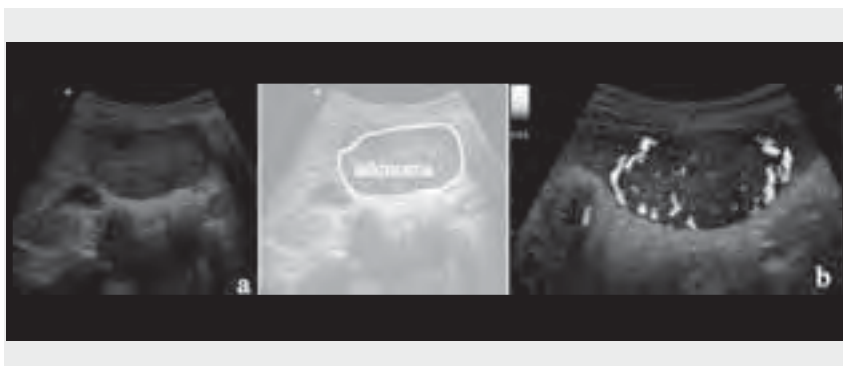
Hepatic adenoma

Hepatic adenoma occurs more commonly in women than men and has been associated with use of oral contraceptives. Patients may present with right upper-quadrant pain secondary to rupture, with bleeding into the tumour. Hepatic adenomas have also been reported in association with glycogen storage or **von Gierke disease**. Because hepatic adenoma has a propensity to haemorrhage and there is a risk for malignant degeneration, surgical resection is recommended. The sonographic appearance of hepatic adenoma is non-specific, and the echogenicity is variable (Fig. 7.25). In haemorrhage, a fluid component may be evident within or around the mass, and free intraperitoneal blood may be seen. The mass may be solitary or multiple. If the liver ruptures, fluid may be found in the peritoneal cavity.

Biliary cystadenoma and biliary cystadenocarcinoma

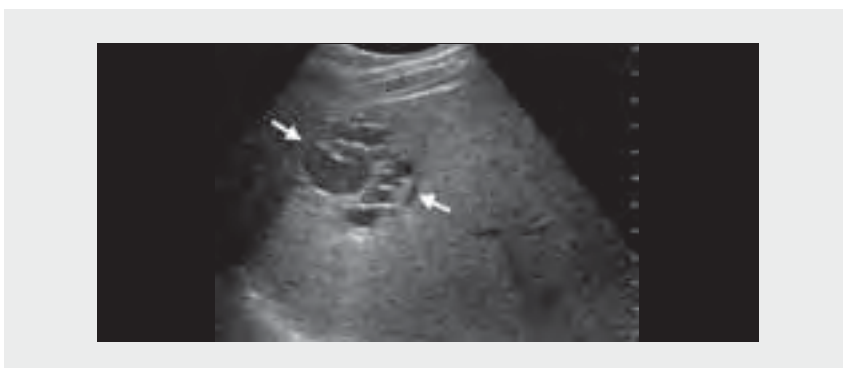
Biliary cystadenoma is a rare cystic neoplasm occurring primarily in middle-aged women. Although it is usually benign, it tends to recur after subtotal excision and can develop into a malignant cystadenocarcinoma. The most striking feature of the gross pathology of a biliary cystadenoma or cystadenocarcinoma is its multiloculated

Fig. 7.25. Large adenoma of the right liver lobe. (a) Echo-poor oval lesion with (b) multiple vascular signals within the lesion detected by power Doppler



appearance. In patients with biliary cystadenoma, the most common sonographic finding is a septated multilocular cyst with no gross nodules or soft-tissue mass (Fig. 7.26). Although cystadenoma usually cannot be differentiated from cystadenocarcinoma by imaging criteria, the presence of solid nodular masses or coarse calcifications along the wall or septa in a multilocular cystic mass indicates a likely diagnosis of biliary cystadenocarcinoma (Fig. 7.27).

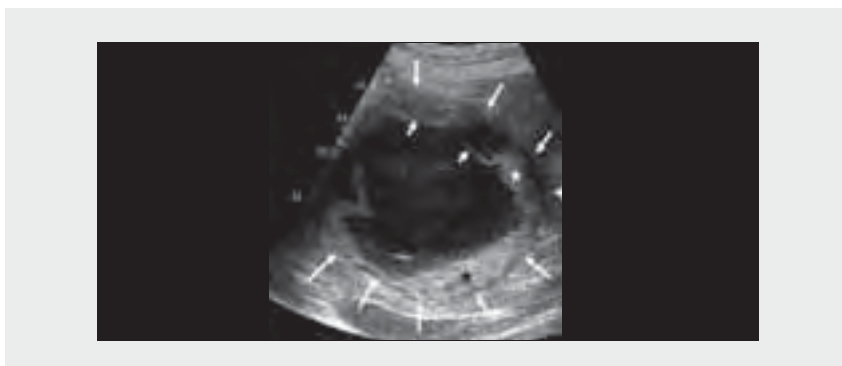
Fig. 7.26. Biliary cystadenoma. A multilocular cystic mass (arrows) with irregular septa is seen



Hepatocellular carcinoma

Hepatocellular carcinoma (HCC) is one of the commonest malignant tumours worldwide and its incidence is increasing, particularly in Africa and Asia. It is strongly associated with cirrhosis (80% of patients with HCC have cirrhosis) and chronic viral hepatitis. Alcoholic cirrhosis is a potential predisposing factor for HCC, and both viral hepatitis B and viral hepatitis C are now widespread. Pathologically, HCC occurs in three forms: solitary, multiple nodules and diffuse infiltrative. The sonographic appearance is variable, but there is a relation to size. Small HCCs (< 3 cm) tend to be hypoechoic (Fig. 7.28). Increasing echogenicity is related to the presence of haemorrhage, fibrosis and necrosis, echogenic lesions being found in about one

Fig. 7.27. Biliary cystadenocarcinoma. A large multilocular cystic mass (long arrows) with thick mural nodules (asterisks) and septa (short arrows) are noted



half of large HCCs. Small HCCs may also appear hyperechoic due to fatty change or sinusoidal dilatation. A mosaic pattern, a hypoechoic halo and lateral shadowing are relatively specific findings in HCCs (Fig. 7.28). The mosaic pattern is due to the presence of multiple compartments of different histological origin in a tumour. A hypoechoic halo and lateral shadowing are caused by a fibrous capsule. Portal or hepatic venous invasion of a tumour is considered to be characteristic of HCC and is associated with a poorer prognosis. Colour and spectral Doppler show high-velocity systolic and diastolic signals in HCC due to arteriovenous shunts and low impedance vasculature. The basket pattern and intratumoral vascular pattern are characteristic of HCCs on colour Doppler sonography (Fig. 7.28). Colour and power Doppler techniques are excellent for detecting neovascularity in tumour thrombi within the portal veins, which is diagnostic of HCC even without the demonstration of the parenchymal lesion.

Fibrolamellar hepatocellular carcinoma

Fibrolamellar HCC is a rare form (2%), occurring in young patients without coexisting liver disease. It has a better prognosis than HCC itself. It is typically large, solitary and slow growing, often with calcification and a central fibrosis scar resembling focal nodular hyperplasia.

Metastases

Metastatic disease is the commonest form of neoplastic involvement of the liver. It is most common in association with colon cancer, with decreasing frequency in gastric, pancreatic, breast and lung cancers. The sonographic appearance of metastatic liver disease varies. Knowledge of a prior or concomitant malignancy and features of disseminated malignancy at the time of sonography are helpful for correct interpretation of sonographically detected liver masses. They may present as a single liver lesion, but do so more commonly as multiple focal masses. Although there are no absolutely confirmatory features of metastatic disease on sonography, the presence of multiple solid nodules of different sizes and the presence of a hypoechoic halo surrounding a liver mass are indicative of metastasis (Fig. 7.29).

Hyperechoic metastases are generally from a gastrointestinal tumour, a renal cell carcinoma, a carcinoid, a choriocarcinoma or an islet cell tumour, and the echogenicity

Fig. 7.28. Small hepatocellular carcinoma (HCC). (a) A small, low echoic tumour measuring 1.7 cm in diameter (arrow) with slight heterogeneous internal echogenicity and a subtle hypoechoic halo; the coarse echo texture indicates chronic liver disease. (b) Echogenic HCC nodule with a subtle hypoechoic halo. (c) This tumour has two echoic areas, with a sharp distinction within the tumour (node-intra-node pattern). Note, in (b) and (c), the hypoechoic halo (long arrows), lateral shadowing (short arrows) and posterior enhancement. (d) Echo-rich, inhomogeneous HCC with hypoechoic halo. (e) Echo-poor HCC with extracapsular growth. (f)–(h) In larger tumours, the echo texture is complex (mosaic pattern and multiple tumour vascular signals are found). Colour Doppler sonography of HCC: (g) basket pattern in which peritumoral and intratumoral vessels are seen (arrows indicate the tumour margin); (h) in the intratumoral vascular pattern, the feeding vessel goes directly into the tumour and branches within it (arrows indicate the tumour margin)

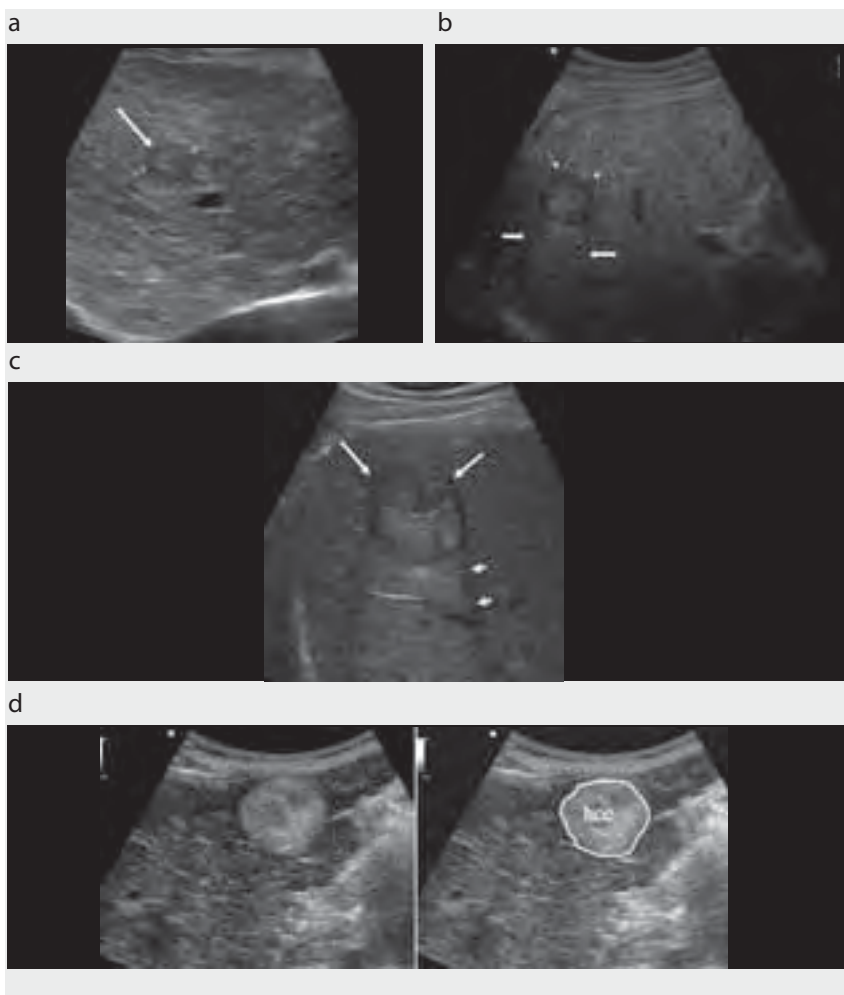
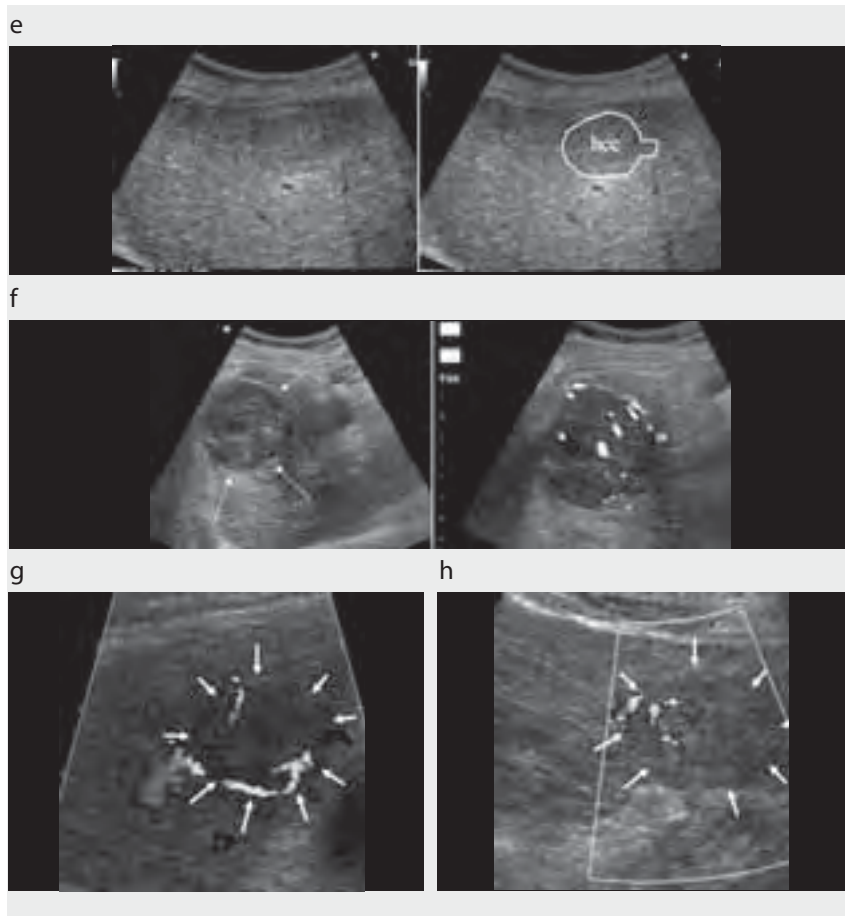


Fig. 7.28. *continued*



of the lesion increases with the vascularity of the tumour (Fig. 7.29). Hypoechoic metastases are typical after breast or lung cancer, but metastases from gastric, pancreatic or oesophageal cancer may also be hypoechoic. Calcific metastases have marked echogenicity and posterior shadowing (Fig. 7.30). They are most frequently associated with mucinous adenocarcinoma. Cystic metastases can generally be differentiated from benign hepatic cysts by their irregular thick walls, mural nodules, fluid–fluid levels and internal septation. Cystadenocarcinoma of the ovary and pancreas and mucinous carcinoma of the colon may be associated with cystic metastases in the liver. More often, cystic neoplasms occur secondary to extensive necrosis, most commonly in metastatic sarcoma (Fig. 7.31). Metastatic neuroendocrine tumours and large necrotic colorectal metastases can be predominantly cystic.

Diffuse infiltrative metastases, which may be confused with chronic liver disease, can occur after breast cancer, lung cancer and malignant melanoma. The ‘bull’s-eye’ pattern or ‘target’ sign indicates a hyperechoic or isoechoic lesion with a peripheral hypoechoic halo and is the result of compression, fibrosis or hypervascularity of adjacent liver parenchyma (see Fig. 7.29). Clinically, the presence of this hypoechoic halo is an important sign of malignancy, such as metastases and HCCs (see Fig. 7.28 and Fig. 7.29).

Fig. 7.29. Multiple metastatic tumours from a carcinoid. Multiple hyperechoic nodules (arrows) have a peripheral hyperechoic halo with a 'target' or 'bull's-eye' pattern

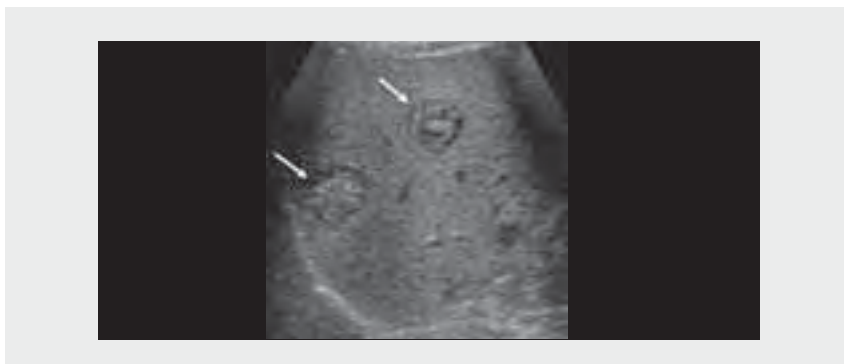


Fig. 7.30. Calcified metastatic tumours from colon cancer. Multiple, very bright echogenic nodules with posterior shadowing are noted

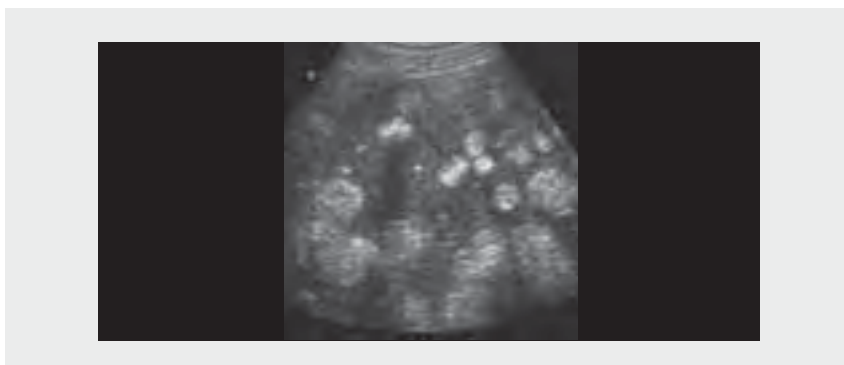
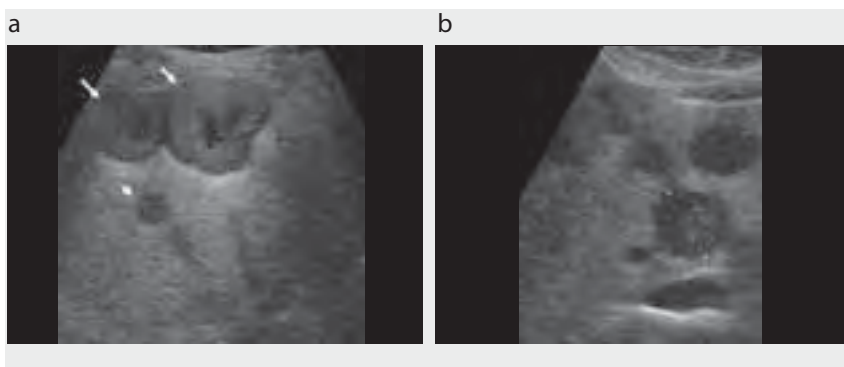


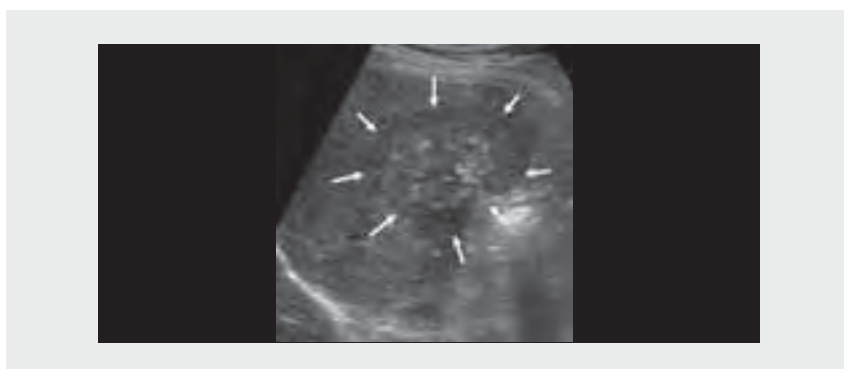
Fig. 7.31. Multiple solid and cystic metastases from gastrointestinal stromal tumours. (a) Multiple hypoechoic nodules (arrows) with a central cystic area are seen. (b) Some nodules show complete or partial cystic change due to extensive tumour necrosis



Intrahepatic cholangiocarcinoma

Intrahepatic cholangiocarcinoma is the second commonest primary hepatic malignant tumour after HCC, accounting for 5–30% of all primary malignant hepatic tumours. They can be classified as peripheral tumours. On sonography, most occur as a single, homogeneous, hypoechoic mass (Fig. 7.32). When detected, they are usually ill defined and poorly reflective. Commonly, dilated intrahepatic bile ducts are seen, which terminate at the level of the tumour. Occasionally, a tumour is intraluminal or causes focal thickening of the bile duct wall, resulting in stenosis in the absence of a mass. The tumour may be multifocal. As a rule, portal vein tumour thrombus is rare.

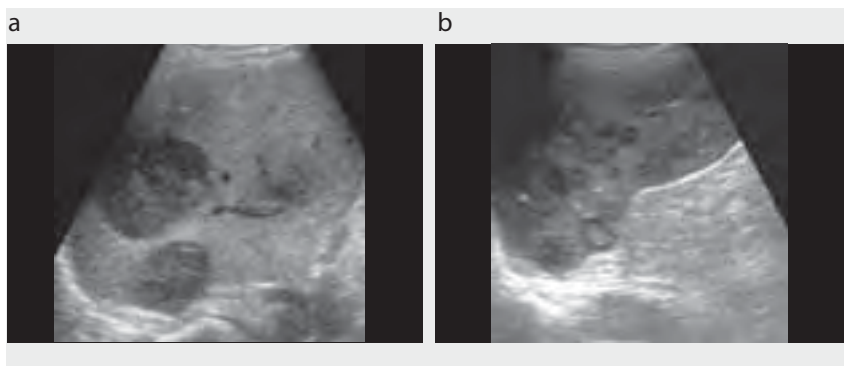
Fig. 7.32. Intrahepatic cholangiocarcinoma. In the right lobe of the liver, a large, ill-defined, heterogeneous, echo-poor mass (arrows) with multiple intratumoral echogenic spots can be seen



Lymphoma

Primary liver lymphoma is rare, and secondary liver lymphoma is also uncommon. Lymphomatous involvement of the liver appears either as a normal or a diffuse alteration of parenchymal echoes with hepatomegaly or as homogeneous hypoechoic masses (Fig. 7.33), which tend to have posterior acoustic enhancement. The pattern of multiple hypoechoic hepatic masses is more typical of primary non-Hodgkin lymphoma of the liver or lymphoma associated with HIV/AIDS.

Fig. 7.33. Lymphoma of the liver. (a) Multiple echo-poor tumours are seen throughout the liver. (b) Some tumours show a typical 'bull's-eye' pattern



Epithelioid haemangioendothelioma

Hepatic epithelioid haemangioendothelioma is a rare tumour of vascular origin that occurs almost exclusively in adults. It is difficult to diagnose on clinical grounds because of its non-specific signs and symptoms and misinterpretation of pathological specimens. On sonography, these tumours usually consist of discrete, mostly peripheral, individual tumour nodules measuring 2–4 cm. As the nodules grow and coalesce with time, they may show peripheral, confluent tumour masses. The echogenicity of the tumours varies, although they are usually hypoechogenic.

Angiosarcoma

Angiosarcoma is a malignant tumour arising from vascular endothelial cells. It is associated with exposure to various toxic materials, such as polyvinyl chloride, arsenic and Thorotrast (previously used as an intravascular contrast agent). The condition occurs almost exclusively in adults, predominantly in men. The tumours are usually large, unencapsulated and nodular or multinodular. Their sonographic appearance is commonly that of a large mass of mixed echogenicity, associated with necrosis and haemorrhage. If these tumours show a diffuse infiltrative pattern, they cannot be differentiated from diffuse hepatocellular disease.

Trauma

Abdominal trauma most frequently affects the spleen, kidney and liver. CT is used more often than sonography to evaluate the presence and extent of liver laceration, while sonography is usually used to monitor serially the pattern of healing. In the sonographic findings of acute trauma to the liver, fresh haemorrhage is echogenic. Within the first week, a hepatic laceration becomes more hypoechoic and distinct as blood becomes resolved (Fig. 7.34). Septations and internal echoes develop 2–4 weeks after trauma. A subcapsular haematoma may appear as anechoic, hypoechoic, septated lenticular or curvilinear. Fluid in the right upper quadrant or in the right upper quadrant and pelvic recess may suggest hepatic injury, as opposed to splenic, renal or enteric injury.

Fig. 7.34. Liver laceration. (a) The irregularly lacerated lesion (arrows) has a track-like zone, which in (b) is shown as an echo-poor zone with a central anechoic area. It suggests resolution of a haematoma in the lacerated zone

